

**Investigation of Drug Metabolism by
Non-Cytochrome P450 Enzymes and
Its Clinical Relevance**

Mitsuhiro Nishihara

2014

CONTENTS

GENERAL INTRODUCTION	1
CHAPTER I.....	3
Main Metabolic Pathways of TAK-802, a Novel Drug Candidate for Voiding Dysfunction, in Humans: The Involvement of Carbonyl Reduction by 11 β -hydroxysteroid Dehydrogenase 1	
CHAPTER II.....	24
Metabolic Fate of Sipoglitazar, a Novel Oral PPAR Agonist with Activities for PPAR- γ , - α and - δ , in Rats and Monkeys and Comparison with Humans <i>In Vitro</i>	
CHAPTER III.....	45
An Unusual Metabolic Pathway of Sipoglitazar: Cytochrome P450-Catalyzed Oxidation of Sipoglitazar Acyl Glucuronide	
CHAPTER IV.....	67
UDP-glucuronosyltransferase 2B15 (UGT2B15) Is the Major Enzyme Responsible for Sipoglitazar Glucuronidation in Humans: Retrospective Identification of the UGT Isoform by <i>In Vitro</i> Analysis and the Effect of UGT2B15*2 Mutation	
CONCLUSION.....	86
ACKNOWLEDGEMENTS.....	88
REFERENCES.....	90

LIST OF TABLES

- Table I-1.** *In vitro* metabolic profiles of [¹⁴C]TAK-802 with liver microsomes from humans and animals
- Table I-2.** Fragmentation profile of the precursor ions of TAK-802 and its metabolites in mass spectrometry analysis
- Table I-3.** Correlation coefficients between the metabolism of [¹⁴C]TAK-802 and CYP isoform-specific activities in microsomes from 16 human livers
- Table I-4.** *In vitro* metabolism of [¹⁴C]TAK-802 by 11β-HSD1-expressing microsomes
- Table I-5.** Correlation coefficients between the metabolism of M-IV and CYP isoform-specific activities in microsomes from 16 human livers
- Table II-1.** Apparent absorption ratio and bioavailability of [¹⁴C]sipoglitazar after a single oral dose in rats and monkeys at a dose of 0.5 mg/kg
- Table II-2.** Pharmacokinetic parameters of ¹⁴C in rats given once-daily oral doses of [¹⁴C]sipoglitazar repeatedly at a dose of 0.5 mg/kg for 14 days
- Table II-3.** Composition of radiolabeled materials in plasma of rats and monkeys given a single oral dose of [¹⁴C]sipoglitazar at a dose of 0.5 mg/kg
- Table II-4.** Composition of the radiolabeled materials in the urine, feces, and bile of rats and monkeys given a single oral dose of [¹⁴C]sipoglitazar at a dose of 0.5 mg/kg
- Table II-5.** Cumulative excretion of ¹⁴C in the urine, feces, and bile of rats and monkeys given a single oral dose of [¹⁴C]sipoglitazar at a dose of 0.5 mg/kg
- Table III-1.** ¹H Chemical shifts of sipoglitazar and its metabolites
- Table III-2.** Correlation coefficients for the metabolism of [¹⁴C]sipoglitazar-G1 with CYP isoform-specific activities
- Table IV-1.** Kinetic parameters of [¹⁴C]sipoglitazar-G1 formation in human UGT1A1-, UGT1A3-, UGT1A6-, UGT2B4-, UGT2B15-expressing supersomes, and liver microsomes
- Table IV-2.** The correlation coefficients among the glucuronidation of sipoglitazar, β-estradiol, trifluoperazine, 1-naphthol, morphine, and S-oxazepam

LIST OF FIGURES

- Figure I-1.** Concentrations and pharmacokinetic parameters of TAK-802 and M-IV in plasma of healthy male Japanese volunteers after a single oral dose of TAK-802 at 0.5 mg
- Figure I-2.** *In vitro* metabolism of [¹⁴C]TAK-802 with human CYP-expressing microsomes
- Figure I-3.** Representative HPLC-UV chromatograms of the incubation mixture of TAK-802 with human liver microsomes or cytosol
- Figure I-4.** Effects of glycyrrhetic acid on *in vitro* formation of M-IV from [¹⁴C]TAK-802 in human liver and 11 β -HSD1-expressing microsomes
- Figure I-5.** Representative HPLC-UV chromatograms of the incubation mixture of M-I, M-II or M-IV with human liver microsomes
- Figure I-6.** *In vitro* metabolism of M-IV with human CYP-expressing microsomes
- Figure I-7.** Postulated metabolic pathways of TAK-802 in humans
-
- Figure II-1.** Chemical structures of [¹⁴C]sipoglitazar, M-I, M-II, sipoglitazar-G and M-I-G
- Figure II-2.** Concentrations of ¹⁴C and pharmacokinetic parameters of sipoglitazar in plasma of rats and monkeys given a single oral dose of [¹⁴C]sipoglitazar at a dose of 0.5 mg/kg
- Figure II-3.** Concentrations of ¹⁴C and its elimination in tissues of rats given a single oral dose of [¹⁴C]sipoglitazar at a dose of 0.5 mg/kg
- Figure II-4.** Concentrations of ¹⁴C and its elimination in tissues of rats after a once-daily oral dose of [¹⁴C]sipoglitazar at a dose of 0.5 mg/kg for 21 days
- Figure II-5.** *In vitro* metabolic profiles of [¹⁴C]sipoglitazar with hepatocytes from humans, rats and monkeys
-
- Figure III-1.** Composition of metabolites of [¹⁴C]sipoglitazar formed by human hepatocytes and liver microsomes
- Figure III-2.** Representative HPLC-radiochromatograms of the incubation mixture of sipoglitazar with human liver microsomes in the presence of UDPGA
- Figure III-3.** Full ion mass spectrum of sipoglitazar-G1 (A), and its product ion mass spectrum of the precursor ion at *m/z* 642 (B)
- Figure III-4.** Full ion mass spectrum of sipoglitazar-G2 (A), and its product ion mass spectrum of the precursor ion at *m/z* 642 (B)
- Figure III-5.** Stability and interconversion of sipoglitazar-G1 and sipoglitazar-G2 in KPBB (pH 7.4), acetate buffer (pH 4.4), rat bile, and human plasma

- Figure III-6.** Representative HPLC-radiochromatograms of the incubation mixture of sipoglitazar-G1 or sipoglitazar-G2 by human liver microsomes with or without an NADPH-generating system
- Figure III-7.** Formation of M-I from [¹⁴C]sipoglitazar-G by specific human CYP-expressing microsomes
- Figure III-8.** Effect of gemfibrozil on the *in vitro* oxidative metabolism and/or glucuronidation of [¹⁴C]sipoglitazar
- Figure III-9.** Postulated metabolic pathways of sipoglitazar
- Figure III-10.** Possible metabolic pathway of sipoglitazar-G1 via lactone-form and metabolic pathway of statin glucuronide
-
- Figure IV-1.** Relative glucuronosyltransferase activity of [¹⁴C]sipoglitazar with human UGT-expressing supersomes
- Figure IV-2.** Kinetics of [¹⁴C]sipoglitazar-G1 formation by UGT1A1-, UGT1A3-, UGT1A6-, UGT2B4-, UGT2B15-expressing supersomes and human liver microsomes
- Figure IV-3.** Correlation analysis between the glucuronidation of [¹⁴C]sipoglitazar and UGT isoform-specific activities in microsomes from 16 human livers
- Figure IV-4.** Identification of His-tagged UGT2B15*1 and UGT2B15*2 protein by Western blotting
- Figure IV-5.** Kinetics of [¹⁴C]sipoglitazar glucuronidation by His-tagged UGT2B15*1 and UGT2B15*2 membrane fractions

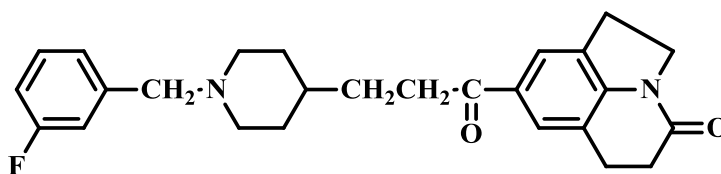
ABBREVIATIONS

ADME	absorption, distribution, metabolism and excretion
AO	aldehyde oxidase
AUC	area under plasma concentration time curve
11 β -HSD	11 β -hydroxysteroid dehydrogenase
β -NADP ⁺	β -nicotinamide adenine dinucleotide phosphate
C _{max}	maximum observed plasma concentration
CID	collisionally induced dissociation
CL _{int}	intrinsic clearance
CR	carbonyl-reducing enzyme
CYP	cytochrome P450
DDI	drug-drug interaction
DMEM	Dulbecco's Modified Eagle medium
DMSO	dimethylsulfoxide
EM and PM	extensive and poor metabolizers
ESI	electrospray ionization
FDA	Food and Drug Administration
HPLC	high-performance liquid chromatography
K _m	Michaelis constant
KPB	potassium phosphate buffer
LC-MS/MS	liquid chromatography-tandem mass spectrometry
NCE	new chemical entity
NMR	nuclear magnetic resonance spectroscopy
PPAR	peroxisome proliferator-activated receptor
SDR	short-chain dehydrogenases/reductase
SRM	selective reaction monitoring
t _{1/2}	elimination half-life
T _{max}	time at which C _{max} occurred
TDZ	thiazolidinedione
TFA	trifluoroacetic acid
TLC	thin layer chromatography
UDPGA	uridine 5'-diphosphoglucuronic acid
UGT	uridine diphosphoglucuronosyltransferase
V _{max}	maximum velocity

GENERAL INTRODUCTION

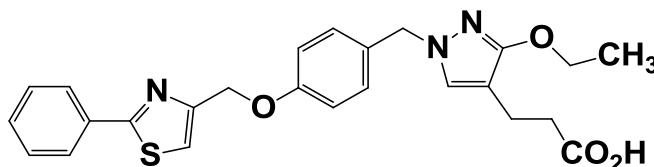
Drug metabolism studies are important for the drug discovery and development processes, to examine whether the drug candidate would have desired pharmacokinetic profiles to exert the pharmacological effects safely and stably, such as bioavailability, elimination rate from the body and drug-drug interaction (DDI). In addition, the identification of metabolic enzymes by *in vitro* metabolism studies is essential to pharmaceutical industries on drug development. Metabolic enzymes are broadly categorized into "phase I" and "phase II" enzymes. Phase I enzymes catalyze the oxidation, reduction and hydrolysis to reduce lipophilicity of the drug, and phase II enzymes mediate conjugation of a hydrophilic moiety with the drug to promote drug elimination from the body. Phase II reaction generally follows the phase I reaction. Cytochrome P450 (CYP) are well known as the major phase I enzyme involved in oxidative metabolism of a variety of drugs. CYP-mediated metabolism has been comprehensively investigated *in vitro* and *in vivo* to date, and the cumulative knowledge and information have often been fed back to drug design [1,2]. However, with advances in such rational drug design for enzymatically stable compounds against CYPs, drugs metabolized by non-CYP enzymes have been increasingly conspicuous instead [3]. Previous literature reported that about a quarter of top 200 prescribed drugs in the USA were metabolized predominantly by non-CYP enzymes, including UDP-glucuronosyltransferase (UGT), flavin monooxygenase (FMO), monoamine oxidase (MAO) and esterase [4]. Recently, aldehyde oxidase (AO), one of non-CYP enzymes, has more often become topics in that extensive metabolism by AO in humans may cause inter-species differences and seriously low bioavailability in humans [5]. To address this issue, several approaches have already been proposed and demonstrated successful prediction of intrinsic clearance (CL_{int}) in humans by *in vitro*-to-*in vivo* extrapolation and computational models [6,7]. Although there are literatures discussing clinical impacts of some specific non-CYP enzymes like AO, basic information on other enzymes is still insufficient. In this thesis, drug metabolism by 11 β -hydroxysteroid dehydrogenase (11 β -HSD) and UGT is focused. Through *in vitro* metabolism studies for candidate drugs developed at Takeda Pharmaceutical Company Limited, clinical relevancies of non-CYP metabolism are discussed.

In Chapter I, drug metabolism by 11 β -HSD1 is discussed and the species difference in the metabolism of TAK-802 (8-[3-[1-[(3-fluorophenyl)methyl]-4-piperidinyl]-1-oxopropyl]-1,2,5,6-tetrahydro-4*H*-pyrrolo[3,2,1-*ij*]quinolin-4-one), a member of a novel non-carbamate class of acetylcholinesterase inhibitors for voiding dysfunction, is addressed from *in vitro* studies [8].



Chemical structure of TAK-802

In Chapter II-IV, conjugation enzymes are focused. UGTs and sulfatases are the phase II enzymes mediating glucuronidation and sulfation, respectively. In general, these conjugations occur at hydroxyl or amine groups originally existing in the chemical structure or generated by phase I reaction of CYPs to increase hydrophilicity of drugs and then encourage drug elimination from the body. As UGT enzymes have become well characterized, Food and Drug Administration (FDA) has recently issued the revised draft guidance for DDI, where *in vitro* metabolism studies of UGT1A family are recommended [9]. Glucuronidation profiles of sipoglitazar (TAK-654, 3-[3-ethoxy-1-[[4-[(2-phenyl-1,3-thiazol-4-yl)methoxy]phenyl]methyl]pyrazol-4-yl]propanoic acid), a novel anti-diabetic agent with triple agonistic activities on human peroxisome proliferator-activated receptor (PPAR) γ , PPAR- α , and PPAR- δ , were investigated as a part of pharmacokinetic evaluation in the drug development process.



Chemical structure of sipoglitazar

Firstly, the *in vivo* pharmacokinetic properties of sipoglitazar were evaluated in animals and the *in vivo* and *in vitro* metabolite profiles in humans and animals were compared (Chapter II) [10]. Secondly, the metabolic pathways of sipoglitazar via glucuronidation in humans were clarified (Chapter III) [11]. Recently, genotyping in clinical studies has revealed that UGT2B15 genetic polymorphism has an influence on the clinical pharmacokinetics of sipoglitazar [12,13]. Finally, the responsible enzymes for the glucuronidation of sipoglitazar in humans were retrospectively identified as UGT2B15 by *in vitro* analysis and the effect of genetic polymorphism of UGT2B15 was examined in Chapter IV [14].

CHAPTER I

Main Metabolic Pathways of TAK-802, a Novel Drug Candidate for Voiding Dysfunction, in Humans: The Involvement of Carbonyl Reduction by 11 β -hydroxysteroid Dehydrogenase 1

Introduction

TAK-802 is a member of a novel non-carbamate class of acetylcholinesterase inhibitors [15]. TAK-802 was more effective than both of the clinically used cholinomimetics, distigmine and bethanechol, in increasing urinary flow and voided volume in urethane-anaesthetized guinea pigs or rats with partial bladder outlet obstruction [16,17]. TAK-802 also had a higher selectivity for muscarinic actions over nicotinic actions than distigmine [18], and did not influence urethral resistance or bladder-storage function, unlike distigmine.

The pharmacokinetic studies using ^{14}C -labeled TAK-802 (^{14}C]TAK-802) in rats, dogs and monkeys have already revealed that TAK-802 is biotransformed to M-I (the metabolite formed by elimination of the fluorobenzyl group), M-II (the reductive metabolite of M-I) and other unidentified metabolites [19]. In addition, the formation of M-III was also confirmed in the animals and M-III was estimated to be the hydroxylated metabolite of TAK-802 (unpublished observation). TAK-802 was extensively metabolized involving first-pass metabolism during the absorption process and its related metabolites were excreted predominantly into the feces via the bile in the tested animals. As calculated from the $\text{AUC}_{0-24\text{h}}$ in rats, given a single oral dose of ^{14}C]TAK-802 at 0.3 mg/kg, 13.3%, 3.3%, 3.2% and 2.2% of the total ^{14}C was accounted for by unchanged TAK-802, M-I, M-II, and M-III, respectively. In the same way, the composition ratio of unchanged TAK-802, M-I, M-II and M-III was 5.2%, 2.1%, 0.9% and 1.3% in dog plasma and 11.7%, 6.9%, 9.2% and 3.8% in monkey plasma, respectively. The major components of ^{14}C in plasma were unidentified polar metabolites in all tested animals. After a single oral administration of ^{14}C]TAK-802 at 0.3 mg/kg, small amounts of unchanged TAK-802, M-I, M-II and M-III were detected in the urine and feces of animals and the bile of rats. However, most of the ^{14}C in excreta consisted of unidentified polar metabolites in all species.

In this study, through the metabolite profiling in human plasma and excreta after administration of TAK-802, M-IV was detected as a newly identified metabolite and M-IV formation was confirmed in human liver microsomes, too. Thus, the amounts of TAK-802 and its metabolites in the plasma of healthy male Japanese volunteers given a single oral dose of TAK-802 at 0.5 mg were preliminarily quantified by liquid chromatography-tandem mass spectrometry (LC-MS/MS) and the metabolic profile was investigated *in vitro* and *in vivo* and compared between humans and animals. M-IV is a reductive metabolite, indicating the involvement of reductive enzymes in the metabolism of TAK-802. In general, phase I

enzymes catalyzing the reduction of ketone moieties include alcohol dehydrogenases, aldo-keto reductases (AKRs), short-chain dehydrogenases/reductases (SDRs) and quinone reductases in humans [20,21]. They are known to be involved in the biotransformation of endogenous compounds such as steroid hormones and some xenobiotic compounds such as tobacco-specific nitrosamines, anthracycline anti-cancer drugs, and HIV integrase inhibitors [22,23,24]. Most of reductive enzymes are located in the cytosol, while only the SDR superfamily, one of carbonyl-reducing enzyme (CR), is located in microsomes [22,25]. Among the microsomal SDRs, 11 β -HSD1 is well-known with respect to xenobiotic metabolism [21,26,27]. Based on this understanding, *in vitro* metabolic studies were carried out using 11 β -HSD-expressing microsomes and the metabolic pathways from TAK-802 to its metabolites in humans were clarified to investigate the species differences in the metabolism of TAK-802.

Materials and Methods

Chemicals

TAK-802, its metabolites (M-I, 8-[3-(4-piperidinyl)-1-oxopropyl]-1,2,5,6-tetrahydro-4*H*-pyrrolo[3,2,1-*ij*]quinolin-4-one, M-II, 8-[1-hydroxyl-3-(4-piperidinyl)propyl]-1,2,5,6-tetrahydro-4*H*-pyrrolo[3,2,1-*ij*]quinolin-4-one) and M-IV, 8-[3-[1-[(3-fluorophenyl)methyl]-4-piperidinyl]-1-hydroxypropyl]-1,2,5,6-tetrahydro-4*H*-pyrrolo[3,2,1-*ij*]quinolin-4-one) and the internal standard of TAK-802 (deuterated TAK-802, TAK-802-*d*₄), were prepared by Takeda Pharmaceutical Company Limited (Osaka, Japan). [¹⁴C]TAK-802 with a specific radioactivity of 4.8 or 5.0 MBq/mg was synthesized by Amersham Pharmacia Biotech UK Ltd. (Buckinghamshire, UK). Glucose 6-phosphate and β -nicotinamide adenine dinucleotide phosphate (β -NADP⁺) were purchased from Oriental Yeast Co., Ltd. (Osaka, Japan). Glucose-6-phosphate dehydrogenase was from Sigma-Aldrich (St. Louis, MO) and glycyrrhetic acid, methanol, acetonitrile, and other reagents of analytical grade from Wako Pure Chemical Industries, Ltd. (Osaka, Japan).

Human samples

Plasma and urine samples were obtained from healthy male volunteers in the Phase I single dose study in Japan. The clinical study was conducted according to Good Clinical Practice standards. The protocol, informed consent, and other relevant study documentation were approved by the appropriate institutional review board at the participating site. All participants provided written informed consent in accordance with institutional guidelines. The dosage of TAK-802 was 0.5 mg. The samples were stored below -20°C until analysis. The pooled samples (plasma; 1-12 or 0.25-48 hours (n=9) and urine; 0-24 hours (n=9) were used for LC-MS/MS analysis. Liver microsomes and cytosol from mixed-gender humans were obtained from Tissue Transformation Technologies (Edison, NJ) and Xenotech, LLC

(Lenexa, KS).

Other materials

Baculovirus-infected-insect cell microsomes expressing human 11 β -HSD1 (hHSD1) and rat 11 β -HSD1 (rHSD1) were prepared by Takeda Pharmaceutical Company Limited. The 11-oxoreduction activity of cortisone was measured by high-performance liquid chromatography (HPLC)-UV quantitation of the conversion from cortisone to cortisol. The activity for hHSD1- and rHSD1-expressing microsomes was 0.353 and 0.499 nmol/min/mg protein, respectively, when cortisone (10 μ M) was incubated with each of the 11 β -HSD-expressing microsomes (0.5 mg microsomal protein/mL) in the presence of NADPH at 37°C for 30 minutes. Liver microsomes and cytosol from male animals were obtained from In Vitro Technologies (Baltimore, MD) and Xenotech, LLC. Baculovirus-infected-insect cell microsomes expressing human CYP isoforms were purchased from BD Biosciences (Woburn, MA).

Metabolism of [¹⁴C]TAK-802, TAK-802, or its metabolites by human and animal liver microsomes or cytosol

A dimethylsulfoxide (DMSO) solution of 0.1 mM [¹⁴C]TAK-802 or a methanol solution of 1 mM TAK-802, M-I, M-II or M-IV was added to the incubation mixture with a 1 % volume of the reaction mixture, consisting of human or animal liver microsomes (0.2 or 1.0 mg protein/mL) or cytosol (0.5 mg protein/mL) and an NADPH-generating system with a final concentration of 5 mM glucose-6-phosphate, 0.5 mM β -NADP⁺, 1.5 unit/mL glucose-6-phosphate dehydrogenase and 5 mM MgCl₂ in 50 mM potassium phosphate buffer (KPB) (pH 7.4). The reaction was initiated by the NADPH-generating system and was conducted at 37°C for 1 hour (microsomes) and 1.5 hours (cytosol). The final concentration of the substrate was 1 μ M ([¹⁴C]TAK-802) and 10 μ M (TAK-802, M-I, M-II or M-IV). All incubations were made in duplicate.

LC-MS/MS Analysis of TAK-802 and its metabolites in human samples

A six fold volume of ethyl acetate was added to the pooled human plasma samples. These mixtures were shaken for 10 minutes and centrifuged at approximately 1,500 \times g for 10 minutes. The ethyl acetate layers were separated from the aqueous layers. Methanol was added to the aqueous layers and these solutions were mixed well and centrifuged at approximately 1,500 \times g for 10 minutes. The ethyl acetate extracts and the methanol extracts were concentrated to dryness separately under a stream of nitrogen gas. Each residue was dissolved in a mixture of acetonitrile and 10 mM ammonium acetate (25:75, v/v). Each solution was centrifuged at approximately 9,500 \times g for 5 minutes and the supernatants were injected into the LC-MS/MS system. The pooled urine sample was centrifuged at approximately 9,500 \times g for 5 minutes and the supernatant was injected into the LC-MS/MS

system. LC-MS/MS analysis was conducted with a 2690 HPLC system (Waters, Milford, MA) coupled to an API3000 (Applied Biosystems, Foster City, CA) equipped with an electrospray source in positive detection mode. The column, a Develosil ODS-SR-5 (150 × 2.0 mm i.d., 5- μ m, Nomura Chemical Co., Ltd., Seto, Japan) was used at 40°C. Ten mM ammonium acetate and acetonitrile were used as the mobile phase (A) [MP (A)] and (B) [MP (B)], respectively and the flow rate was 0.2 mL/min. The time program for the gradient elution was as follows: The concentration of MP(B) was started at 5 v/v% for 5 minutes, increased linearly from 5 to 80% (B) over a period of 35 minutes, held at 80% (B) for 5 minutes, and then cycled back to the initial condition [5% (B)].

Quantitation for TAK-802 and M-IV in human plasma by LC-MS/MS

The amounts of TAK-802 and M-IV in human plasma were roughly estimated by the following procedure. An equivalent volume of 50 mM KPB (pH 7) containing TAK-802-*d*₄ was added to the individual or pooled human plasma sample. These mixtures were extracted with a six-fold volume of diethyl ether against the plasma. The diethyl ether extracts were dried under a stream of nitrogen gas. Each of the residues was dissolved in a mixture of acetonitrile and 10 mM ammonium acetate (25:75, v/v) by ultrasonication and mixing. After each solution was filtered and centrifuged, the aliquot of each filtrate was injected into the LC-MS/MS system. LC-MS/MS analysis was conducted with a 2690 HPLC system coupled to an API3000. The column, XTerra RP18 (150 × 2.0 mm i.d., 5- μ m, Waters) was used at 40°C. A mixture of acetonitrile and 10 mM ammonium acetate (65:35, v/v) was used as the mobile phase and the flow rate was 0.2 mL/min. All spectra were obtained in the positive ion mode. The monitoring ions of TAK-802, M-IV and TAK-802-*d*₄ were *m/z* 421→109, *m/z* 423→405 and *m/z* 425→111, respectively. In advance of the quantitation study of TAK-802 and M-IV in human plasma, the linearity of the analytes (0.1–50 ng/mL), the recovery from the human plasma, and the precision and accuracy of the analytical method by LC-MS/MS were confirmed to ensure the reliability for the determination of TAK-802 and M-IV.

Pharmacokinetic analysis

The pharmacokinetic parameters (T_{\max} , C_{\max} , $t_{1/2}$ and AUC_{0-48h}) of TAK-802 and M-IV were calculated using WinNonlin 6.3 (Pharsight Corporation, Mountain View, CA).

Identification of the CYP isoforms involved in the metabolism from [¹⁴C]TAK-802 to M-I and from M-IV to M-II

To identify the CYP isoforms involved in the metabolism from [¹⁴C]TAK-802 to M-I and from M-IV to M-II, a CYP metabolic study using 100 pmol P450/mL CYP-expressing microsomes and a correlation study using 0.2 mg protein/mL individual liver microsomes from 16 humans provided as the Reaction Phenotyping Kit (Version 5.0 and 6.0) were

performed. The correlation analysis was carried out using the least-square method with SAS System (SAS Institute) and $p < 0.01$ or $p < 0.05$ was considered statistically significant. The biochemical activity data for the specific CYP enzymes provided with the kit were used for the correlation analysis. The DMSO solution of 0.1 mM [^{14}C]TAK-802 or the methanol solution of 1 mM M-IV was added to the incubation mixture with a 1% volume of the reaction mixture, consisting of the respective microsomal protein, and an NADPH-generating system as described above in 50 mM KPB (pH 7.4) or Tris-HCl buffer (pH 7.4). The incubation was conducted at 37°C for 1 hour (the [^{14}C]TAK-802 incubation) or 30 minutes (the M-IV incubation). The final concentration of the substrate was 1 μM for the [^{14}C]TAK-802 incubation or 10 μM for the M-IV incubation. All incubations were made in duplicate. In advance of the study of reaction phenotyping in the metabolism of M-IV, the linearity, the recovery from the reaction mixture, the precision, the accuracy, and the stability of the analytical method by HPLC were confirmed to ensure the reliability for the determination of M-I, M-II, and M-IV.

Effect of glycyrrhetic acid on metabolism of [^{14}C]TAK-802 with human liver microsomes or 11 β -HSD1-expressing microsomes

A methanol solution of 1 mM [^{14}C]TAK-802 was added to the incubation mixture, consisting of 0.2 mg protein/mL human liver microsomes, hHSD1- or rHSD1-expressing microsomes, with an NADPH-generating system as described above and with/without glycyrrhetic acid in 50 mM KPB (pH 7.4). Glycyrrhetic acid was dissolved in methanol and its final concentrations were 0, 0.003, 0.01, 0.03, 0.1, 0.3, 1 and 10 μM . The incubation was conducted at 37°C for 30 minutes. The final concentration of [^{14}C]TAK-802 was 10 μM . All incubations were made in duplicate.

Analytical procedures for the incubation mixture of [^{14}C]TAK-802, TAK-802, or its metabolites

The incubation procedures described above were terminated by the addition of a five-fold volume of methanol or acetonitrile. After centrifugation at approximately 1,500 $\times g$ for 10 minutes, the supernatants were evaporated under a nitrogen gas stream and the residues were dissolved in the mobile phase with initial flow composition. The re-dissolved supernatants were separated by an HPLC (LC-10 gradient system; Shimadzu Corp., Kyoto, Japan). The HPLC analytical method for [^{14}C]TAK-802 incubation was as follows: Separation of the metabolites was carried out on a YMC-Pack Pro C18 AS-302 (5- μm particle size, 150 \times 4.6 mm I.D.; YMC, Tokyo, Japan), with a gradient elution using 50 mM NaH_2PO_4 (pH 7.4) and acetonitrile. The acetonitrile concentration was increased from 10% to 50% over a period of 50 minutes and held at 50% for 10 minutes and then cycled back to the initial condition (10%). The HPLC analytical method for the incubation of TAK-802, M-I, M-II or M-IV and the inhibition study of glycyrrhetic acid was as follows: Separation of the metabolites

was carried out on a CAPCELL PAK C₁₈ UG120, (5- μ m particle size, 250 \times 4.6 mm I.D.; SHISEIDO Co., LTD, Tokyo, Japan), with a gradient elution using 10 mM ammonium acetate and acetonitrile. The acetonitrile concentration was increased from 10% to 62% over a period of 30 minutes, jumped up to 90% and held at 90% for 10 minutes and then cycled back to the initial condition (10%). Throughout the elution, the column temperature and the flow-rate were 40°C and 1.0 mL/min, respectively. The column effluent was collected for each 0.5 minutes into scintillation-counting vials, and the radioactivity was measured by a liquid scintillation counter (LSC-5100, Aloka Co., Ltd., Tokyo, Japan). The formation amounts of TAK-802, M-I, M-II and M-IV were measured at UV280 nm. For the inhibition study with glycyrrhetic acid, the incubation mixture of [¹⁴C]TAK-802 was terminated by the addition of acetonitrile equivalent to the reaction volume. After centrifugation at approximately 1,500 \times g for 10 minutes, the supernatant was analyzed with an on-line RI detector (D505TR Flow Scintillation Analyzer, Packard Instrument Company, Meriden, CT) using Ultima-Flo as the flow scintillation cocktail.

Results

Metabolic profiles of [¹⁴C]TAK-802 with liver microsomes from humans and animals

The *in vitro* metabolism of [¹⁴C]TAK-802 with liver microsomes from rats, dogs, monkeys and humans was investigated. [¹⁴C]TAK-802 was metabolized to M-I, M-II, M-III, M-IV and other unidentified metabolites (others) by the liver microsomes (Table I-1). In case of human liver microsomes, TAK-802 was mainly biotransformed to M-I and M-IV. The amount of M-IV formation was the largest in humans followed by monkeys, dogs and rats in the same reactive condition. The composition ratio of each unidentified metabolite in others was less than 2% in human liver microsomes.

Table I-1. *In vitro* metabolic profiles of [¹⁴C]TAK-802 with liver microsomes from humans and animals

Species	Composition ratio of TAK-802 and its metabolites (%)					
	TAK-802	M-I	M-II	M-III	M-IV	Others
Human	47.5	14.2	4.1	2.4	17.3	14.5
Rat	31.4	5.3	0.4	7.1	0.2	55.6
Dog	31.2	2.0	0.1	6.5	0.3	59.9
Monkey	36.7	17.3	1.1	10.0	2.7	32.2

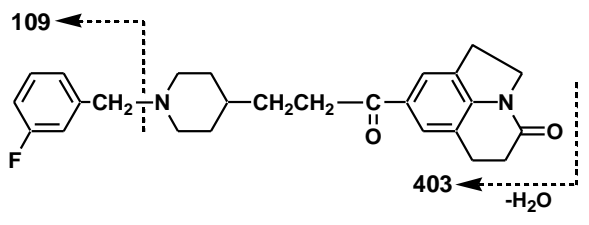
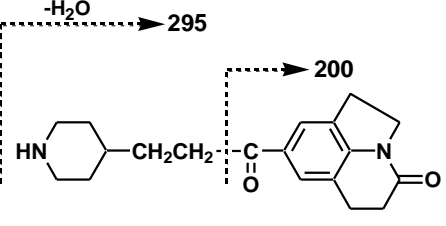
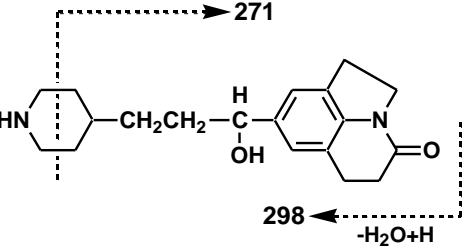
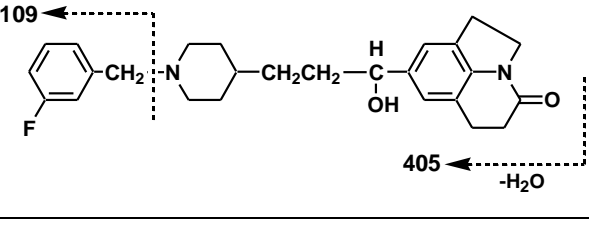
The composition ratio represents the ratio of TAK-802 and its metabolites in the presence of an NADPH-generating system, when the total radioactivity in the incubation mixture is regarded as 100%. The composition ratio of others was calculated by subtracting the sum of TAK-802 and its metabolites from 100%. Data represent the means of duplicate determinations.

Metabolite characterization in human plasma and urine by mass spectrometry

The plasma and urine samples from Japanese healthy male volunteers given a single oral dose of TAK-802 were analyzed by the full ion scan mode of the LC-MS/MS. In each full ion mass chromatogram of the ethyl acetate extracts from the plasma samples, unchanged TAK-802 and M-IV were observed. In the full ion mass chromatograms of the urine samples, unchanged TAK-802, M-I, M-II, and M-IV were detected at the retention times of about 33, 17, 14, and 27 minutes, respectively. These peaks of unchanged TAK-802, M-I, M-II, and M-IV correspond to the protonated molecules ([M+H]⁺) at *m/z* 421, 313, 315, and 423, respectively. The fragmentation profile of the precursor ions at *m/z* 421, 313, 315, and 423 is shown in Table I-2. These mass spectra and the retention times were in agreement with those of unchanged TAK-802, M-I, M-II, and M-IV standard samples. Other unknown metabolites and the conjugated metabolites were not detected by LC-MS/MS analysis of either these ethyl acetate extracts or methanolic extracts of the plasma samples and the urine

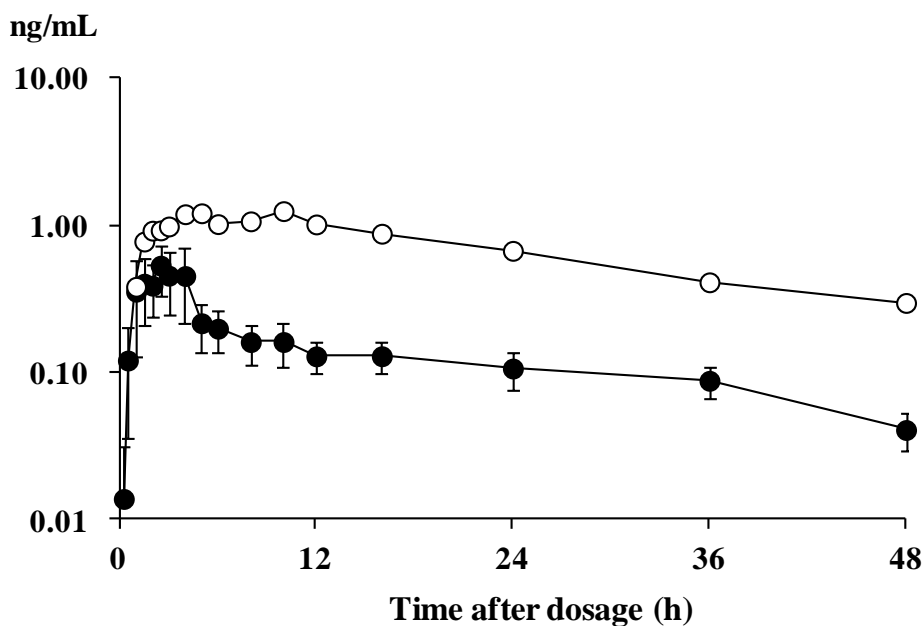
samples.

Table I-2. Fragmentation profile of the precursor ions of TAK-802 and its metabolites in mass spectrometry analysis

Compound	Structure	Precursor ion (m/z)	Product ion (m/z)
TAK-802		421	403 109
M-I		313	295 200
M-II		315	298 271
M-IV		423	405 109

Concentrations and pharmacokinetic parameters of TAK-802 and M-IV in plasma of healthy male Japanese volunteers after a single oral dose of TAK-802 at 0.5 mg

The maximum measured concentration of TAK-802 and M-IV in human plasma was 0.59 and 1.26 ng/mL (C_{max}) at 2.6 and 10.0 hours (T_{max}) after oral dosing with TAK-802, respectively (Figure I-1). The concentrations of TAK-802 and M-IV declined monophasically thereafter with an apparent half-life ($t_{1/2}$) of 21.3 and 19.9 hours, respectively. The AUC_{0-48h} value of M-IV (32.8 ng·h/mL) was approximately five-fold of that of TAK-802 (6.40 ng·h/mL). The concentrations of M-I and M-II were less than the lower limit of quantitation.



Analyte	Pharmacokinetic parameters			
	T _{max} (h)	C _{max} (ng/mL)	t _{1/2} (h)	AUC _{0-48h} (ng·h/mL)
TAK-802	2.6 ± 0.8	0.59 ± 0.24	21.3 ± 3.6	6.40 ± 1.85
M-IV	10.0	1.26	19.9	32.8

Figure I-1. Concentrations and pharmacokinetic parameters of TAK-802 and M-IV in plasma of healthy male Japanese volunteers after a single oral dose of TAK-802 at 0.5 mg. Symbols represent the mean plasma concentrations of TAK-802 (●) and the pooled plasma concentrations of M-IV (○) (n=9).

Identification of the CYP isoform involved in the metabolism of [¹⁴C]TAK-802

The CYP isoforms involved in the biotransformation of [¹⁴C]TAK-802 were identified by the metabolism of TAK-802 with microsomes expressing human CYP isoforms and by a correlation study using liver microsomes from 16 individual humans (Table I-3 and Figure I-2). As shown in Figure I-2, microsomes expressing CYP2C8, CYP2C19, CYP2D6, CYP2E1 and CYP3A4 metabolized [¹⁴C]TAK-802. Among the CYP-expressing microsomes, [¹⁴C]TAK-802 was extensively metabolized by microsomes expressing CYP2D6 and CYP3A4 and M-I was significantly formed by CYP3A4-expressing microsomes. A little formation of M-II was observed in CYP2E1- and CYP3A4-expressing microsomes and M-III formation was observed in CYP2D6- and CYP3A4-expressing microsomes. In the correlation study, the elimination rate of [¹⁴C]TAK-802 and the formation rate of M-I correlated with *S*-mephenytoin *N*-demethylation (CYP2B6) activity,

paclitaxel 6 α -hydroxylase (CYP2C8) activity, and testosterone 6 β -hydroxylase (CYP3A4/5) activity. The formation rate of M-II also correlated with CYP2B6 activity and CYP3A4 activity. The correlation analysis for the formation rate of M-III was not conducted with its limited formation. The involvement of CYP2B6 was suggested in the metabolism of [¹⁴C]TAK-802 by the correlation analysis, but the possibility of CYP2B6 metabolism might be excluded due to the high internal correlation between CYP2B6 and CYP3A4 ($r=0.736$, $p<0.01$) in this panel of individual microsomes and little metabolism observed with the CYP2B6-expressing microsomes. In addition, the metabolism of the CYP2C8-expressing microsomes was considered small compared to that of the CYP3A4-expressing microsomes. The contribution of CYP2D6 was also considered to be insignificant compared to that of CYP3A4, since CYP2D6 did not show any correlation in the correlation analysis for human liver microsomes. Moreover, most of [¹⁴C]TAK-802 eliminated by CYP2D6-expressing microsomes could account for M-III and an unidentified metabolite, and their formation amounts were much smaller than those of other metabolites in human liver microsomes. Thus, it was concluded that the oxidative metabolism of TAK-802 and M-I formation were mainly catalyzed by CYP3A4. Although the M-II formation rate correlated with CYP3A4/5 activity in human liver microsomes, it is difficult to elucidate whether CYP3A4 is responsible for M-II formation with little formation of M-II observed in CYP3A4-expressing microsomes. No M-IV formation was observed in any CYP-expressing microsomes and the formation rate for M-IV was not correlated to the marker activities of any CYP isoforms in the correlation study, although M-IV was one of the major metabolites observed with human liver microsomes. This is reasonable because CYP enzymes do not function as carbonyl reductases and exemplifies the involvement of non-CYP enzymes in the M-IV formation.

Table I-3. Correlation coefficients between the metabolism of [¹⁴C]TAK-802 and CYP isoform-specific activities in microsomes from 16 human livers

Isoform-specific activity	CYP enzymes	Correlation coefficient (<i>r</i>)			
		TAK-802 elimination	M-I formation	M-II formation	M-IV formation
7-Ethoxyresorufin <i>O</i> -dealkylation	CYP1A2	-0.076	-0.106	-0.035	0.097
<i>S</i> -Mephenytoin <i>N</i> -demethylation	CYP2B6	0.516 ^b	0.797 ^a	0.608 ^b	-0.551 ^b
Paclitaxel 6 α -hydroxylation	CYP2C8	0.545 ^b	0.570 ^b	0.413	-0.308
Diclofenac 4'-hydroxylation	CYP2C9	-0.009	0.295	0.033	-0.474
<i>S</i> -Mephenytoin 4'-hydroxylation	CYP2C19	0.155	0.334	0.323	-0.332
Dextromethorphan <i>O</i> -demethylation	CYP2D6	0.093	0.181	-0.031	-0.288
Chlorzoxazone 6-hydroxylation	CYP2E1	0.115	-0.108	-0.225	0.072
Testosterone 6 β -hydroxylation	CYP3A4/5	0.732 ^a	0.960 ^a	0.940 ^a	-0.517 ^b
Lauric acid 12-hydroxylation	CYP4A9/11	0.138	-0.017	0.063	0.293

^a $p < 0.01$

^b $p < 0.05$

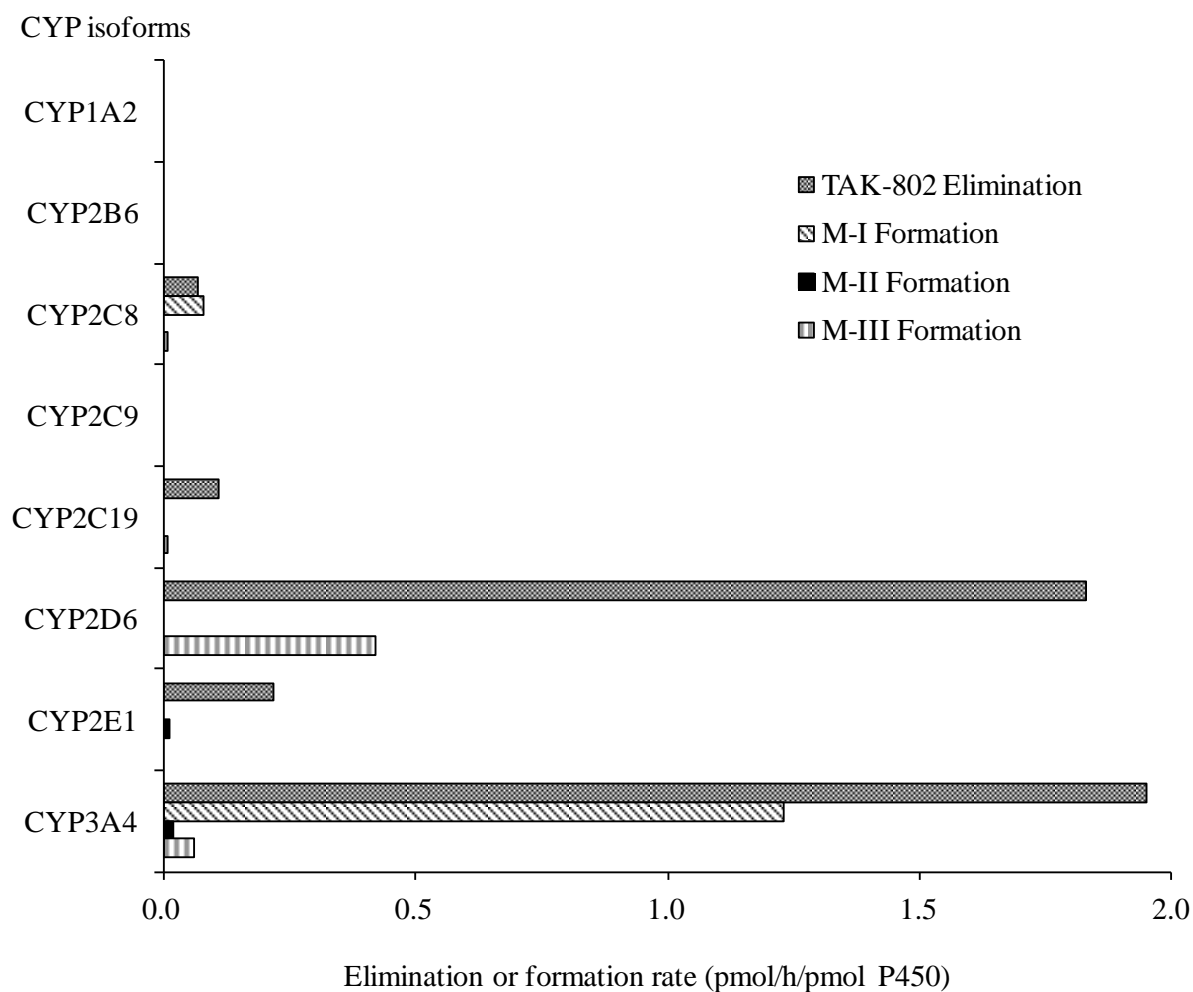


Figure I-2. *In vitro* metabolism of [¹⁴C]TAK-802 with human CYP-expressing microsomes. Data represent the means of duplicate determinations.

Comparison of the metabolic profiles of TAK-802 with human liver microsomes and cytosol

In vitro metabolism of TAK-802 with human liver microsomes and cytosol were investigated (Figure I-3). In human liver cytosol, limited M-IV formation was observed, and the formation of M-IV and elimination of TAK-802 were smaller compared with those by the human liver microsomes even in the reactive condition with more protein and longer incubation time.

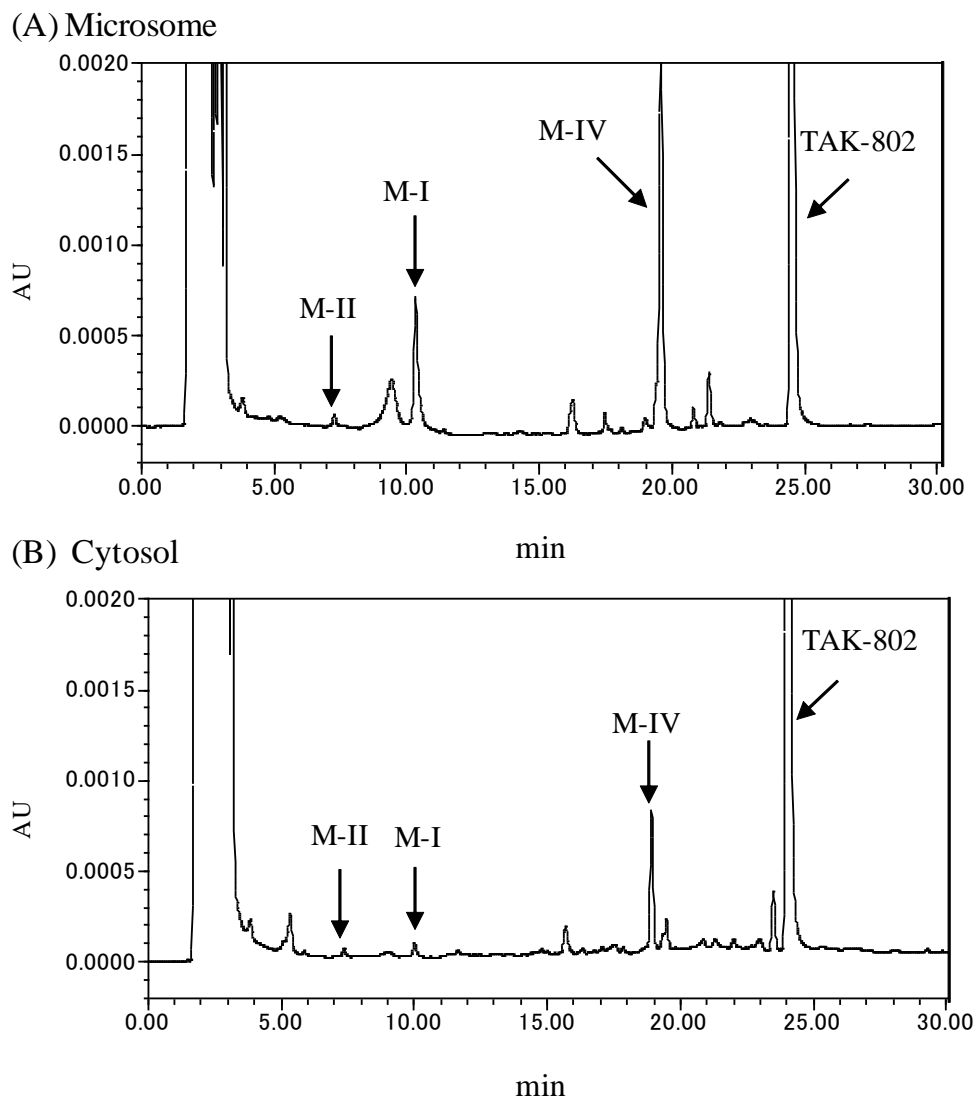


Figure I-3. Representative HPLC-UV chromatograms of the incubation mixture of TAK-802 with human liver microsomes or cytosol

TAK-802 (10 μ M) was incubated with human liver microsomes (A, 0.2 mg protein/mL) or cytosol (B, 0.5 mg protein/mL) in the presence of an NADPH-generating system at 37°C for 1 hour (A) and 1.5 hours (B).

The inhibitory effect of glycyrrhetic acid on the *in vitro* reductive metabolism of [14 C]TAK-802

[14 C]TAK-802 was metabolized to M-IV by human liver microsomes or 11 β -HSD1-expressing microsomes in the presence of NADPH (Table I-4 and Figure I-3). M-IV formation in rHSD1-expressing microsomes was limited and much less than that in hHSD1-expressing microsomes. M-IV formation was concentration-dependently inhibited by nanomolar concentrations of glycyrrhetic acid, a short-chain dehydrogenase inhibitor [28], in human liver microsomes and hHSD1-expressing microsomes (Figure I-4).

Table I-4. *In vitro* metabolism of [¹⁴C]TAK-802 by 11 β -HSD1-expressing microsomes

11 β -HSD- expressing microsomes	Elimination rate (pmol/min/mg protein)	Formation rate (pmol/min/mg protein)		
	TAK-802	M-I	M-II	M-IV
hHSD1	1231	0	0	1243
rHSD1	34	< 1	< 1	27

[¹⁴C]TAK-802 (10 μ M) was incubated with 11 β -HSD1-expressing microsomes (0.2 mg protein/mL) in the presence of an NADPH-generating system at 37°C for 30 minutes. Data represent the means of duplicate determinations.

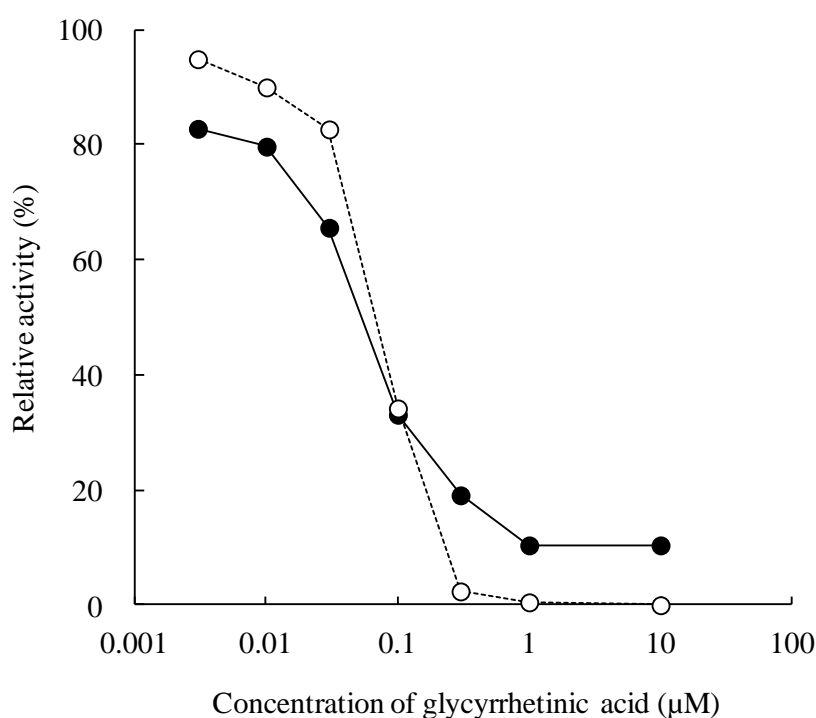


Figure I-4. Effects of glycyrrhetic acid on *in vitro* formation of M-IV from [¹⁴C]TAK-802 in human liver and 11 β -HSD1-expressing microsomes

Relative activities represent the percentage (%) of the M-IV formation rate at each concentration of glycyrrhetic acid when the M-IV formation rate in the absence of glycyrrhetic acid was regarded as 100%. Symbols represent the means of duplicate samples in human liver microsomes (●) and 11 β -HSD1-expressing microsomes (○).

Metabolic profiles of M-I, M-II or M-IV with human liver microsomes

In vitro metabolism of M-I, M-II or M-IV with human liver microsomes was investigated. Consequently, M-II was formed from M-IV and neither M-II formation from M-I, TAK-802

formation from M-IV nor M-I formation from M-II was observed (Figure I-5).

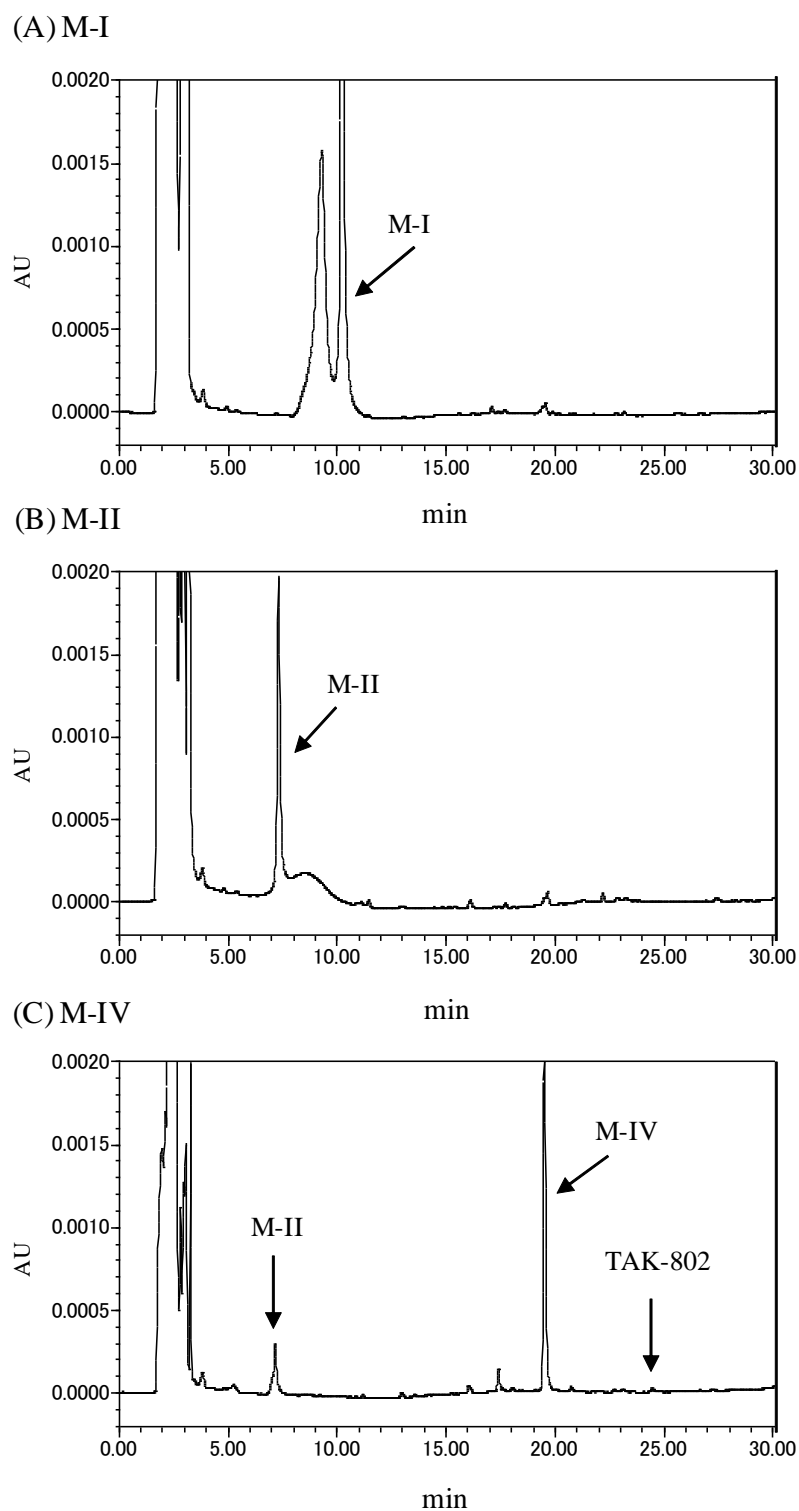


Figure I-5. Representative HPLC-UV chromatograms of the incubation mixture of M-I, M-II or M-IV with human liver microsomes
(A) M-I, (B) M-II or (C) M-IV (10 μ M) was incubated with human liver microsomes (0.2 mg protein/mL) in the presence of an NADPH-generating system at 37°C for 1 hour.

Identification of the CYP isoform involved in the metabolism of M-IV

In the study of CYP reaction phenotyping, M-IV was mainly metabolized to M-II (Table I-5). M-I was not detected as a metabolite of M-IV. The elimination rate of M-IV and the formation rate of M-II most strongly correlated with CYP3A4/5 activity, and also correlated with CYP2B6 and CYP2C8 activities. Within the panel of microsomes, CYP3A4/5 activity correlated with CYP2B6 ($r=0.788$, $p<0.01$) and CYP2C8 ($r=0.617$, $p<0.05$) activities. The correlation of CYP3A4/5 activity with CYP2B6 and CYP2C8 activities affected the correlation of CYP2B6 and CYP2C8 activities with elimination of M-IV and formation of M-II. In the study of CYP-expressing microsomes, M-IV was metabolized to M-II (Figure I-6). The elimination rate of M-IV was the highest with CYP3A4 followed by CYP2D6 and the other CYP isoforms. M-II was mainly formed by CYP3A4-expressing microsomes and the M-II formation by other CYP isoforms was minor.

Table I-5. Correlation coefficients between the metabolism of M-IV and CYP isoform-specific activities in microsomes from 16 human livers

Isoform-specific activity	CYP enzymes	Correlation coefficient (r)	
		M-IV elimination	M-II formation
7-Ethoxyresorufin <i>O</i> -dealkylation	CYP1A2	0.045	0.180
<i>S</i> -Mephenytoin <i>N</i> -demethylation	CYP2B6	0.747 ^a	0.767 ^a
Paclitaxel 6 α -hydroxylation	CYP2C8	0.614 ^b	0.550 ^b
Diclofenac 4'-hydroxylation	CYP2C9	0.230	0.208
<i>S</i> -Mephenytoin 4'-hydroxylation	CYP2C19	0.460	0.557 ^b
Dextromethorphan <i>O</i> -demethylation	CYP2D6	-0.189	-0.241
Chlorzoxazone 6-hydroxylation	CYP2E1	-0.287	-0.313
Testosterone 6 β -hydroxylation	CYP3A4/5	0.988 ^a	0.940 ^a
Lauric acid 12-hydroxylation	CYP4A9/11	0.145	0.237

^a $p<0.01$

^b $p<0.05$

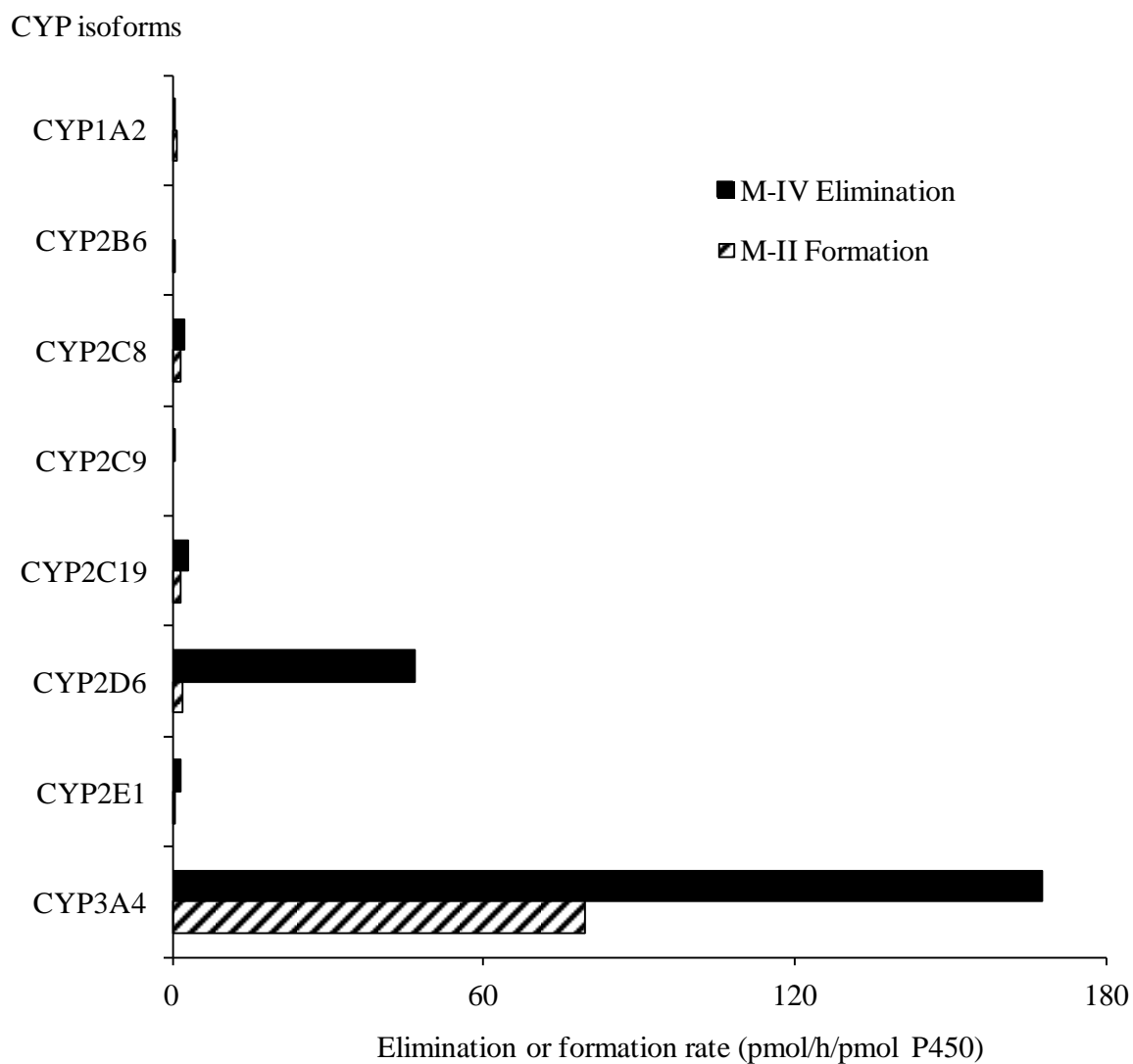


Figure I-6. *In vitro* metabolism of M-IV with human CYP-expressing microsomes
Data represent the means of duplicate determinations.

Discussion

In vitro metabolism studies of [¹⁴C]TAK-802 showed that TAK-802 was mainly metabolized to M-I, M-II, M-III, and M-IV in human liver microsomes (Table I-1). Especially, the composition ratio of M-IV in human liver microsomes was larger than those in animals in the same reactive conditions. *In vivo* animal pharmacokinetic studies of [¹⁴C]TAK-802 showed that the formation of M-I, M-II and M-III was confirmed [19]. However, M-IV was not considered due to the lower level as an important metabolite in rat, dog and monkey plasma and excreta. On the other hand, M-IV was the main metabolite detected in plasma of humans orally administered with TAK-802 and the concentrations of M-I and M-II were less than lower limit of quantitation. The AUC_{0-48h} value of M-IV was estimated to be approximately five-fold higher than that of TAK-802 in human plasma (Figure I-1). In addition, M-I, M-II and M-IV were detected in human urine. These results indicate that *in vitro* metabolic profile reflects the *in vivo* condition in humans and animals and the formation of M-IV was relatively specific to humans. Thus, to explain the species differences in the metabolic profiles between humans and animals, the enzyme responsible for forming M-IV was identified and the metabolic pathway from TAK-802 to its metabolites in humans was elucidated *in vitro*. Considering its chemical structures, M-IV was presumed as a reductive metabolite, indicating the involvement of non-CYP enzymes in the metabolism of TAK-802. This was confirmed by a study using microsomes expressing 8 human CYP isoforms and a correlation study using 16 individual human liver microsomes (Table I-3 and Figure I-2). No M-IV formation was observed in any CYP-expressing microsomes and the formation rate for M-IV did not correlate to the marker activities of any CYP isoforms in the correlation study despite its being the major metabolite observed in human liver microsomes. These CYP identification studies also showed that the oxidative metabolism of TAK-802 and M-I formation from TAK-802 were mainly catalyzed by CYP3A4.

In general, many reductive enzymes are located in the cytosol and the formation of M-IV in human liver cytosol was observed, indicating the involvement of some carbonyl reductase located in human cytosol. However, the formation amounts of M-IV were limited and smaller even in the reactive condition with a greater amount of protein and longer incubation time, compared with the formation by human liver microsomes (Figure I-3). In addition, M-IV was not formed at all in the liver microsomes and cytosol without NADPH (data not shown). Thus, the enzyme systems involved in TAK-802 reduction were mainly microsomal and NADPH-dependent. Among the reductive enzymes, the major CR located in human microsomes is only the SDR superfamily [22,25]. NADPH-dependent SDRs have been reported to be located not only in the microsomes, but also in the mitochondrial fractions of mouse, guinea pig, and pig lung [23,29] and this mitochondrial enzyme is known as tetrameric lung carbonyl reductase [30,31]. However, to our knowledge, no SDR of the human liver mitochondrial fraction has ever been identified and the possibility of its involvement in TAK-802 reduction was excluded in this study. Among the microsomal

SDRs, 11 β -HSD was first focused as the responsible enzyme, since 11 β -HSD1 is currently the only known microsomal carbonyl reductase of the SDRs [27]. 11 β -HSD1 is responsible for the interconversion of the active glucocorticoid, cortisol, from its hormonally inactive 11-keto metabolite, cortisone and 11 β -HSD2 acts exclusively as dehydrogenase and catalyzes the reverse reaction [26]. To examine whether M-IV formation is catalyzed by human 11 β -HSD1, TAK-802 was incubated with 11 β -HSD1-expressing microsomes in the presence of NADPH. Consequently, M-IV was formed by the incubation of TAK-802 with human 11 β -HSD1-expressing microsomes (Table I-4). Moreover, M-IV formation from TAK-802 in human liver and HSD1-expressing microsomes was concentration-dependently (in nanomolar concentrations) inhibited by glycyrrhetic acid, an inhibitor for 11 β -HSD (Figure I-4). These results indicate that M-IV is principally formed by human 11 β -HSD1. In addition, the formation of M-IV was limited in rat 11 β -HSD1-expressing microsomes and the amount of its formation was less than that in human 11 β -HSD1-expressing microsomes, which coincides with the *in vivo* and *in vitro* metabolic profile of TAK-802 in rats and indicates that the species difference is due to the involvement of 11 β -HSD1. The species difference of 11 β -HSD1 has already been investigated using cortisone, 11-dehydrocorticosterone and 7-ketocholesterol and huge variability was found in different species [32]. Compared with human 11 β -HSD1 for cortisone and 11-dehydrocorticosterone by kinetic analysis, rat and dog 11 β -HSD1 displayed higher K_m values in common, which would account for the difference of M-IV formation amount observed between human, rat and dog liver microsomes. In addition, human 11 β -HSD1 reduced triadimefon to triadimenol and bupropion to threohydrobupropion in a more efficient way than the rat and mouse enzymes [33,34]. Thus, the species difference of metabolic profile between humans and animals is presumed to be due to the substrate affinity of 11 β -HSD1 to TAK-802. This information is valuable in the development of new chemical entities (NCEs), since there are few reports in which the species-specific variability of 11 β -HSD1 is confirmed in both *in vivo* and *in vitro* metabolic profiles.

Considering the formation of M-II, two metabolic pathways could be postulated: One is via the reduction of M-I and the other is via the elimination of the fluorobenzyl group of M-IV. To examine which metabolic pathway is involved in the formation of M-II, formation of M-II was confirmed by the incubation of M-I, M-II or M-IV with human liver microsomes in the presence of NADPH (Figure I-5). The representative UV-chromatograms showed that M-II was formed only from M-IV, and neither M-II formation from M-I, TAK-802 formation from M-IV nor M-I formation from M-II was observed by the incubation with human liver microsomes in the presence of NADPH. Moreover, although little M-II formation from M-I was observed in both liver microsomes and cytosol from animals, M-II formation from M-IV in the liver microsomes was observed in rats and monkeys as well as in humans (data not shown). Thus, M-II observed in plasma and excreta of humans and animals was considered to be formed via the M-IV formation by 11 β -HSD1 or other reductive enzymes. These

results indicate that the fluorobenzyl group of TAK-802 is indispensable for the substrate specificity of the 11 β -HSD1 enzyme and the species difference related to the formation of M-II was due to the involvement of 11 β -HSD1 in the formation of M-IV. Further investigations were conducted to identify the CYP isoform responsible for M-IV metabolism as well as for TAK-802 metabolism (Table I-5 and Figure I-6). Consequently, M-II formation from M-IV was catalyzed by CYP3A4.

In conclusion, TAK-802 is principally metabolized to M-I by CYP3A4 and to M-IV by 11 β -HSD1 and M-IV is metabolized to M-II by CYP3A4 in humans (Figure I-7). Especially the involvement of 11 β -HSD1 in the metabolism of TAK-802 and the difference of its affinity to the fluorobenzyl group of TAK-802 is presumed to contribute to the species differences in the metabolic profiles between humans and animals. Hereafter, we should pay more attention to species-specific variability when the non-CYP enzymes such as 11 β -HSD are involved in the metabolism of NCEs. In addition, the present study may provide a better insight into the elucidation of the metabolic pathway in a complicated system in which both oxidation and reduction are involved in the metabolism.

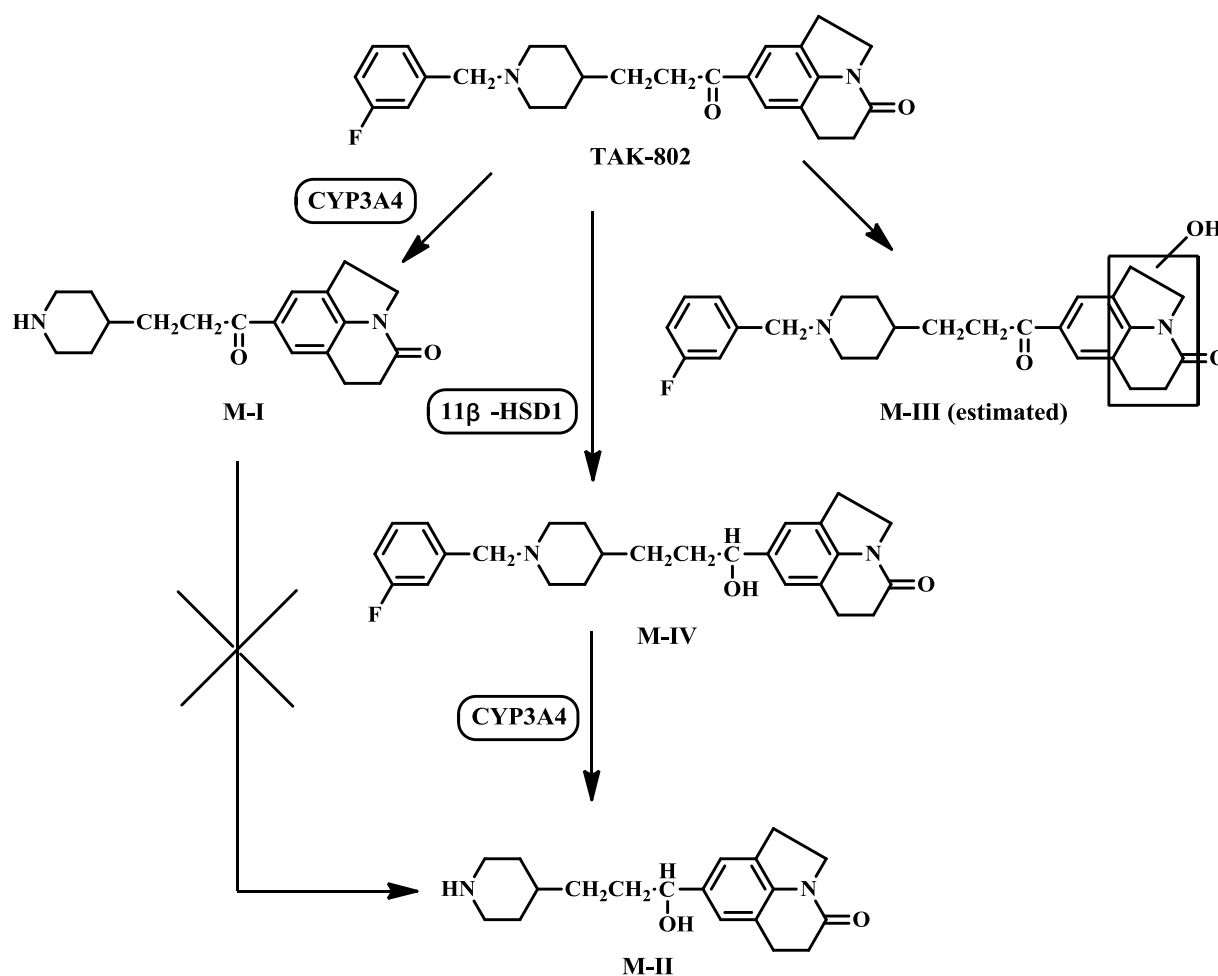


Figure I-7. Postulated metabolic pathways of TAK-802 in humans

Summary

To investigate species differences in the metabolism of TAK-802, a novel drug candidate for voiding dysfunction, *in vitro* and *in vivo* metabolic profiles were compared between humans and animals. TAK-802 was mainly metabolized to M-I, M-II, M-III and M-IV in human and animal liver microsomes. Especially the M-IV formation in humans was greater than that in animals. Likewise, M-IV was detected to a lower extent in the plasma and excreta of animals administered with TAK-802, whereas the AUC_{0-48h} of M-IV was approximately five-fold higher than that of TAK-802 in human plasma. These results indicate that the *in vitro* metabolic profile reflects the *in vivo* condition. Thus, to identify the metabolic pathway of TAK-802 in humans, the responsible enzyme to form M-IV was elucidated *in vitro*. Since M-IV is a reductive metabolite formed in microsomes, the possibility of involvement of 11 β -HSD1, a carbonyl reductase located in microsomes, was first investigated. Consequently, M-IV formation was confirmed by incubation with human 11 β -HSD1-expressing microsomes and was concentration-dependently inhibited by glycyrrhetic acid, an inhibitor for 11 β -HSD enzymes, indicating the involvement of 11 β -HSD1 in the M-IV formation. In contrast, little M-IV formation was observed using rat 11 β -HSD1, suggesting species differences between humans and rats. In addition, M-II was formed via M-IV, not via M-I and the CYP identification studies revealed that both M-I formation from TAK-802 and M-II formation from M-IV were mainly catalyzed by CYP3A4. In conclusion, 11 β -HSD1 and CYP3A4 are principally responsible for the metabolism of TAK-802 in humans and 11 β -HSD1 may be responsible for the observed species difference.

CHAPTER II

Metabolic Fate of Sipoglitazar, a Novel Oral PPAR Agonist with Activities for PPAR- γ , - α and - δ , in Rats and Monkeys and Comparison with Humans *In Vitro*

Introduction

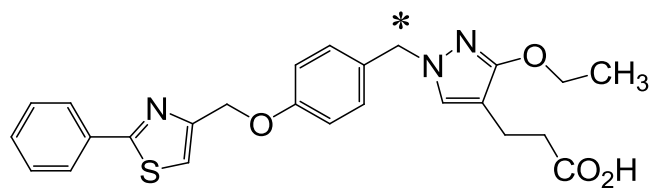
The peroxisome proliferator-activated receptors (PPARs) are members of the nuclear receptor superfamily of ligand-activated transcription factors. Three PPAR subtypes have been identified so far, dubbed PPAR- α , PPAR- γ , and PPAR- δ (also called PPAR- β) [35]. PPAR- α receptors are expressed primarily in the liver, play a critical role in lipid metabolism and are the target of the fibrate class of hypolipidemic drugs such as fenofibrate [36,37] and gemfibrozil [38]. PPAR- γ receptors play a key role in energy storage, glucose homeostasis, and vascular biology [39]. Thiazolidinediones (TZDs) such as pioglitazone and rosiglitazone are known as typical agents to activate these receptors [40,41]. TZDs work via activation of PPAR- γ and activation of this receptor leads to increased insulin sensitivity in the liver, fat, and skeletal muscle cells. Although much less is known about the function of PPAR- δ , its activation exerts beneficial effects on lipoprotein and glucose metabolism [42]. Sipoglitazar (TAK-654) was attempted to be developed as a novel anti-diabetic agent with triple agonistic activities on human PPAR- γ , PPAR- α , and PPAR- δ (Figure II-1). Here I investigate the absorption, distribution, metabolism and excretion (ADME) profile of sipoglitazar in rats and monkeys. Animal studies using [^{14}C]sipoglitazar are essential to understand the fate of new drugs and these ADME data are helpful to understand the pharmacological properties of sipoglitazar, an activator for PPARs. Furthermore, to predict the metabolic profile and main excretion route from the body in humans, the *in vitro* metabolism of sipoglitazar was examined using human and animal hepatocytes and compared for their relationship *in vivo* and *in vitro*. These studies contribute to minimize negative effects from these species differences, which often have been a bottleneck problem in the development of new drugs. Sipoglitazar is a typical example to evaluate the non-clinical ADME properties before clinical studies, taking into account both the *in vivo* animal data and *in vitro* human data.

Materials and Methods

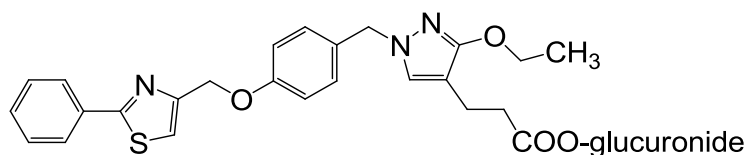
Chemicals

Sipoglitazar and its metabolites (M-I, 3-(3-hydroxy-1-{4-[(2-phenyl-1,3-thiazol-4-yl)methoxy]benzyl}-1*H*-pyrazol-4-yl)propanoic acid and M-II, 3-[3-ethoxy-1-(4-

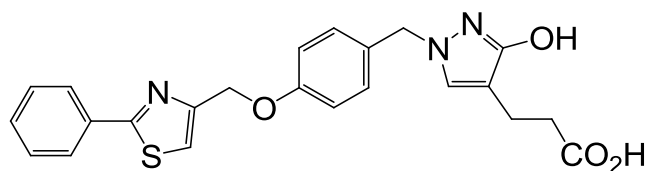
hydroxybenzyl)-1*H*-pyrazol-4-yl]propanoic acid) were prepared by Takeda Pharmaceutical Company Limited (Osaka, Japan) (Figure II-1). [¹⁴C]sipoglitazar with a specific radioactivity of 4.58 MBq/mg was synthesized by Amersham Pharmacia Biotech UK Ltd. (Buckinghamshire, UK). The radiopurity (>98 %) and chemical identity of the labeled compound were verified by thin-layer chromatography (TLC) and HPLC. All other reagents and chemicals were of the highest quality obtained from commercial suppliers such as Sigma-Aldrich (St. Louis, MO), ICN Pharmaceuticals, Inc. (Costa Mesa, CA), ULTRAFINE Chemicals (Manchester, UK), Oriental Yeast Co., Ltd. (Osaka, Japan), Dojindo (Kumamoto, Japan) and Wako Pure Chemical Industries, Ltd. (Osaka, Japan).



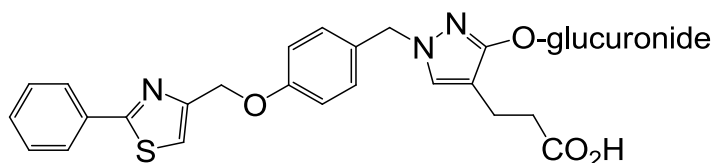
[¹⁴C]sipoglitazar



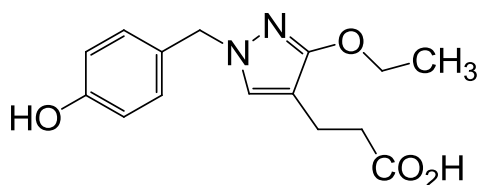
Sipoglitazar-G (presumed)



M-I



M-I-G (presumed)



M-II

Figure II-1. Chemical structures of [¹⁴C]sipoglitazar, M-I, M-II, sipoglitazar-G and M-I-G.

* : Radiolabeled position

Administration of [¹⁴C]sipoglitazar and collection of biological samples in rats and monkeys

A series of experiments were conducted to investigate the absorption, distribution, metabolism, and excretion of [¹⁴C]sipoglitazar after single and multiple oral administrations to rats and monkeys. These studies were conducted according to protocols approved by Experimental Animal Ethical Committee at Takeda Pharmaceutical Company Limited (Osaka,

Japan) and Nemoto Science Co., Ltd. (Ibaraki, Japan). The animals used in this study were male Crj:CD(SD)IGS rats (weight, 266 to 349 g; Charles River Japan Inc., Yokohama, Japan) and male cynomolgus monkeys (weight, 2.60 to 3.64 kg; Kearsy Co., Ltd., Osaka, Japan). They were fed laboratory chow (CR-LPF; Oriental Yeast Co., Ltd., Tokyo, Japan for the rats, and Monkey Bit, Nosan Corporation, Yokohama, Japan, or Primate Chow #5048, Purina Mills, Inc., St. Louis, MO for the monkeys), had free access to water, and were housed in temperature- and humidity-controlled rooms (20 to 26°C and 40 to 70%) with 12-hour light-dark cycles for more than one week before use. The applied dose was determined by considering the pharmacological dose and the detection limit of the radioactivity. [¹⁴C]sipoglitazar, diluted appropriately with unlabeled compound, was suspended in a 0.5% (w/v) methylcellulose solution for oral (PO) or intraduodenal (ID) administration at a dose of 0.5 mg/10 mL/kg to the rats or 0.5 mg/2 mL/kg to the monkeys. [¹⁴C]sipoglitazar was dissolved in a mixture of dimethyl acetamide and physiological saline (1:1, by volume) for intravenous (IV) injection at a dose of 0.5 mg/mL/kg to the rats or 0.5 mg/0.2 mL/kg to the monkeys. The vehicle used for IV injection, dimethyl acetamide has been reported to cause some toxicity in animals and humans, but there were no harmful effects in this study [43]. The formulated sipoglitazar was administered to fed animals. After dosing, blood was taken from the tail vein or abdominal aorta at appropriate times in the rats or from the femoral vein in the monkeys. Urine and feces were collected in metabolic cages equipped with separators for urine and feces. Radioactive carbon dioxide in the expired air of the rats was absorbed in a mixture of methylcellosolve and monoethanolamine (2:1, by volume). Bile samples from the rats were obtained after cannulation of the common bile duct. In the enterohepatic circulation study, the collected bile was injected into the duodenum of other biliary-cannulated rats (10 mL/kg). After determination of the radioactivity, the samples were kept frozen at -20°C until analysis.

Tissue distribution of [¹⁴C]sipoglitazar in rats

To determine ¹⁴C concentrations in the rat tissues, the following tissues were excised after a single oral dose of [¹⁴C]sipoglitazar and after a once daily oral dose of [¹⁴C]sipoglitazar for 21 days: blood, brain, spinal cord, hypophysis, eyes, Harderian glands, submaxillary glands, thyroid gland, thymus, heart, lungs, liver, spleen, pancreas, adrenals, kidneys, testes, skeletal muscle, skin, fat, brown fat, bone marrow, stomach and intestine.

Identification and quantification of the metabolites in the biological samples from the rats and monkeys

[¹⁴C]sipoglitazar and its metabolites in plasma, urine, feces, bile and tissues were quantified by TLC as follows. Plasma or aqueous homogenates of the feces were extracted with acetonitrile (5 vol.) and then the extracts were evaporated to dryness under a nitrogen gas stream at room temperature. The residues were dissolved in methanol. Then the solutions

were subjected to TLC using plates precoated with silica gel 60F₂₅₄ (0.25-mm thick; E. Merck, Darmstadt, Germany), which were developed in dichloromethane-methanol (85:15, by vol.). The urine and bile samples were diluted with acetonitrile and put on TLC plates, which were then developed under the same conditions as described above. The component in the rat fat was also examined by alkaline hydrolysis and the same TLC analysis after extraction with acetone and ethylacetate. After development, the radioactive materials on the plate were located by radioluminography using a Bio-image Analyzer (BAS-2000II; Fuji Photo Film Co., Ltd., Tokyo, Japan) and imaging plate (BAS III; Fuji Photo Film Co., Ltd.) and by the UV-absorption of authentic sipoglitazar, M-I and M-II being added to the test samples as internal standards. The silica gel sections corresponding to sipoglitazar, M-I and M-II were scraped off the plate, the radioactivity in each section was counted and [¹⁴C]sipoglitazar and its metabolites labeled with ¹⁴C were identified by LC-MS/MS. The remaining material on the plates was also removed, counted, and referred to as "others".

For the measurement of the conjugated metabolites, portions of the urine, bile and aqueous homogenates of feces were incubated overnight at 37°C with sulfatase of type H-1 (including β-glucuronidase activity, pH 5, Sigma-Aldrich). After incubation, 5 vol. of acetonitrile were added to the mixtures and the mixtures were centrifuged. The supernatants were analyzed in the same way as described above. Sipoglitazar-G and M-I-G were identified by LC-MS/MS and calculated by subtracting the unchanged values from the value of each fraction obtained by enzymatic treatment.

Structural analysis of sipoglitazar and its metabolites in the biological samples of rats and monkeys by LC-MS/MS

Sipoglitazar and M-I were extracted from the plasma of monkeys and M-II from the urine of rats as described above. The extracts were subjected to LC-MS/MS for analysis. The rat bile and monkey urine were directly subjected to LC-MS/MS for analysis of sipoglitazar-G and M-I-G, respectively. LC-MS and MS/MS analyses of the unchanged sipoglitazar, M-I, M-II, sipoglitazar-G and M-I-G were performed using HPLC (a Waters Alliance system with a Waters 2690 pump; Waters Assoc., Milford, MA) and an ion trap mass spectrometer (LCQ, Thermo Finnigan, San Jose, CA) equipped with an electrospray ionization (ESI) interface system. The HPLC conditions are described in "Analytical procedures". The spectra were obtained in the positive ion mode. The interface and mass spectrometer were operated under the following conditions: heated capillary temperature, 200°C; spray voltage, 4.5 kV; sheath gas and auxiliary gas flow rate (arbitrary units), 80 and 15, respectively; and capillary voltage, 3.0 V. The collisionally induced dissociation (CID) fragment ions were generated using helium as a target gas, and the CID energy was 40%.

Measurement of the radioactivity

The radioactivity in the biological samples, organic solvent extracts, silica gel from the TLC

plates, and column effluent from the HPLC was determined with liquid scintillation counters (LSC-5100 and LSC-6100; Aloka Co., Ltd., Tokyo, Japan, LS-6000; Beckman Coulter, Inc., Brea, CA and 2700TR; Packard Instrument Co., Inc., Downers Grove, IL) or flow scintillation analyzers (500TR; Packard Instrument Co., Inc., Meriden, CT). The radioactivity in each rat tissue and the feces was measured by the combustion method. All sample combustions were performed in a Sample Oxidizer from Packard Instrument Co. and the resulting $^{14}\text{CO}_2$ was trapped in a mixture of Carbo-Sorb[®]E (Packard) and Liquid scintillator B (Wako Pure Chemical Industries, Ltd.).

Pharmacokinetic analysis

The half-life ($t_{1/2}$) in plasma for sipoglitazar was calculated by non-compartmental analysis using WinNonlin version 1.1 from Pharsight Corporation, Inc. (Mountain View, CA). The area under the plasma concentration-time curve (AUC) was calculated by the trapezoidal rule. The oral bioavailability of sipoglitazar was calculated by dividing the area under the curve ($\text{AUC}_{0-24\text{h}}$) for sipoglitazar normalized by the oral dose molar equivalent of sipoglitazar by the $\text{AUC}_{0-24\text{h}}$ for sipoglitazar normalized by the intravenous dose molar equivalent of sipoglitazar.

Incubation of [^{14}C]sipoglitazar with hepatocytes

Cryopreserved hepatocytes from rats, monkeys and humans (Celsis In Vitro Technologies, Baltimore, MD) were suspended using published procedures with minor modifications [44,45]. Hepatocytes, suspended in 0.5 mL of ice-cold Dulbecco's Modified Eagle medium (DMEM) were dispensed onto 24-well culture plates at a density of 3×10^5 viable cells/well, and 10 μM of [^{14}C]sipoglitazar were incubated at 37°C for 1, 2, 4 and 6 hours. The reactions were terminated by the addition of a volume of acetonitrile equivalent to the volume of the reaction medium. After centrifugation at 1500 $\times g$ for 10 minutes, the supernatants were applied to the HPLC. The ratios of sipoglitazar and its metabolites were calculated, with the total radioactivity in the incubation mixture regarded as 100%. All incubations were made in duplicate.

Analytical procedures

[^{14}C]sipoglitazar and its metabolites in the samples for structural analysis and the *in vitro* study with hepatocytes were analyzed by HPLC. The supernatants were mainly analyzed by HPLC (LC-10 gradient system; Shimadzu Corp., Kyoto, Japan) with an on-line RI detector (D505TR Flow Scintillation Analyzer, Packard Instrument Company, Meriden, CT). The principal HPLC analytical method was as follows: The column was an Inertsil ODS-3 (5- μm particle size, 150 \times 4.6 mm or 250 \times 4.6 mm I.D.; GL Sciences, Tokyo, Japan). The mobile phase (A) [MP(A)] was H₂O-acetonitrile-trifluoroacetic acid (TFA) (90:10:0.1, v/v) and the mobile phase (B) [MP(B)] was H₂O-acetonitrile-TFA (10:90:0.1, v/v). The column

temperature and the flow-rate were 40°C and 0.5 or 1 mL/min. The scheduled program for the gradient elution was as follows: The concentration of MP(B) was linearly increased from 30 % to 70 % over a period of 40 minutes, held at 95 % for 10 minutes and then cycled back to the initial condition (30 %). On-line RI detection was carried out using Ultima-Flo M as the flow scintillation cocktail.

Results

Apparent absorption ratio and bioavailability of [¹⁴C]sipoglitazar after a single or repeated oral dose in rats and monkeys at a dose of 0.5 mg/kg

As calculated from the AUC ratios for ¹⁴C after single oral and intravenous administration of [¹⁴C]sipoglitazar, 95.1% and 80.3% of the orally dosed drug were apparently absorbed in rats and monkeys, respectively. The component of sipoglitazar was separated by TLC analysis using the same plasma samples and its concentrations were quantified. The maximum measured concentration of sipoglitazar in rat plasma was 1.172 µg/mL (C_{max}) at 6.7 hours (T_{max}) after oral dosing with [¹⁴C]sipoglitazar. The concentrations of sipoglitazar declined monophasically thereafter with an apparent half-life (t_{1/2}) of 6.5 hours and AUC_{0-24h} of 16.88 µg·h/mL (Table II-1 and Figure II-2A). In monkeys given [¹⁴C]sipoglitazar orally, the T_{max}, C_{max}, t_{1/2α}, t_{1/2β}, and AUC_{0-24h} values for sipoglitazar were 1.1 hours, 1.499 µg/mL, 2.5 hours, 6.5 hours and 6.99 µg·h/mL, respectively (Table II-1 and Figure II-2B). Based on the ratio of AUC_{po} and AUC_{iv}, the bioavailability of sipoglitazar was calculated to be 95.0% and 72.6% in rats and monkeys respectively, showing the high bioavailability in both species. During repeated oral administration of [¹⁴C]sipoglitazar to rats for 14 days, the pharmacokinetic behavior of ¹⁴C in the plasma hardly changed (Table II-2).

Table II-1. Apparent absorption ratio and bioavailability of [¹⁴C]sipoglitazar after a single oral dose in rats and monkeys at a dose of 0.5 mg/kg

Species	Dosage Route	Total ¹⁴ C		Sipoglitazar	
		AUC _{0-24h} ^(a) (µg·h/mL)	Absorption ^(b) Ratio (%)	AUC _{0-24h} (µg·h/mL)	Bioavailability ^(b) (%)
Rat	PO	17.55 ± 0.46	95.1 ± 15.8 ^(c)	16.88 ± 0.46	95.0 ± 16.0 ^(c)
	IV	18.45 ± 3.02		17.76 ± 2.95	
Monkey	PO	11.25 ± 2.53	80.3 ± 14.6	6.99 ± 2.13	72.6 ± 15.7
	IV	14.01 ± 1.84		9.55 ± 1.21	

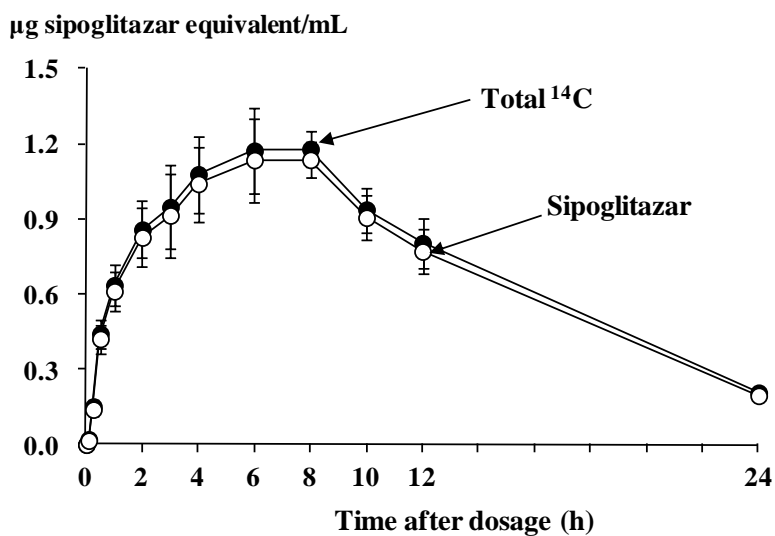
Values are the mean ± standard deviation (SD) of 3 rats or 4 monkeys.

(a) Sipoglitazar equivalent

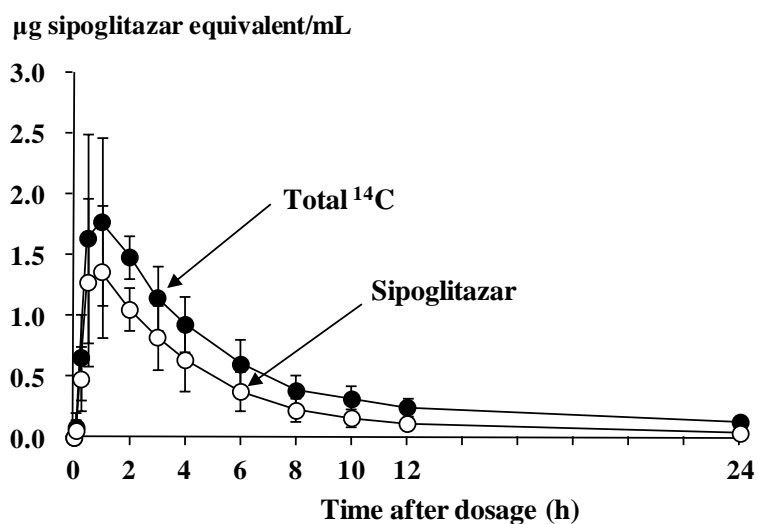
(b) (AUC_{po}/AUC_{iv}) × 100

(c) The SD was calculated by the following equation; SD = PO/IV ratio or bioavailability × ([SD of AUC_{po}/AUC_{po}]² + [SD of AUC_{iv}/AUC_{iv}]²)^{1/2}.

(A) Rat



(B) Monkey



Species	Pharmacokinetic parameters of sipoglitazar			
	T _{max} (h)	C _{max} (µg/mL)	t _{1/2} (h)	
			α	β
Rat	6.7 ± 1.2	1.172 ± 0.105	6.5 ± 0.1	
Monkey	1.1 ± 0.6	1.499 ± 0.458	2.5 ± 0.5	6.5 ± 1.0

Figure II-2. Concentrations of ¹⁴C and pharmacokinetic parameters of sipoglitazar in plasma of rats and monkeys given a single oral dose of [¹⁴C]sipoglitazar at a dose of 0.5 mg/kg. Values are the mean ± standard deviation (SD) for 3 rats or 4 monkeys.

Table II-2. Pharmacokinetic parameters of ^{14}C in rats given once-daily oral doses of [^{14}C]sipoglitazar repeatedly at a dose of 0.5 mg/kg for 14 days

Days on Drug	T_{\max} (h)	C_{\max} ($\mu\text{g}/\text{mL}$)	$C_{\min}^{(a)}$ ($\mu\text{g}/\text{mL}$)	$t_{1/2}$ (h)	$\text{AUC}_{0-24\text{h}}^{(b)}$ ($\mu\text{g}\cdot\text{h}/\text{mL}$)
1	6.7 ± 2.3	1.172 ± 0.153	0.248 ± 0.086	7.7 ± 1.8	16.97 ± 1.61
4	4.0 ± 3.6	1.019 ± 0.271	0.136 ± 0.035	5.9 ± 0.3	13.54 ± 3.24
7	5.3 ± 1.2	1.030 ± 0.230	0.128 ± 0.038	5.8 ± 0.5	13.53 ± 2.80
11	1.7 ± 1.2	0.962 ± 0.260	0.122 ± 0.034	6.1 ± 0.6	12.20 ± 2.67
14	4.0 ± 3.5	0.910 ± 0.155	0.133 ± 0.054	6.5 ± 1.2	12.16 ± 2.19

Values are the mean \pm standard deviation (SD) of 3 rats.

(a) Concentration at 24 h after each dose

(b) Sipoglitazar equivalent

Distribution of [^{14}C]sipoglitazar and its related compounds

The ^{14}C concentrations in the tissues were examined at 2, 4, 8, 24, 72, 120 and 168 hours after a single oral administration of [^{14}C]sipoglitazar to the rats (Figure II-3). In most tissues, ^{14}C was maximal at 4 hours after dosing (0.5 mg/kg). At 4 hours, the concentration of ^{14}C was the highest in the liver, followed in decreasing order by the plasma, Harderian glands, blood, intestine, kidneys, brown fat, adrenals, lungs, heart, skin, hypophysis, thyroid gland, submaxillary glands, pancreas, stomach, testes, bone marrow, spleen, thymus, fat, skeletal muscle and eyes; it was lowest in the spinal cord and brain. Although the elimination of ^{14}C in the adrenals, fat and brown fat was relatively slow, the ^{14}C in most other tissues then decreased to very low concentrations within 168 hours.

On repeated oral dosing of [^{14}C]sipoglitazar (0.5 mg/kg) to rats for 21 days, the concentrations of ^{14}C in most tissues increased gradually and attained steady state within 21 days (data not shown). After the 21st dose, the ^{14}C concentration was the highest in the brown fat, followed in decreasing order by the fat, adrenals and skin and thereafter ^{14}C in most tissues except for these adipose tissues decreased to low concentrations within 28 days. Especially in the fat, although elimination of ^{14}C was observed, its rate was much slower than that in the other tissues (Figure II-4). A major component of ^{14}C in the fat was elucidated to be sipoglitazar as ester-conjugates by alkaline hydrolysis after extraction with acetone and ethylacetate (data not shown).

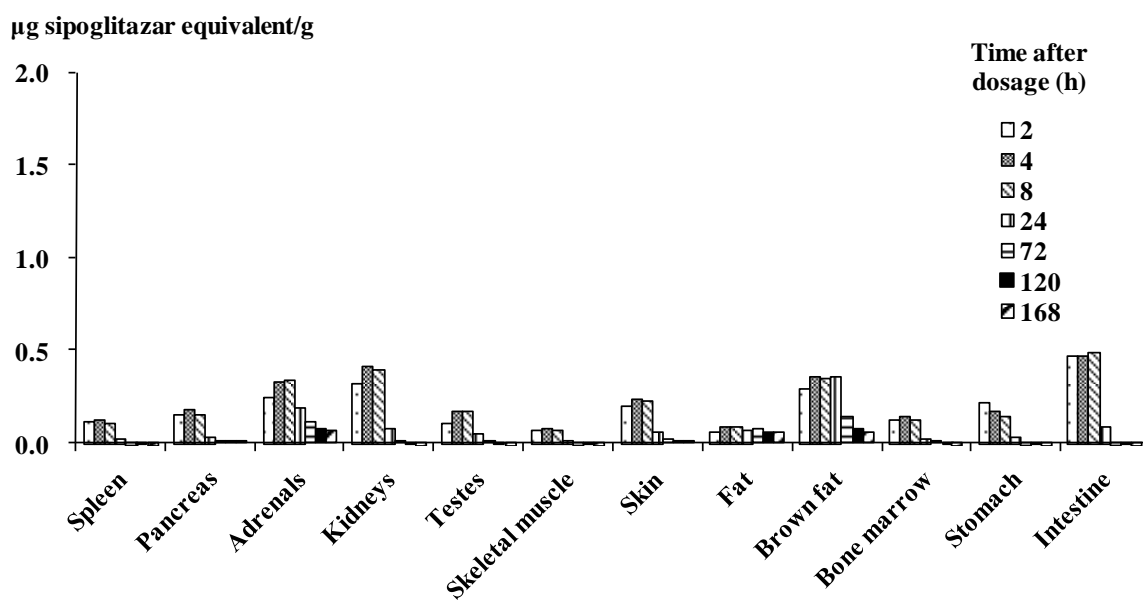
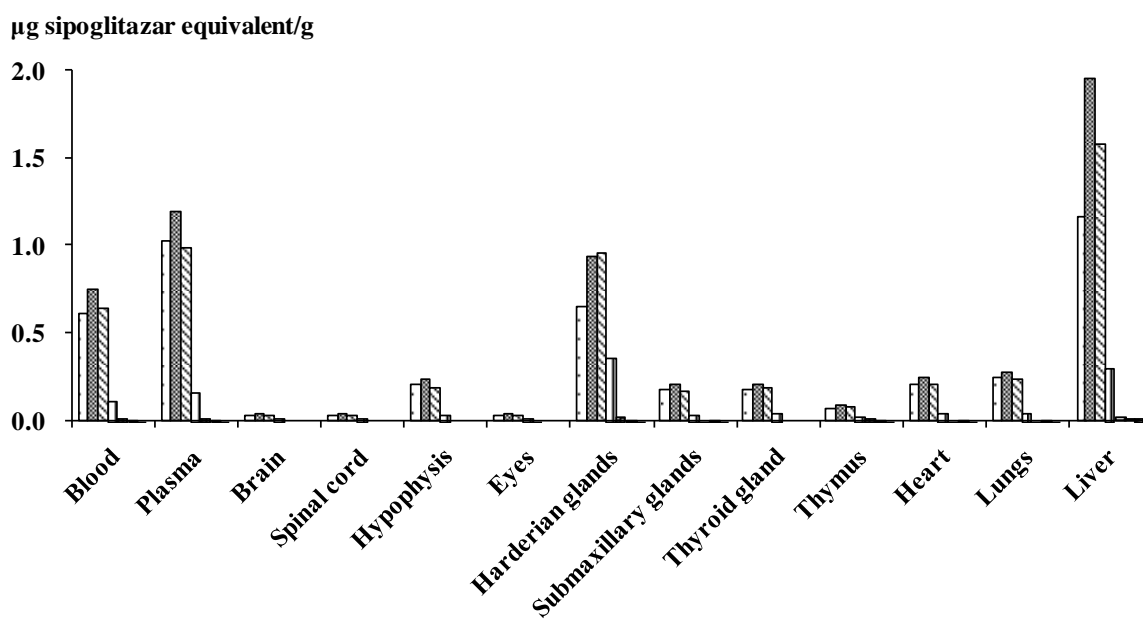


Figure II-3. Concentrations of ^{14}C and its elimination in tissues of rats given a single oral dose of [^{14}C]sipoglitazar at a dose of 0.5 mg/kg

Values are the mean \pm standard deviation (SD) for 3 rats.

Blood and plasma: $\mu\text{g/mL}$

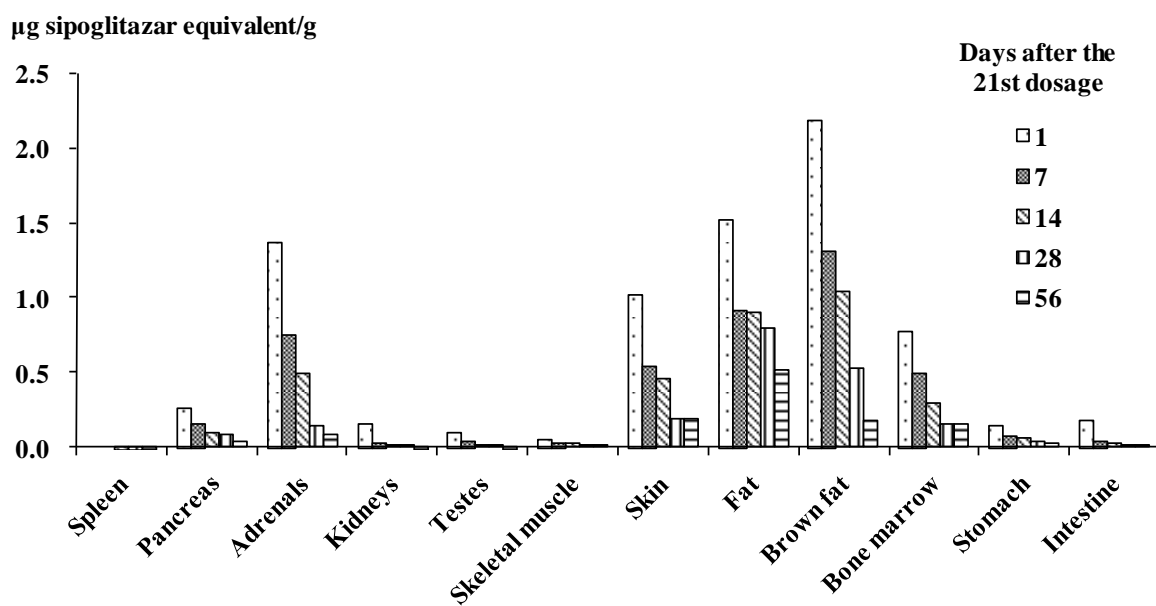
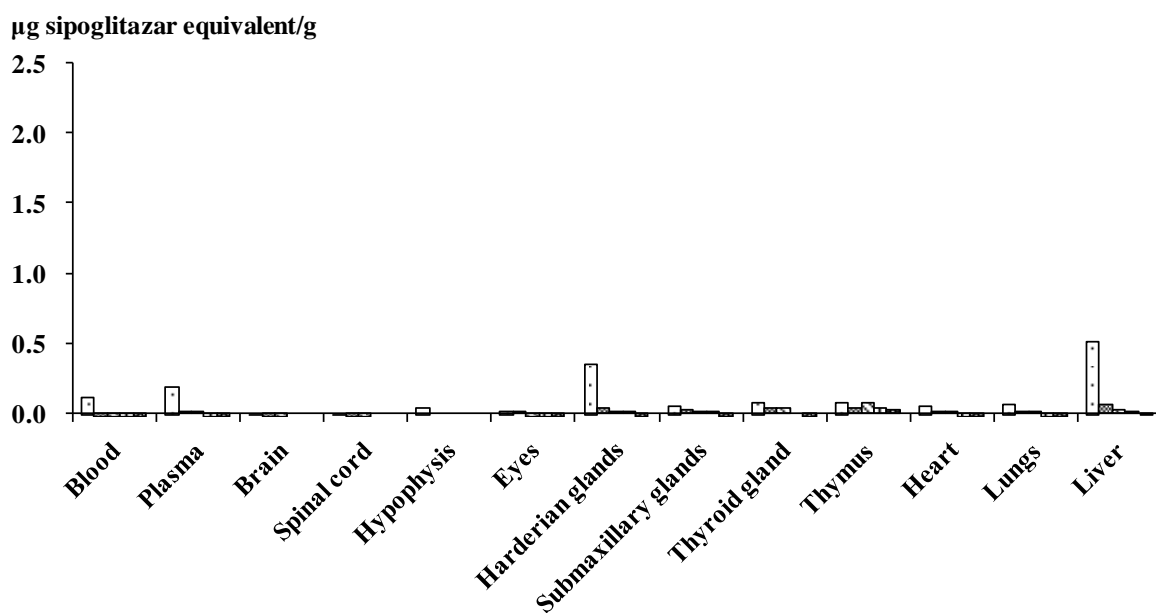


Figure II-4. Concentrations of ¹⁴C and its elimination in tissues of rats after a once-daily oral dose of [¹⁴C]sipoglitazar at a dose of 0.5 mg/kg for 21 days

Values are the mean ± standard deviation (SD) of 3 rats.

Blood and plasma: µg/mL

***In vivo* metabolic profiles of plasma and excreta of rats and monkeys given a single oral dose of [¹⁴C]sipoglitazar at a dose of 0.5 mg/kg**

From the AUC_{0-24h} values calculated by the composition analysis of the plasma, 96.2% and 62.1% of the total ¹⁴C were accounted for by sipoglitazar in the rats and monkeys, respectively (Table II-3). Small amounts of M-I and M-II were also detected in the plasma of both species, but the glucuronides of sipoglitazar and M-I were not detected. The other components in the plasma were minor and summarized as others. In the excreta of the rats and monkeys, various metabolites were detected (Table II-4). Over 48 hours after administration of [¹⁴C]sipoglitazar to the rats, 3.3% and 88.1% of the total ¹⁴C were excreted in the urine and feces and the main component was M-II in the urine and sipoglitazar containing unabsorbed drug in the feces, respectively. In rat bile, 83.6% of the total ¹⁴C was recovered in 24 hours after administration and 56.1% of the total ¹⁴C was detected as sipoglitazar-G. Over 96 hours after administration of [¹⁴C]sipoglitazar to the monkeys, 35.7% and 48.8% of the total ¹⁴C were excreted in the urine and feces and the main component was M-I-G in the urine and M-I in the feces, respectively. Therefore, sipoglitazar was metabolized to M-I, M-II, sipoglitazar-G, M-I-G and other unidentified metabolites with high polarity in the rats and monkeys.

Table II-3. Composition of radiolabeled materials in plasma of rats and monkeys given a single oral dose of [¹⁴C]sipoglitazar at a dose of 0.5 mg/kg

Compound	AUC _{0-24h} (µg·h/mL) ^(a)	
	Rat	Monkey
Total ¹⁴ C	17.55 ± 0.46 (100.0)	11.25 ± 2.53 (100.0)
Sipoglitazar	16.88 ± 0.46 (96.2)	6.99 ± 2.13 (62.1)
M-I	0.08 ± 0.01 (0.5)	0.86 ± 0.24 (7.6)
M-II	0.19 ± 0.01 (1.1)	0.13 ± 0.03 (1.2)
Others	0.41 ± 0.02 (2.2)	3.27 ± 0.56 (29.1)

Values are the mean ± standard deviation (SD) of 3 rats or 4 monkeys.

Figures in parentheses denote % of total ¹⁴C.

(a) Sipoglitazar equivalent

Table II-4. Composition of the radiolabeled materials in the urine, feces, and bile of rats and monkeys given a single oral dose of [¹⁴C]sipoglitazar at a dose of 0.5 mg/kg

Compound	Composition of ¹⁴ C (% of Dose)				
	Rat			Monkey	
	Urine (0-48 h)	Feces (0-48 h)	Bile ^(a) (0-24 h)	Urine (0-96 h)	Feces (0-96 h)
Total ¹⁴ C	3.3 ± 0.2 (100)	88.1 ± 1.3 (100)	83.6 ± 5.9 (100)	35.7 ± 4.7 (100)	48.8 ± 11.0 (100)
Sipoglitazar	< 0.1 (0)	44.1 ± 0.2 (50.1)	8.7 ± 2.3 (10.4)	0.7 ± 0.2 (2.0)	3.5 ± 1.3 (7.2)
Sipoglitazar-G	< 0.1 (0)	5.7 ± 0.4 (6.5)	46.9 ± 6.4 (56.1)	0.6 ± 0.2 (1.7)	0.3 ± 0.2 (0.6)
M-I	< 0.1 (0)	6.3 ± 0.4 (7.2)	0.4 ± 0.1 (0.5)	1.2 ± 0.5 (3.4)	17.0 ± 6.8 (34.8)
M-I-G	0.1 ± 0.1 (3.0)	< 0.1 (0)	1.6 ± 0.3 (1.9)	14.0 ± 6.2 (39.2)	0.4 ± 0.6 (0.8)
M-II	2.0 ± 0.1 (60.6)	4.9 ± 0.6 (5.6)	0.5 ± 0.2 (0.6)	1.3 ± 0.2 (3.6)	0.4 ± 0.1 (0.8)
Others	1.1 ± 0.0 (36.4)	27.2 ± 2.0 (30.6)	25.6 ± 3.2 (30.5)	18.0 ± 5.1 (50.1)	27.3 ± 6.0 (55.8)

Values are the mean ± standard deviation (SD) of 3 rats or 4 monkeys.

Figures in parentheses denote % of total ¹⁴C.

(a) Biliary-cannulated rats (n=4; intraduodenal administration)

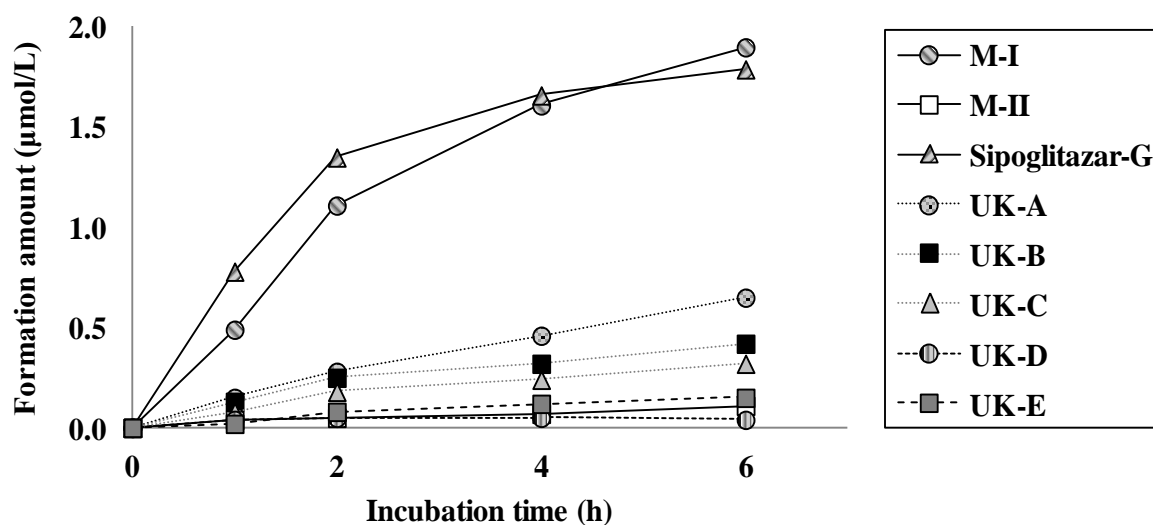
***In vitro* metabolic profiles of [¹⁴C]sipoglitazar with hepatocytes of humans, rats and monkeys**

The *in vitro* metabolism of [¹⁴C]sipoglitazar was studied using hepatocytes from humans, rats, and monkeys (Figure II-5). In human hepatocytes, sipoglitazar was metabolized to M-I, M-II, sipoglitazar-G and unidentified metabolites (UK-A, -B, -C, -D and -E). The concentration of each metabolite in human hepatocytes increased with incubation time and some metabolites attained saturation at 6 hours (Figure II-5A). The composition ratios of sipoglitazar, M-I and sipoglitazar-G were 44.9%, 19.0% and 17.9%, respectively and these two metabolites were the major ones in the human hepatocytes incubated for 6 hours (Figure II-5B). In rat hepatocytes, sipoglitazar was the main component and M-I, M-II,

sipoglitazar-G were also detected, although the amount formed was very limited. In monkey hepatocytes incubated for 6 hours, the composition ratios of sipoglitazar, M-I and sipoglitazar-G were 35.4%, 8.2% and 29.6%, respectively. The metabolic profile with the monkey hepatocytes was similar to that with humans and there was no metabolite specific for humans.

(A)

Human hepatocytes



(B)

Hepatocytes

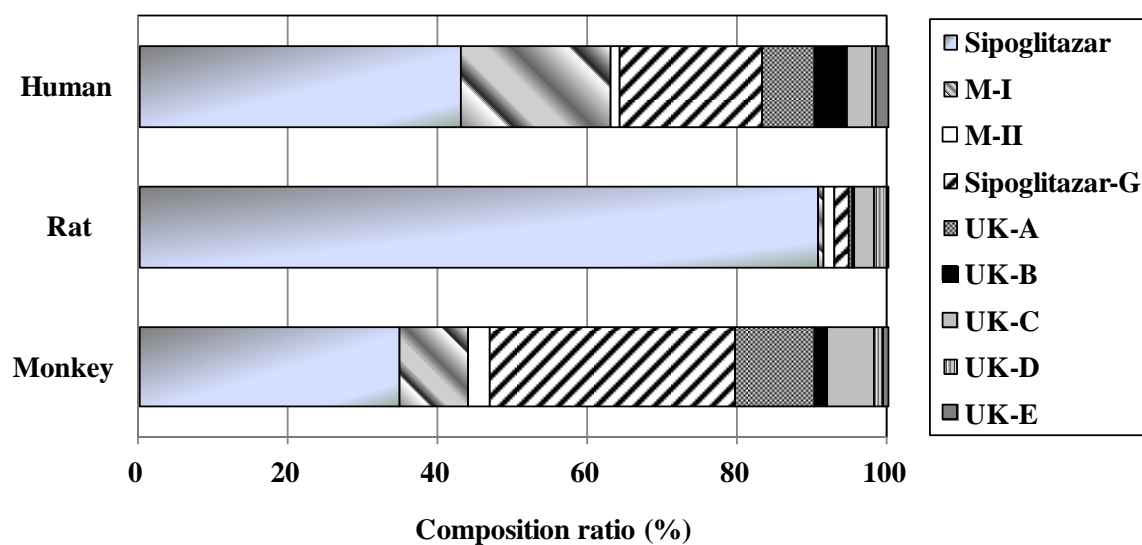


Figure II-5. *In vitro* metabolic profiles of [14 C]sipoglitazar with hepatocytes from humans, rats and monkeys

(A) The time-course of formation of each metabolite in human hepatocytes

(B) Composition profile in the reaction mixture of sipoglitazar incubated with hepatocytes from humans, rats and monkeys for 6 hours

Values are the mean of duplicate determinations.

Structural analysis of sipoglitazar and its metabolites

The structural analysis of M-I, M-II, sipoglitazar-G and M-I-G was confirmed by LC-MS/MS. For M-I and M-II, their mass spectral data and the HPLC retention time were in agreement with those of the authentic compounds.

The full ion mass spectrum of sipoglitazar-G gave the $[M+H]^+$ at m/z 642, which was 176 amu higher than that of sipoglitazar. The characteristic fragment ions in the product ion mass spectrum at m/z 642 were detected at m/z 624, 282 and 174. The ion at m/z 624 was a dehydrated ion. The ions at m/z 282 and 174 were the same as those of sipoglitazar. Alkaline hydrolysis (0.1 mol/L sodium hydroxide solution, at 37°C for 2 hours) and enzymatic hydrolysis [5 w/v% of sulfatase containing β -glucuronidase (type H-1), at 37°C for 2 hours] of the peak at m/z 642 of sipoglitazar-G gave sipoglitazar in the LC-MS.

The full ion mass spectrum of M-I-G gave the $[M+H]^+$ at m/z 614, which was 176 amu higher than that of M-I. The characteristic fragment ions in the product ion mass spectrum at m/z 614 were detected at m/z 438 and 282. The ions at m/z 438 and 282 were derived by diagnostic loss of the sugar moiety (-176 amu) and were the same as that of M-I. Although M-I was not obtained by alkaline hydrolysis, enzymatic hydrolysis [5 w/v% of sulfatase containing β -glucuronidase (type H-1), 37°C, for 14 hours] of its peak gave M-I.

Cumulative excretion of ^{14}C in the urine, feces, and bile of rats and monkeys given a single oral dose of [^{14}C]sipoglitazar at a dose of 0.5 mg/kg

Following oral administration of [^{14}C]sipoglitazar to the rats, most of the radioactivity was recovered within 96 hours, with 3.4% and 92.3% of the dose appearing in the urine and feces, respectively and less than 0.1% of the dose excreted in expired air (Table II-5). In monkeys, 36.6% and 55.5% of the orally administered radioactivity were excreted in the urine and feces within 168 hours, respectively (Table II-5). The dosed ^{14}C was largely excreted into the feces in rats and was excreted in both urine and feces in monkeys.

In biliary-cannulated rats given [^{14}C]sipoglitazar intraduodenally, 83.6% of the administered radioactivity was excreted in the bile over 24 hours (Tables II-4 and 5). Within 24 hours after ID administration of the radioactive bile to other biliary-cannulated rats, 66.9% and 1.3% of the dosed radioactivity were excreted in bile and urine, respectively. It is thus evident that the major part of biliary radioactivity undergoes enterohepatic circulation in rats.

Table II-5. Cumulative excretion of ^{14}C in the urine, feces, and bile of rats and monkeys given a single oral dose of [^{14}C]sipoglitzar at a dose of 0.5 mg/kg

Species	Time after dosage (h)	Cumulative Excretion (% of Dose)			
		Urine	Feces	Bile	Total ^{14}C
Rat	4	0.4 ± 0.1	---	---	N.E.
	8	1.0 ± 0.1	---	---	N.E.
	24	2.7 ± 0.1	61.8 ± 0.3	---	64.4 ± 0.2
	48	3.3 ± 0.2	88.1 ± 1.3	---	91.4 ± 1.1
	72	3.4 ± 0.2	91.7 ± 0.7	---	95.1 ± 0.6
	96	3.4 ± 0.2	92.3 ± 0.7	---	95.7 ± 0.7
	120	3.4 ± 0.2	92.5 ± 0.7	---	95.9 ± 0.7
Rat ^(a)	2	---	---	15.0 ± 3.1	N.E.
	4	0.5 ± 0.1	---	40.8 ± 9.1	N.E.
	8	0.8 ± 0.3	---	62.6 ± 9.8	N.E.
	24	1.4 ± 0.7	6.1 ± 1.0 ^(b)	83.6 ± 5.9	91.0 ± 4.4
Monkey	4	8.2 ± 1.5	---	---	N.E.
	8	17.0 ± 2.1	---	---	N.E.
	24	27.2 ± 2.3	16.2 ± 8.1	---	43.4 ± 6.6
	48	32.5 ± 3.5	33.1 ± 11.9	---	65.6 ± 9.2
	72	34.8 ± 4.3	44.3 ± 12.4	---	79.1 ± 8.6
	96	35.7 ± 4.7	48.8 ± 11.0	---	84.5 ± 6.8
	120	36.1 ± 4.8	51.8 ± 9.8	---	87.9 ± 5.4
	144	36.4 ± 4.9	53.9 ± 8.8	---	90.3 ± 3.9
168	36.6 ± 5.0	55.5 ± 8.2	---	92.1 ± 3.1	

Values are the mean ± standard deviation (SD) of 3 rats or 4 monkeys.

--- indicates not examined.

N.E. indicates not estimated.

(a) Biliary-cannulated rats (n=4; intraduodenal administration)

(b) Includes ^{14}C in the gut contents.

Discussion

To examine the fate of sipoglitazar in experimental animals, the absorption, distribution, metabolism and excretion of the radioactivity and sipoglitazar were investigated in rats and monkeys after single or multiple administration of [^{14}C]sipoglitazar. Furthermore, *in vitro* metabolism of sipoglitazar was also examined using human and animal hepatocytes. By comparing their relationship *in vivo* and *in vitro*, the metabolic profile and the main excretion route from the body in humans could be presumed.

Sipoglitazar exhibited good oral absorption and bioavailability in both species and the apparent absorption ratios and bioavailability showed similar values (Table II-1 and Figure II-2). Sipoglitazar accounted for a major part of the radioactivity in the plasma of both species (Table II-3). These findings indicated that sipoglitazar was significantly absorbed without first pass metabolism. With repeated oral administration of [^{14}C]sipoglitazar to rats for 14 days, the pharmacokinetic parameters remained generally unchanged (Table II-2). This property would be helpful for the dosing plan of sipoglitazar in humans to control the plasma concentrations safely.

Absorbed sipoglitazar and its metabolites were distributed in rat tissues with relatively high concentrations in the liver after a single oral administration, resulting in the metabolic stimulation of sipoglitazar (Figure II-3). The distribution of [^{14}C]sipoglitazar after single administration was also observed in the target tissues of PPAR- γ , skeletal muscle and adipose tissue, although their distributed concentrations were low. The concentrations of ^{14}C in adipose tissues remained relatively high after multiple administrations, although ^{14}C was gradually excreted from almost all the tissues (Figure II-4). The main component of ^{14}C for the fat, one of the target tissues to activate PPAR- γ , was elucidated to be sipoglitazar by alkaline hydrolysis and the same as that for the plasma in rats. These results indicated that the main component could be same for all the tissues in rats and the pharmacologically active substance sipoglitazar was distributed to the target tissues, in which PPAR- α and PPAR- γ are predominantly expressed [35]. Furthermore, sipoglitazar was considered to exist as an ester-conjugate with the triglyceride of fatty acids in the fat, because alkaline hydrolysis could elucidate the component in the fat, while only liquid-liquid extraction with organic solvents like acetone or ethylacetate could not yield sipoglitazar in the fat, probably due to the endogenous fatty acids. Thus, the fatty acids with triglyceride in the fat could play an important role in retaining sipoglitazar in the tissues. The rapid elimination of ^{14}C from skeletal muscle, one of the target tissues to activate PPAR- γ , was likely due to the low level of fatty acids. Considering these results in total, sipoglitazar is stored as the ester-form in the fat after multiple administrations, released into the plasma gradually by hydrolysis and thus contributes to the action on the PPARs. Adipose PPAR especially would work as an essential mediator for the maintenance of whole body insulin sensitivity [46]. This could be consistent with the pharmacological results that sipoglitazar enhanced glucose uptake in white adipose tissue of Wistar fatty rats administered sipoglitazar (1.2 mg/kg/day) repeatedly

for 7 days and after the final administration on day 7, its effect was maintained even on day 8 (Matsumoto M., personal communications). These results indirectly indicate that the distribution properties of sipoglitazar contribute to the duration of the pharmacological effects.

Sipoglitazar was metabolized to M-I, M-II, their glucuronide conjugates (sipoglitazar-G and M-I-G), and unidentified metabolites in rats and monkeys and these identified metabolites could account for the major part of the metabolic profile in rats and monkeys (Tables II-3 and 4). The larger formation amount of M-I and others in monkeys than that in rats indicates that the metabolism of sipoglitazar in monkeys is more extensive than in rats (Table II-3). Moreover, there was an apparent difference between rats and monkeys in the metabolic profile in the excreta (Table II-4). In rats after single oral administration of [¹⁴C]sipoglitazar, the dosed ¹⁴C was largely excreted in the feces and the major component was sipoglitazar, while the minor components sipoglitazar-G, M-I and M-II were also detected (Tables II-4 and 5). In biliary cannulated rats given [¹⁴C]sipoglitazar intraduodenally, 83.6% of the dose was excreted in the bile and the major part of biliary radioactivity underwent enterohepatic circulation (Tables II-4 and 5). Thus, sipoglitazar and its metabolites were eliminated via biliary excretion into the feces in rats and sipoglitazar-G was a key metabolite. In monkeys, the excretion route was via both the urine and feces and the major component was M-I-G in the urine and M-I in the feces, indicating that the metabolic pathway from M-I to M-I-G was very important (Tables II-4 and 5). The excretion ratio in urine was significantly higher in the monkeys than in rats, which might be due to the enhanced metabolism from M-I to the more water-soluble M-I-G in monkeys. These results indicated that the important metabolite in the metabolic profile of sipoglitazar was sipoglitazar-G in rats and M-I and M-I-G in monkeys. However, the involvement of sipoglitazar-G as the excretion route in monkeys could not be denied, because sipoglitazar-G could be also observed as a minor metabolite in the excreta of monkeys. On the other hand, the *in vitro* metabolism with hepatocytes of humans and animals showed that the metabolism of sipoglitazar in humans appeared to be similar with that in the monkeys and there was no metabolite specific for humans (Figure II-5B). Considering that there was a good correlation for the oxidative metabolites between the feces and hepatocytes of rats and monkeys, M-I was a key metabolite in the elimination process in humans *in vivo*. Meanwhile, there was little correlation for the glucuronidation between the excreta and hepatocytes of animals. The sipoglitazar-G formation was limited in the rat hepatocytes and excreta, but actually sipoglitazar was shown to be excreted via biliary excretion as sipoglitazar-G in rats (Table II-4 and Figure II-5B). These differences probably come from two reasons; one is the enterohepatic circulation of sipoglitazar-G *in vivo* and the other is the unstable properties of sipoglitazar-G in the medium with neutral pH *in vitro*, which is reported as the acyl migration and degradation of the glucuronides [47,48]. These will cause the discrepancy between the *in vitro* and *in vivo* studies. Furthermore, sipoglitazar-G was formed in the hepatocytes of

humans and monkeys more extensively than in rats. Considering these results in total, glucuronidation of sipoglitazar could be also presumed to be an important elimination route in humans and monkeys. Moreover, the glucuronidation of M-I was presumed to occur in humans from the high composition ratio of M-I-G in monkey urine.

In conclusion, sipoglitazar has no fatal non-clinical ADME profile for clinical evaluation. The compound exhibits good oral absorption and bioavailability in rats and monkeys, distribution to target tissues such as fat and excretion. The main component in the plasma of rats and monkeys dosed with sipoglitazar was the parent compound. In rats, sipoglitazar was mainly excreted into the feces via biliary excretion as sipoglitazar-G, while the major component was M-I-G in the urine and M-I in the feces of monkeys. Comparing the metabolic profiles in the hepatocytes, the metabolism of sipoglitazar in monkeys rather than that in rats would be more helpful in understanding that in humans and the formation of M-I was considered to be crucial in humans. Moreover, glucuronidation was also presumed to be an important excretion route in humans from the biliary excretion as sipoglitazar-G in rats and the high composition ratio of M-I-G in monkey urine. These results suggest that sipoglitazar will be cleared primarily by oxidation and glucuronidation in humans. Further investigation of the biotransformation of sipoglitazar is also necessary.

Summary

Sipoglitazar is a novel anti-diabetic agent with triple agonistic activities on the human peroxisome proliferator-activated receptors, hPPAR- γ , - α , and - δ . The bioavailability for sipoglitazar was 95.0% and 72.6% in rats and monkeys respectively and sipoglitazar is hardly subject to first pass metabolism in either species. Following oral administration of [^{14}C]sipoglitazar to rats, sipoglitazar and its metabolites were distributed to the rat tissues with relatively high concentrations in the liver and also to the target tissue, the adipose tissue. The major component was sipoglitazar in the plasma of rats and monkeys. In rats, sipoglitazar was mainly excreted into the feces via biliary excretion as sipoglitazar-G, while the major component was M-I-G in the urine and M-I in the feces of monkeys. In hepatocytes, the metabolism was not extensively advanced in rats and the main metabolites were M-I and sipoglitazar-G in humans, similar to the metabolic profile in monkeys. There was no metabolite specific for humans *in vitro*. In conclusion, the formation of M-I, M-I-G and sipoglitazar-G is considered to be crucial and sipoglitazar is presumed to be cleared primarily by oxidation and glucuronidation in humans, when examined *in vivo* and *in vitro*.

CHAPTER III

An Unusual Metabolic Pathway of Sipoglitazar: Cytochrome P450-Catalyzed Oxidation of Sipoglitazar Acyl Glucuronide

Introduction

Animal pharmacokinetic studies using [¹⁴C]sipoglitazar in rats and monkeys revealed that sipoglitazar was biotransformed to the deethylated metabolite (M-I), the hydroxyl metabolite (M-II), the glucuronide conjugate of sipoglitazar (sipoglitazar-G), the glucuronide of M-I (M-I-G) and other unidentified metabolites [10]. Among the metabolites, M-I and sipoglitazar-G were shown to be the key metabolites in the elimination process, because sipoglitazar was mainly excreted into the feces via biliary excretion as sipoglitazar-G in rats and M-I was detected as the main metabolite in the monkey plasma. Furthermore, metabolite M-I was also measured as the main metabolite in plasma of humans orally administered sipoglitazar.

In the present study, to clarify the metabolic pathways from sipoglitazar to M-I in humans, *in vitro* metabolic studies using human hepatocytes and liver microsomes, identification of metabolites by LC-MS/MS and nuclear magnetic resonance spectroscopy (NMR) and a stability study of the metabolites were carried out.

Materials and Methods

Chemicals

Sipoglitazar and its metabolites (M-I and M-II) were prepared by Takeda Pharmaceutical Company Limited (Osaka, Japan). [¹⁴C]sipoglitazar with a specific radioactivity of 4.58 MBq/mg was synthesized by Amersham Pharmacia Biotech UK Ltd. (Buckinghamshire, UK). Glucose 6-phosphate and β -NADP⁺ were purchased from Oriental Yeast Co., Ltd. (Osaka, Japan). Glucose-6-phosphate dehydrogenase, uridine 5'-diphospho-glucuronic acid (UDPGA), gemfibrozil and β -glucuronidase (type H-1) were from Sigma Chemical Co. (St. Louis, MO), alamethicin was from MP Biomedicals, LLC. (Solon, OH), and methanol, acetonitrile, and other reagents of analytical grade were from Wako Pure Chemical Industries, Ltd. (Osaka, Japan).

Other materials

Cryopreserved primary human hepatocytes (Lot No. 69, from a 63-year-old female, Caucasian) were obtained from Celsis In Vitro Technologies (Baltimore, MD). Human liver microsomes were obtained from Tissue Transformation Technologies (Edison, NJ) and Xenotech, LLC (Lenexa, KS). Dog liver microsomes were also obtained from Xenotech,

LLC. Baculovirus-infected-insect cell microsomes expressing human CYP isoforms were purchased from BD Biosciences (Woburn, MA). Rat bile was collected from Crj:CD(SD)IGS rats, which were obtained from Charles River Japan Inc. (Yokohama, Japan). Human plasma (Lot No. MT116523) was purchased from Kojin Bio (Saitama, Japan).

Preparation of [¹⁴C]sipoglitazar-G, [¹⁴C]sipoglitazar-G1 and [¹⁴C]sipoglitazar-G2

In the course of this study, the glucuronide of sipoglitazar, sipoglitazar-G was revealed to be composed of two glucuronides, which were defined as sipoglitazar-G1 and sipoglitazar-G2. For the *in vitro* metabolic study, [¹⁴C]sipoglitazar-G, [¹⁴C]sipoglitazar-G1 and [¹⁴C]sipoglitazar-G2 were isolated from the glucuronidation reactant obtained by the incubation of [¹⁴C]sipoglitazar (100 μM) with human liver microsomes (2 mg protein/mL) at 37°C for 4 hours. After the termination of the reaction and centrifugation, the supernatant was concentrated under a nitrogen gas stream and applied to an HPLC. To isolate these glucuronides, the column temperature for HPLC analysis was set at 40°C for [¹⁴C]sipoglitazar-G (the mixture of [¹⁴C]sipoglitazar-G1 and [¹⁴C]sipoglitazar-G2), and the column temperature for HPLC analysis was set at 4°C for the isolation of [¹⁴C]sipoglitazar-G1 and [¹⁴C]sipoglitazar-G2, respectively. The HPLC analytical conditions are described in "Analytical procedures for [¹⁴C]sipoglitazar and its metabolites". Each eluate was dried under a nitrogen gas stream and resolved in 50% or 70% acetonitrile. For the structural analysis, [¹⁴C]sipoglitazar-G1 was prepared from the glucuronidation reactant with human liver microsomes (2 mg protein/mL) or dog liver microsomes (1 mg protein/mL), and [¹⁴C]sipoglitazar-G2 was prepared from the bile of rats after a single intraduodenal administration of [¹⁴C]sipoglitazar (0.5 mg/kg). The HPLC analytical condition is described in "Analytical procedures for [¹⁴C]sipoglitazar and its metabolites". The column temperature was set at 40°C for the structural analysis.

Incubation of [¹⁴C]sipoglitazar with human hepatocytes

Cryopreserved hepatocytes were suspended using published procedures with minor modifications [44,45]. Hepatocytes, suspended in 0.5 mL of DMEM were dispensed on 24-well culture plates at a density of 3×10^5 viable cells/well with 10 μM of [¹⁴C]sipoglitazar and incubated at 37°C for 6 hours.

Structural analysis of [¹⁴C]sipoglitazar-G1 and [¹⁴C]sipoglitazar-G2 by LC-MS/MS and NMR

LC-MS and LC-MS/MS analyses were performed using an ion trap mass spectrometer (LCQ and TSQ-7000; Thermo Fisher Scientific, Waltham, MA) equipped with an electrospray ionization (ESI) interface system. The spectra were obtained in the positive ion mode. The interface and mass spectrometer were operated under the following conditions. For

LCQ (target analytes: sipoglitazar, M-I and M-II), heated capillary temperature was 200°C, spray voltage was 4.5 kV, sheath gas and auxiliary gas flow rates were 80 and 15 arbitrary units, respectively, and capillary voltage was 3.0 V. The CID fragment ions were generated using helium as a target gas, and the CID energy was 40%. For TSQ-7000 (target analytes: sipoglitazar-G1 and -G2), heated capillary temperature was 230°C, spray voltage was 4.5 kV, and sheath gas pressure was 483 kPa. The CID fragment ions were generated within quadrupole 2, using argon as a target gas, and the CID energy (quadrupole 2 offset voltage) and the target gas pressure were -25 eV and 0.2 Pa, respectively.

¹H-NMR spectrometry was performed using a Varian Gemini-300 (Varian Instruments Ltd., Palo Alto, CA). The conditions for measurement were as follows: spectral width, 4500.5 Hz; acquisition time, 3.498 s; measurement solvent, deuterated acetonitrile and deuterium oxide (7:3, by vol.); temperature, ambient. Chemical shifts (parts per million) were referenced to the residual solvent peak at 1.95 ppm. Signals of the ¹H-NMR spectrum were assigned by the observed coupling patterns.

Stability of [¹⁴C]sipoglitazar-G1 and [¹⁴C]sipoglitazar-G2

[¹⁴C]sipoglitazar-G1 or [¹⁴C]sipoglitazar-G2 (final concentration: 10 μM) was incubated at 37°C in 50 mM KPB (pH 7.4), acetate buffer (pH 4.4), rat bile and human plasma. An aliquot was withdrawn from the reaction mixture after incubation for 0, 5, and 30 minutes and 1, 2, and 4 hours for sipoglitazar-G1 and after incubation for 0, 1, 2, and 4 hours for sipoglitazar-G2.

Oxidative metabolism of [¹⁴C]sipoglitazar, [¹⁴C]sipoglitazar-G1 and [¹⁴C]sipoglitazar-G2 by human liver microsomes

An acetonitrile solution of 1 mM [¹⁴C]sipoglitazar, [¹⁴C]sipoglitazar-G1 or [¹⁴C]sipoglitazar-G2 was added to the incubation mixture, consisting of 1 mg protein/mL human liver microsomes, 5 mM MgCl₂, and an NADPH-generating system with a final concentration of 5 mM glucose-6-phosphate, 0.5 mM β-NADP⁺ and 1.5 unit/mL glucose-6-phosphate dehydrogenase in 50 mM KPB with a final volume of 0.25 mL. The incubation was conducted at 37°C for 1 hour ([¹⁴C]sipoglitazar) or 10 minutes ([¹⁴C]sipoglitazar-G1 or [¹⁴C]sipoglitazar-G2). The final concentration of the substrate was 10 μM.

Glucuronidation of [¹⁴C]sipoglitazar by human liver microsomes

The acetonitrile solution of 1 mM [¹⁴C]sipoglitazar was added to the incubation mixture, consisting of 1 mg protein/mL human liver microsomes, 5 mM MgCl₂, 50 μg/mL alamethicin, and 5 mM of UDPGA in 50 mM KPB (pH 7.4) with a final volume of 0.25 mL. The incubation was conducted at 37°C for 1 hour. The final concentration of [¹⁴C]sipoglitazar was 10 μM.

Identification of the CYP isoform involved in the metabolism from sipoglitazar-G1 to M-I

To identify the CYP isoform involved in the metabolism from sipoglitazar-G1 to M-I, a CYP metabolic study using 80 pmol P450/mL CYP-expressing microsomes and a correlation study using 0.5 mg protein/mL liver microsomes from 16 humans provided as the Reaction Phenotyping Kit (Version 5.0) were performed. The correlation analysis was performed with the SAS System (SAS Institute). The biochemical activity data for the specific CYP enzymes provided with the kit were used for the correlation analysis. In the CYP metabolic study, [¹⁴C]sipoglitazar-G was used, and in the correlation study, [¹⁴C]sipoglitazar-G1 was used as the substrate. An acetonitrile solution of 0.5 mM [¹⁴C]sipoglitazar-G or 1 mM [¹⁴C]sipoglitazar-G1 was added to the incubation mixture, consisting of the respective microsomal protein, 5 mM MgCl₂, and an NADPH-generating system as described above in 50 mM KPB (pH 7.4) or Tris-HCl buffer (pH7.4) with a final volume of 0.25 mL. The incubation was conducted at 37°C for 15 minutes (the CYP metabolic study) or 10 minutes (the correlation study). The final concentration of the substrate was 10 μM in the both studies.

Incubation of [¹⁴C]sipoglitazar and gemfibrozil with human liver microsomes in the presence of UDPGA with or without an NADPH-generating system

The acetonitrile solution of 1 mM [¹⁴C]sipoglitazar was added to the incubation mixture, consisting of 0.5 mg protein/mL human liver microsomes, 5 mM MgCl₂, 50 μg/mL alamethicin, 5 mM of UDPGA with or without an NADPH-generating system and gemfibrozil in 50 mM KPB (pH 7.4) with a final volume of 0.25 mL. Gemfibrozil was prepared to dissolve in acetonitrile and its final concentration was 0, 10, 30, 100, or 300 μM. The incubation was conducted at 37°C for 30 minutes. The final concentration of [¹⁴C]sipoglitazar was 10 μM.

Analytical procedures for [¹⁴C]sipoglitazar and its metabolites

The incubation procedures described above were terminated by the addition of acetonitrile at a volume equivalent to the volume of the reaction mixture and centrifuging at approximately 1500×g for 10 minutes. The supernatant was analyzed by an HPLC (LC-10 gradient system; Shimadzu Corp., Kyoto, Japan) with an on-line RI detector (D505TR Flow Scintillation Analyzer, PerkinElmer Life and Analytical Sciences, Waltham, MA). The typical HPLC analytical method was as follows: Separation of the metabolites was carried out on an Inertsil ODS-3 (5-μm particle size, 150 or 250 × 4.6 mm I.D.; GL Sciences, Tokyo, Japan) at 40°C or 4°C, after gradient elution using acetonitrile, H₂O and TFA. The acetonitrile concentration was increased from 34% to 66% over a period of 40 minutes and held at 86% for 10 minutes. Throughout the elution, the flow of 0.1% of TFA was continued, and the flow rate was 0.5 or

1 mL/min. On-line RI detection was carried out using Ultima-Flo as the flow scintillation cocktail.

Results

Metabolic profiles of [¹⁴C]sipoglitazar with human hepatocytes and liver microsomes

The metabolic profile of [¹⁴C]sipoglitazar was examined using human hepatocytes and liver microsomes (Figure III-1). In the reactions with hepatocytes, the deethylated metabolite (M-I) and the glucuronide conjugate of sipoglitazar (sipoglitazar-G) were the main metabolites and the hydrolyzed metabolite (M-II) was also detected as a minor metabolite. To separate the reactions of oxidation and glucuronidation, metabolic studies using liver microsomes with or without their cofactors, NADPH-generating system, and UDPGA were conducted. When both an NADPH-generating system and UDPGA were added, the metabolites were detected with similar profiles in the reactions with hepatocytes. Addition of only an NADPH-generating system to the reaction mixture resulted in the formation of M-II and a limited amount of M-I. When only UDPGA was added to the microsomal reaction mixture, sipoglitazar-G was formed extensively.

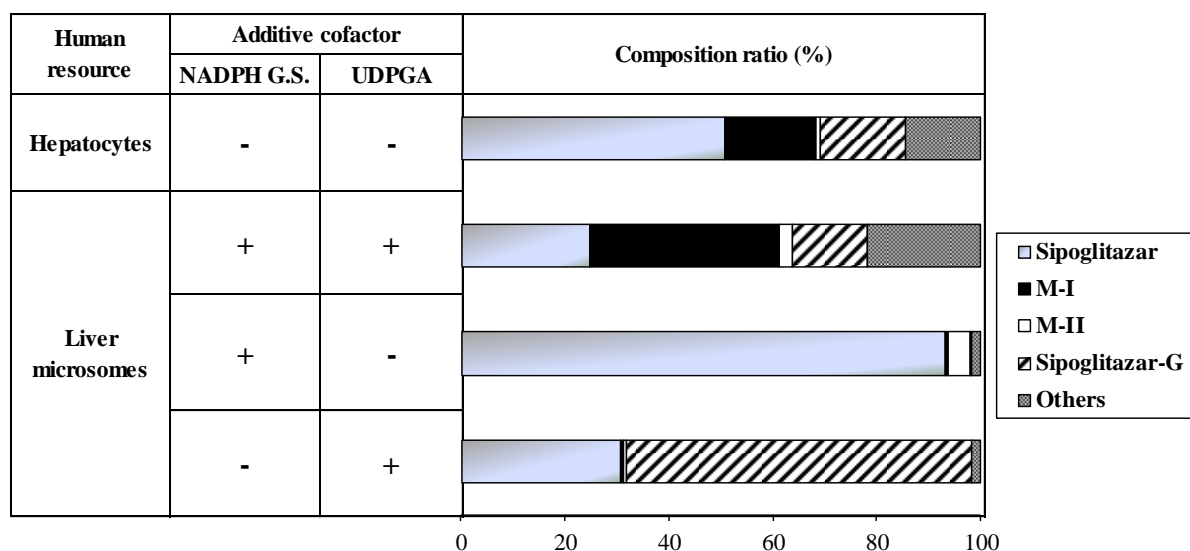


Figure III-1. Composition of metabolites of [¹⁴C]sipoglitazar formed by human hepatocytes and liver microsomes

The composition ratio represents the ratio of sipoglitazar and its metabolites, when the total radioactivity in the incubation mixture is regarded as 100%. Other compositions were calculated by subtracting the sum of sipoglitazar and its metabolites from 100%. Data represent the means of duplicate determinations.

NADPH G.S.: NADPH-generating system

Preparation of sipoglitazar-G1 and sipoglitazar-G2

In the course of metabolic analysis of sipoglitazar-G formed by liver microsomes, sipoglitazar-G in the reaction mixture was revealed to consist of two isomers. In the HPLC analysis with the column set at 40°C, sipoglitazar-G was detected as one peak (Figure III-2A),

but two separate peaks originating from sipoglitazar-G were detected, when the temperature of the column for HPLC analysis was changed to 4°C and these were named sipoglitazar-G1 and sipoglitazar-G2 according to the elution order (Figure III-2B).

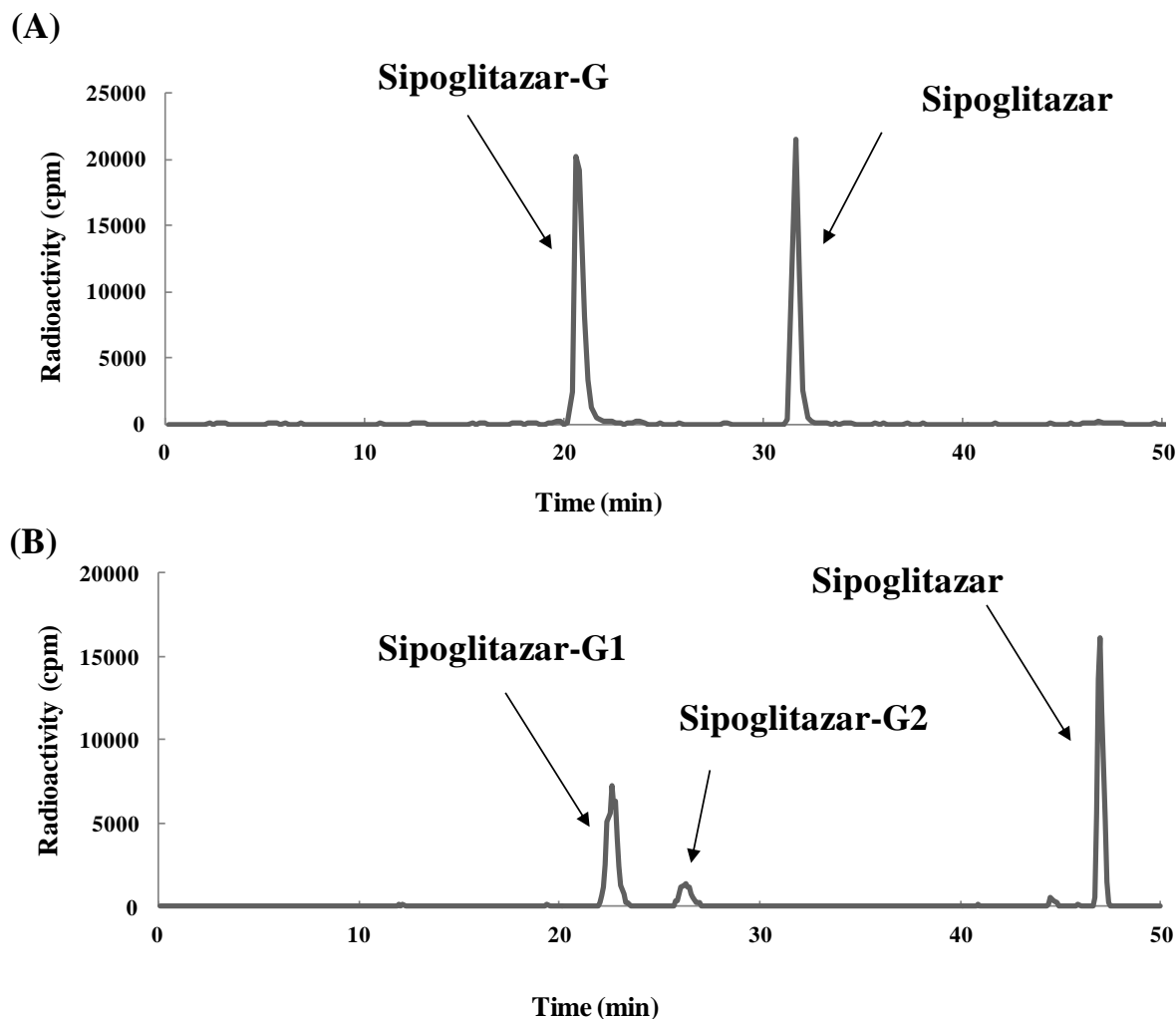


Figure III-2. Representative HPLC-radiochromatograms of the incubation mixture of sipoglitazar with human liver microsomes in the presence of UDPGA

This HPLC-radiochromatogram is for the preparation of [^{14}C]sipoglitazar-G (A) and for that of [^{14}C]sipoglitazar-G1 and [^{14}C]sipoglitazar-G2 (B). [^{14}C]sipoglitazar (100 μM) was incubated with human liver microsomes (2 mg protein/mL) in the presence of UDPGA (5 mM) at 37°C for 4 hours. The metabolites were separated on an Inertsil ODS-3 (5- μm particle size, (A) 150 \times 4.6 mm I.D., (B) 250 \times 10 mm I.D.; GL Sciences, Tokyo, Japan) at 40°C (A) and 4°C (B), after gradient elution using acetonitrile, H₂O and TFA. The acetonitrile concentrations were as follows: (A), it was increased from 34% to 66% over a period of 40 minutes and held at 86% for 10 minutes. (B), it was held at 45.2% for 30 minutes, increased from 45.2% to 90% over a period of 10 minutes and held at 90% for 10 minutes. Throughout the elution, the flow of 0.1% TFA was continued and the flow rate was 1.0 mL/min (A) and 2.4 mL/min (B).

LC-MS/MS analysis of sipoglitazar-G1 and sipoglitazar-G2

To elucidate the properties of the two types of sipoglitazar glucuronides, [¹⁴C]sipoglitazar-G1 and [¹⁴C]sipoglitazar-G2 were each analyzed by LC-MS/MS. The full ion mass spectrum of sipoglitazar-G1 gave the [M+H]⁺ at *m/z* 642 (Figure III-3A), which was 176 amu higher than that of the parent compound. The characteristic fragment ions in the product ion mass spectrum at *m/z* 642 were detected at *m/z* 466, 282 and 174 (Figure III-3B). The ion at *m/z* 466 was derived by diagnostic loss of the sugar moiety (-176 amu). The ions at *m/z* 282 and 174 were the same as those of unchanged sipoglitazar. The full ion mass spectrum of sipoglitazar-G2 gave the [M+H]⁺ at *m/z* 642 (Figure III-4A), which was 176 amu higher than that of the parent compound. The characteristic fragment ions in the product ion mass spectrum at *m/z* 642 were detected at *m/z* 624, 282 and 174 (Figure III-4B). The ion at *m/z* 624 was a dehydrated ion. The ions at *m/z* 282 and 174 were the same as those of the parent compound. Alkaline hydrolysis (0.1 M sodium hydroxide solution, at 37°C for 2 hours) of the peaks at *m/z* 642 of sipoglitazar-G1 and -G2 gave sipoglitazar in the LC-MS, whereas enzymatic hydrolysis [5 w/v% of sulfatase containing β-glucuronidase (type H-1) at 37°C for 2 hours] of the peaks at *m/z* 642 of sipoglitazar-G1 gave sipoglitazar in the LC-MS, but that of sipoglitazar-G2 could not show the cleave (data not shown). From these results, sipoglitazar-G1 and sipoglitazar-G2 are shown to be isomers with respect to the site of glucuronidation.

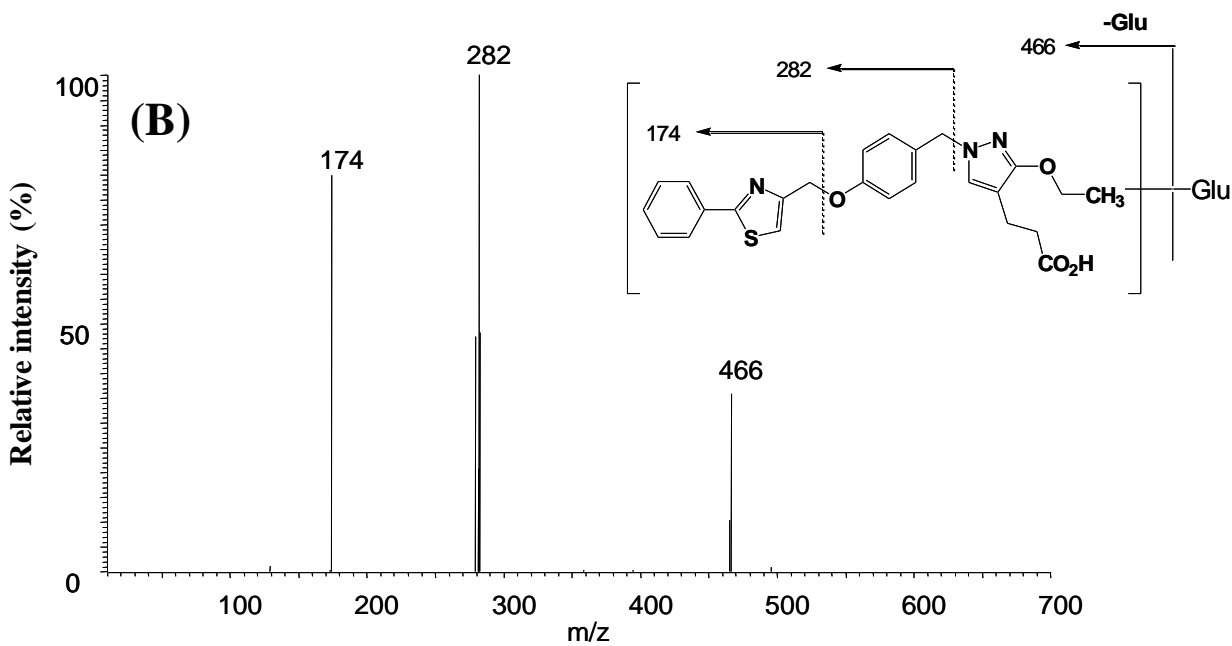
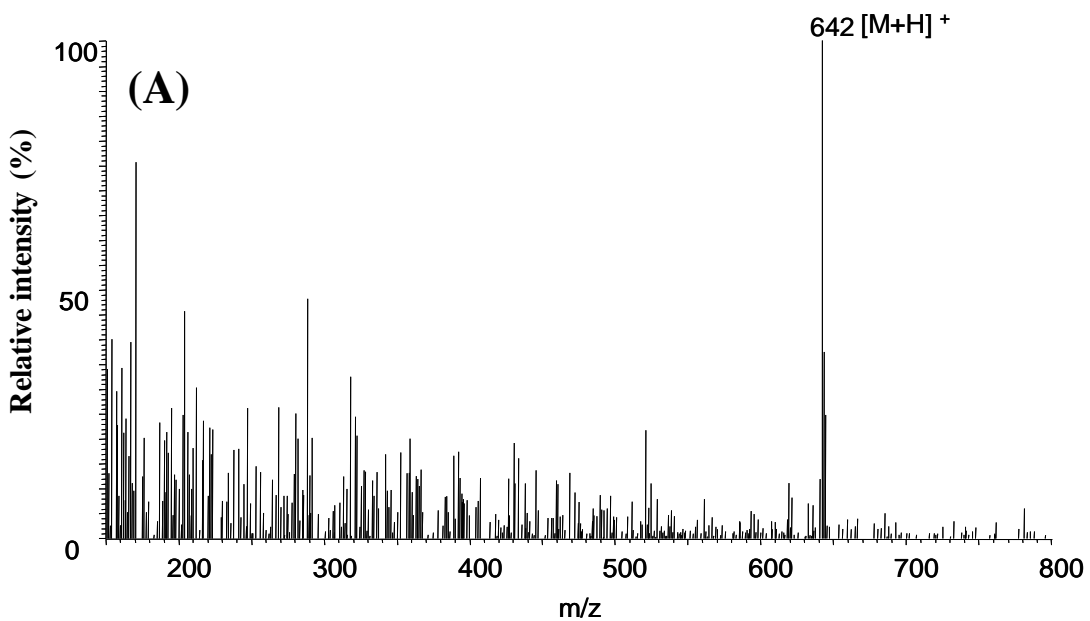


Figure III-3. Full ion mass spectrum of sipoglitazar-G1 (A), and its product ion mass spectrum of the precursor ion at m/z 642 (B)

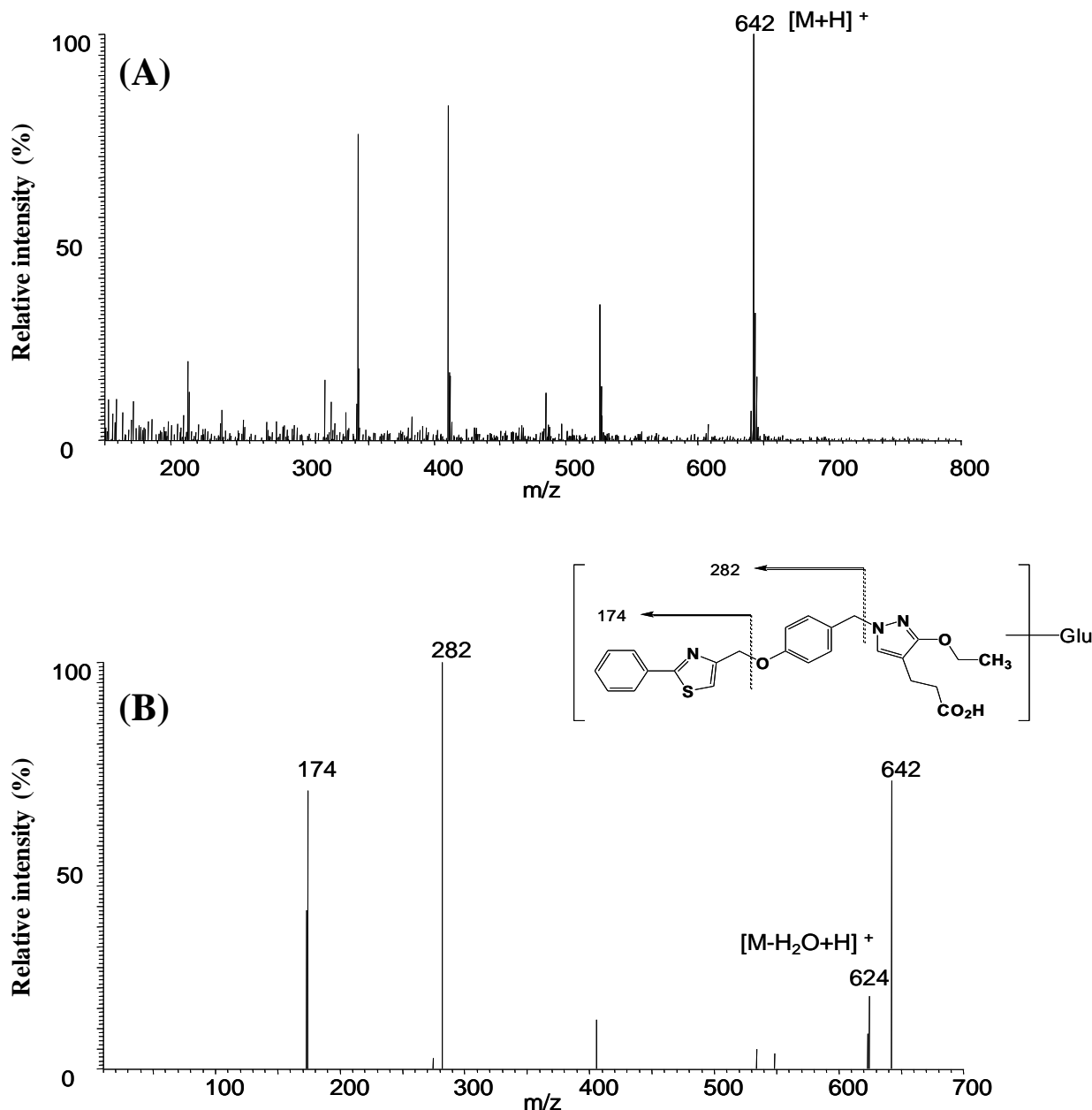


Figure III-4. Full ion mass spectrum of sipoglitazar-G2 (A), and its product ion mass spectrum of the precursor ion at m/z 642 (B)

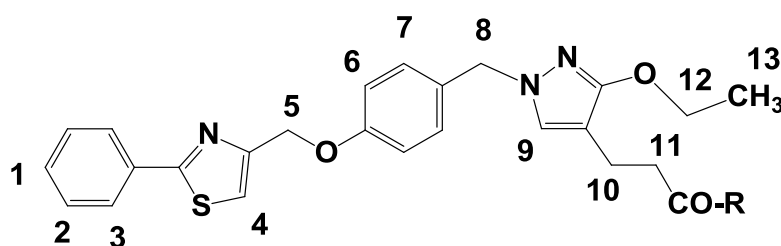
NMR analysis of sipoglitazar-G1 and sipoglitazar-G2

To determine the site of glucuronidation of sipoglitazar-G1 and sipoglitazar-G2, an $^1\text{H-NMR}$ spectrum analysis was performed (Table III-1). In the $^1\text{H-NMR}$ spectrum of sipoglitazar-G1, proton signals assigned to H-10 and H-11 shifted downfield (δ 2.48 to 2.54-2.62 ppm) compared with those of sipoglitazar. This metabolite showed novel signals indicative of a glucuronic acid moiety (five protons, δ 3.38-5.45 ppm) and the split of the anomeric proton signal (δ 5.45 ppm, d, $J=7.7$ Hz) showed a β -glucuronide. The $^1\text{H-NMR}$ spectrum of sipoglitazar-G2 was similar to that of sipoglitazar-G1 except for a glucuronic acid moiety,

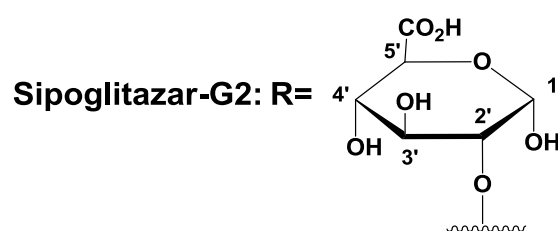
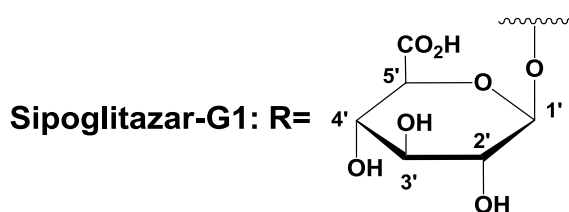
namely, (a) the anomeric proton signal shifted downfield (δ 5.45-5.20 ppm) and the coupling constants were 3.6 Hz, and (b) the proton signal assigned to H-2' shifted upfield (δ 3.38-4.57 ppm). From these results, sipoglitazar-G1 was estimated to be the β -1-*O*-acyl glucuronide of sipoglitazar and sipoglitazar-G2 was the α -2-*O*-acyl glucuronide.

Table III-1. ^1H Chemical shifts of sipoglitazar and its metabolites

H No.	$\delta(\text{ppm}), J(\text{Hz})$		
	Sipoglitazar	Sipoglitazar-G1	Sipoglitazar-G2
1	7.45-7.48 (m)	7.45-7.49 (m)	7.45-7.50 (m)
2	7.45-7.48 (m)	7.45-7.49 (m)	7.45-7.50 (m)
3	7.90 (m)	7.90 (m)	7.91 (m)
4	7.22 (s)	7.25 (s)	7.26 (s)
5	5.16 (s)	5.17 (s)	5.17 (s)
6	6.97 (d, $J=8.7$)	6.97 (d, $J=8.5$)	6.97 (d, $J=8.6$)
7	7.15 (d, $J=8.7$)	7.14 (d, $J=8.5$)	7.16 (d, $J=8.6$)
8	4.94 (s)	4.92 (s)	4.94 (s)
9	7.49 (s)	7.50 (s)	7.51 (s)
10	2.48 (m)	2.54-2.62 (m)	2.54-2.58 (m)
11	2.48 (m)	2.54-2.62 (m)	2.54-2.58 (m)
12	4.07 (q, $J=7.0$)	ca. 4.1 (hidden)	4.08 (q, $J=7.0$)
13	1.25 (t, $J=7.0$)	1.25 (t, $J=7.0$)	1.26 (t, $J=7.0$)
1'	---	5.45 (d, $J=7.7$)	5.20 (d, $J=3.6$)
2'	---	3.38 (m)	4.57 (dd, $J=9.6, 3.6$)
3'	---	3.45-3.52 (m)	3.80 (m)
4'	---	3.45-3.52 (m)	3.55 (m)
5'	---	3.89 (d, $J=8.8$)	4.20 (d, $J=10.2$)



Sipoglitazar: R=H



Stability and interconversion of sipoglitazar-G1 and sipoglitazar-G2

To investigate the stability and interconversion between [¹⁴C]sipoglitazar-G1 and [¹⁴C]sipoglitazar-G2, these compounds were incubated in KPB (pH 7.4), acetate buffer (pH 4.4), rat bile and human plasma (Figure III-5). In acetate buffer (pH 4.4), sipoglitazar-G1 and sipoglitazar-G2 were stable, and neither degradation nor interconversion was observed. In both KPB (pH 7.4) and rat bile, a similar composition change was shown, and sipoglitazar-G1 was gradually eliminated to form sipoglitazar-G2 and sipoglitazar. Sipoglitazar-G2 was slightly eliminated to form sipoglitazar, but conversion from sipoglitazar-G2 to -G1 was not observed. More significant deglucuronidation and sipoglitazar-G1 to sipoglitazar-G2 conversion were also observed in rat bile. In human plasma, sipoglitazar-G1 was converted to sipoglitazar-G2 immediately after the mixing with human plasma, and thereafter both sipoglitazar-G1 and sipoglitazar-G2 were gradually eliminated to form sipoglitazar. Sipoglitazar-G2 was gradually eliminated to form sipoglitazar, but conversion from sipoglitazar-G2 to sipoglitazar-G1 was not observed. These results indicate that sipoglitazar-G1 could be converted to sipoglitazar-G2 and then to sipoglitazar from both sipoglitazar-G1 and -G2.

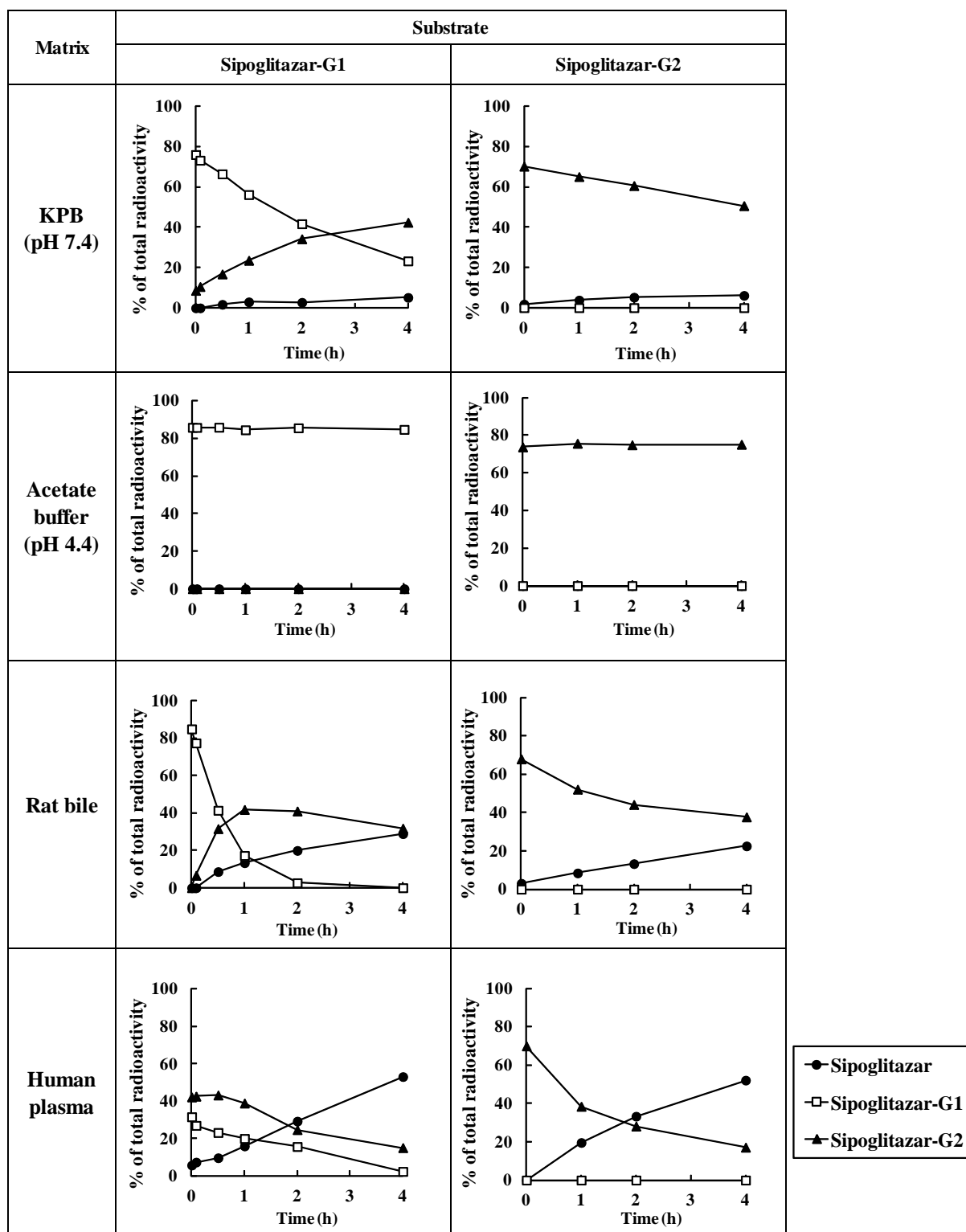


Figure III-5. Stability and interconversion of sipoglitazar-G1 and sipoglitazar-G2 in KPB (pH 7.4), acetate buffer (pH 4.4), rat bile, and human plasma

Each ratio of radioactivity of sipoglitazar (●), sipoglitazar-G1 (□) and sipoglitazar-G2 (▲) was expressed, whereas the total radioactivity in the incubation mixture is regarded as 100%.

Oxidative metabolisms of sipoglitazar-G1 and sipoglitazar-G2

[¹⁴C]sipoglitazar-G1 and [¹⁴C]sipoglitazar-G2 were metabolized by human liver microsomes with or without an NADPH-generating system (Figure III-6A-D). Sipoglitazar was formed from both [¹⁴C]sipoglitazar-G1 and [¹⁴C]sipoglitazar-G2 regardless of the presence of an NADPH-generating system. M-I was formed only when [¹⁴C]sipoglitazar-G1 was metabolized with an NADPH-generating system (Figure III-6A). In this study, HPLC analysis was performed under conditions in which sipoglitazar-G1 and sipoglitazar-G2 could not be detected separately; therefore, the interconversion between sipoglitazar-G1 and sipoglitazar-G2 could not be evaluated.

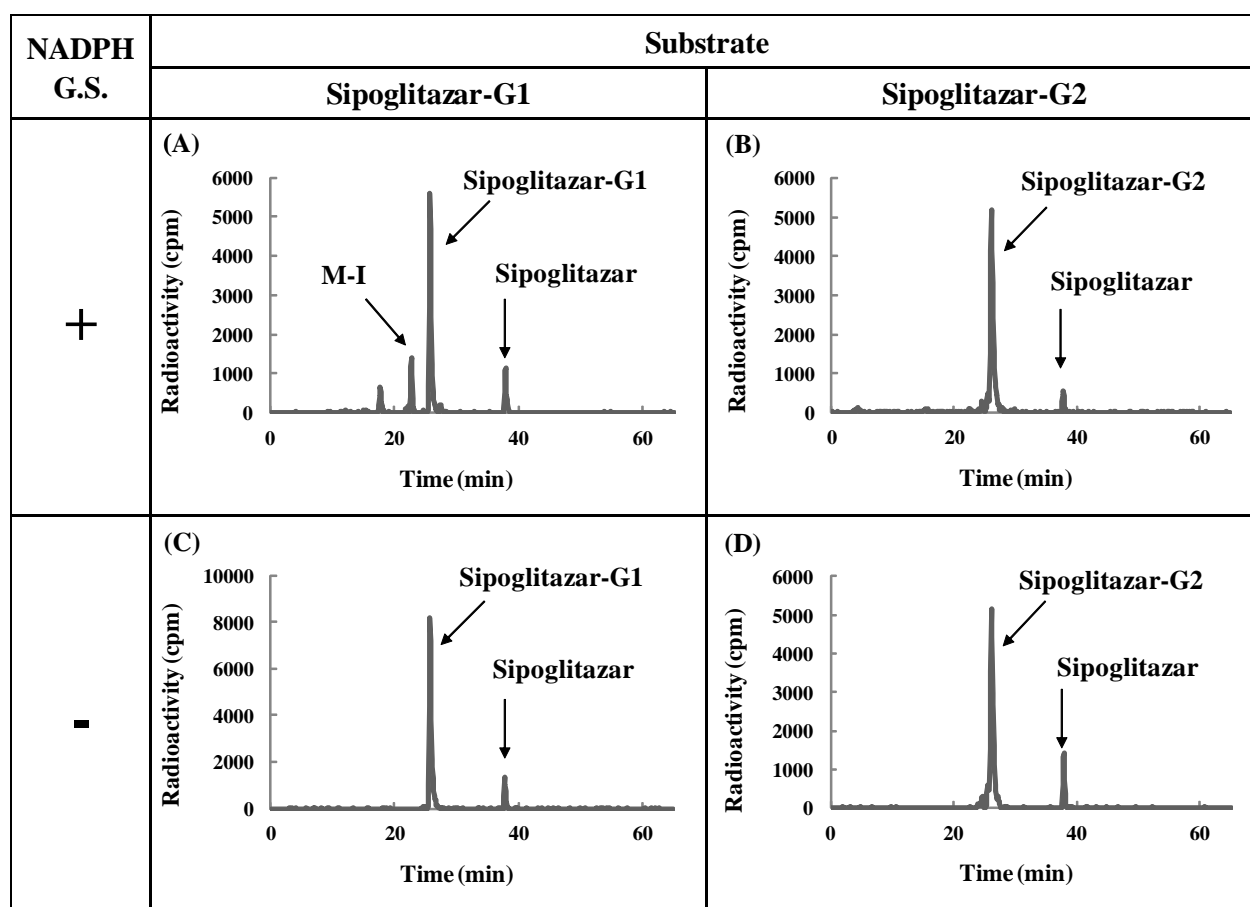


Figure III-6. Representative HPLC-radiochromatograms of the incubation mixture of sipoglitazar-G1 or sipoglitazar-G2 by human liver microsomes with or without an NADPH-generating system (NADPH G.S.)

Identification of the CYP isoform involved in the metabolism of [¹⁴C]sipoglitazar-G1

The CYP isoform involved in the formation of M-I from sipoglitazar-G1 was identified by a metabolic study using microsomes expressing human CYP isoforms and a correlation study using liver microsomes from 16 individual humans (Figure III-7 and Table III-2). CYP2C8-expressing microsomes showed extensive activity to form M-I (Figure III-7). In the correlation study, the elimination rate of [¹⁴C]sipoglitazar-G1 and the formation rate of

M-I correlated most strongly with paclitaxel 6 α -hydroxylase activity (CYP2C8) (Table III-2). Sipoglitazar-G1 elimination and M-I formation were also correlated with the *S*-mephenytoin *N*-demethylation activity (CYP2B6) and chlorzoxazone 6-hydroxylation activity (CYP2E1). However, sipoglitazar-G1 was hardly metabolized by CYP2B6 and CYP2E1 enzymes (Figure III-7). From these results, CYP2C8 is considered to be the main CYP isoform involved in the formation of M-I from sipoglitazar-G1.

Table III-2. Correlation coefficients for the metabolism of [¹⁴C]sipoglitazar-G1 with CYP isoform-specific activities

Isoform-Specific Activity	CYP enzymes	Correlation Coefficient (<i>r</i>)	
		Sipoglitazar-G1 elimination	M-I formation
7-Ethoxyresorufin <i>O</i> -dealkylation	CYP1A2	-0.189	-0.062
Coumarin 7-hydroxylation	CYP2A6	0.498	0.287
<i>S</i> -Mephenytoin <i>N</i> -demethylation	CYP2B6	0.769	0.704
Paclitaxel 6 α -hydroxylation	CYP2C8	0.896	0.977
Diclofenac 4'-hydroxylation	CYP2C9	0.486	0.326
<i>S</i> -Mephenytoin 4'-hydroxylation	CYP2C19	0.078	0.076
Dextromethorphan <i>O</i> -demethylation	CYP2D6	0.152	0.353
Chlorzoxazone 6-hydroxylation	CYP2E1	0.698	0.609
Testosterone 6 β -hydroxylation	CYP3A4/5	0.475	0.439
Lauric acid 12-hydroxylation	CYP4A9/11	0.351	0.310

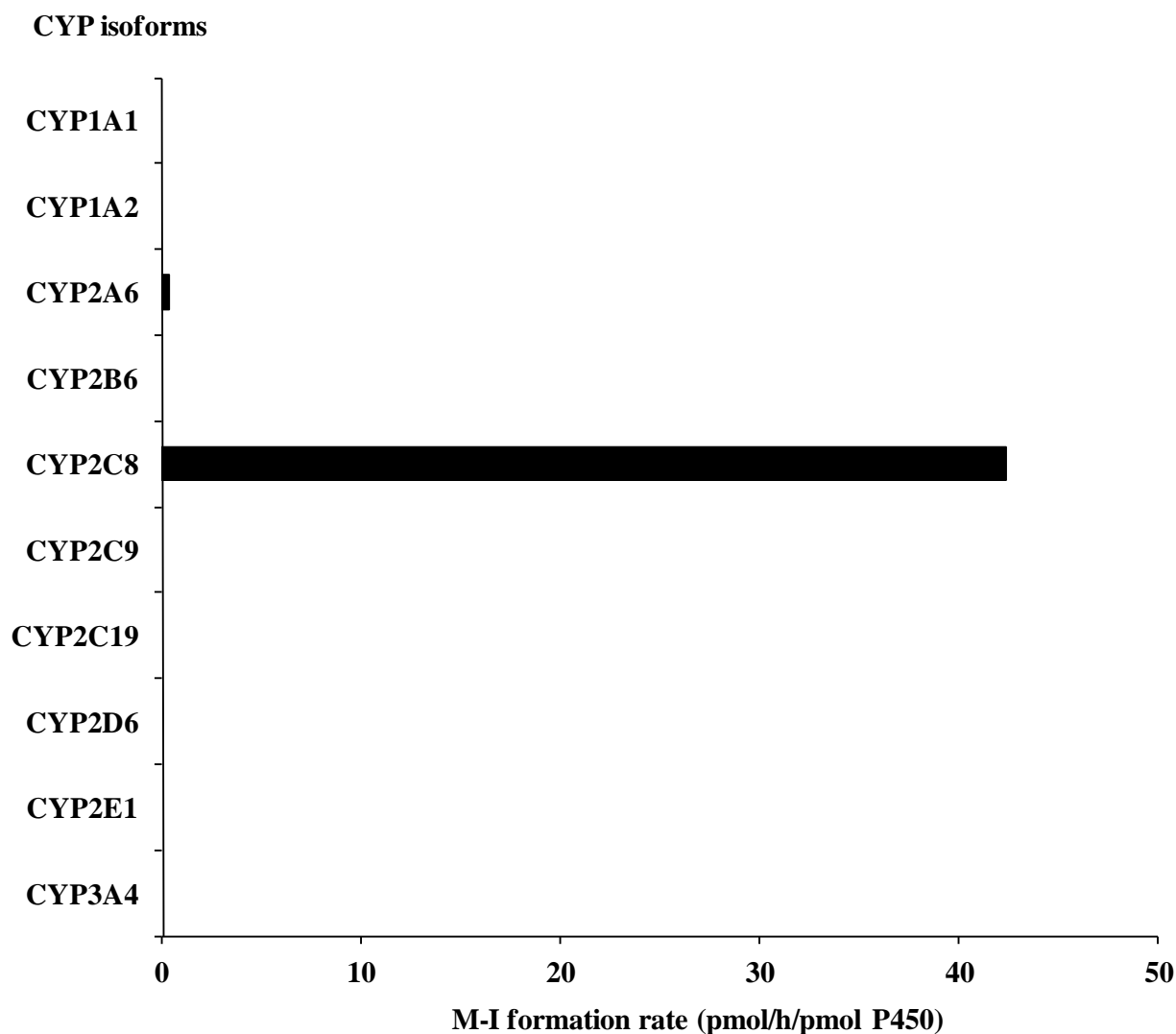


Figure III-7. Formation of M-I from [¹⁴C]sipoglitazar-G by specific human CYP-expressing microsomes

Data represent the means of duplicate determinations.

Effect of gemfibrozil on the *in vitro* oxidative metabolism and/or glucuronidation of [¹⁴C]sipoglitazar

In the presence of both an NADPH generating system and UDPGA, sipoglitazar was metabolized to M-I, M-II, sipoglitazar-G1, sipoglitazar-G2, and unidentified metabolites. Elimination of sipoglitazar and formation of M-I and M-II were inhibited by gemfibrozil, and the relative activities at 300 μM gemfibrozil were 58.7%, 9.1%, and 13.4%, respectively (Figure III-8). However, sipoglitazar-G1 formation was increased rather than inhibited and the relative activities at 10, 30, 100, and 300 μM gemfibrozil were 103.5%, 110.3%, 130.3%, and 125.9%, respectively.

In the presence of UDPGA without an NADPH-generating system, sipoglitazar was mainly

metabolized to sipoglitazar-G1. Elimination of sipoglitazar and formation of sipoglitazar-G1 were inhibited by gemfibrozil, and the relative activities at 300 μM gemfibrozil were 66.8% and 65.7%, respectively (Figure III-8).

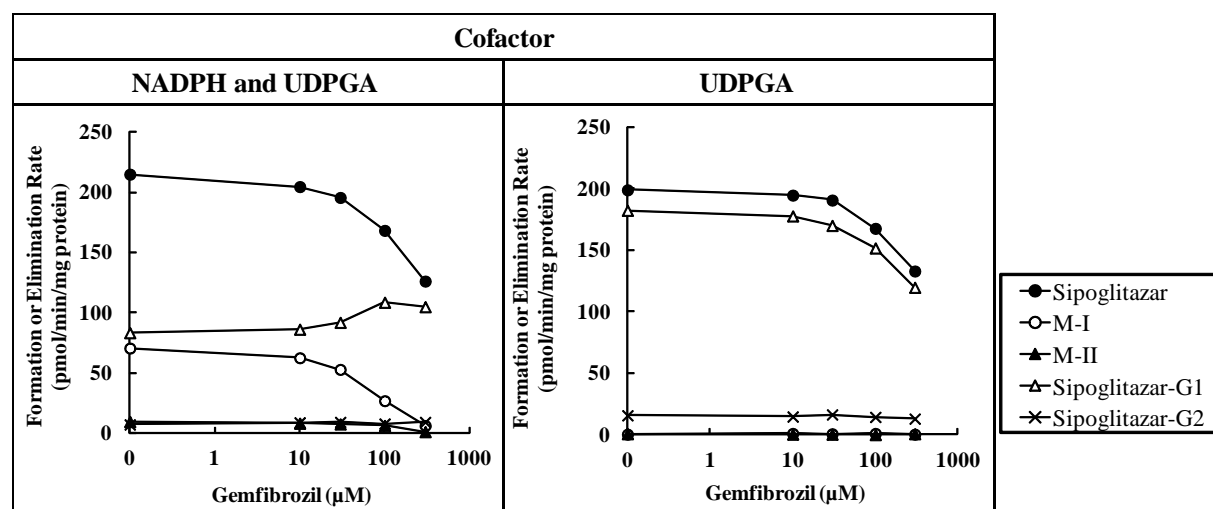


Figure III-8. Effect of gemfibrozil on the *in vitro* oxidative metabolism and/or glucuronidation of [^{14}C]sipoglitazar

Data represent the means of duplicate determinations.

Discussion

In general, drug metabolism reactions are divided into the reactions of such functional groups such as oxidation, reduction, and hydrolysis (phase I) and conjugative reactions such as glucuronidation and sulfation (phase II). In *in vivo* animal ADME studies and *in vitro* studies using hepatocytes, the deethylated metabolite of sipoglitazar (M-I), hydrolyzed metabolite of sipoglitazar (M-II), and glucuronide conjugate of sipoglitazar (sipoglitazar-G) were observed [10]. Furthermore, M-I was also measured as the main metabolite in the plasma of humans orally administered sipoglitazar. Therefore, sipoglitazar M-I and M-II were considered to be formed by phase I oxidative enzymes such as CYP, and sipoglitazar-G was formed by UGT, a phase II metabolic enzyme. To separate the reactions of oxidation and glucuronidation, an *in vitro* metabolic study was conducted using human liver microsomes with and without an NADPH-generating system and UDPGA [49] (Figure III-1), because an NADPH-generating system and UDPGA are essential cofactors for CYP and UGT, respectively. When both the cofactors were added to the *in vitro* reaction mixture, M-I, M-II and sipoglitazar-G were formed from sipoglitazar. However, in oxidative conditions, formation of M-II was observed and M-I could hardly be detected, whereas only sipoglitazar-G was formed in the glucuronidation condition. These results indicated that M-I formation requires both CYP and UGT and also suggested that sipoglitazar-G could be an intermediate in the formation of M-I from sipoglitazar.

To examine the metabolism of sipoglitazar-G in detail, isolation of sipoglitazar-G from an *in*

vitro sample was performed. Of interest, under an appropriate HPLC condition, sipoglitazar-G prepared by liver microsomes was revealed to consist of two isomers (Figure III-2). The main isomer observed in the *in vitro* reactant was named sipoglitazar-G1. The other sipoglitazar-G isomer with the longer retention time, named sipoglitazar-G2, showed the same retention time in the HPLC and LC-MS/MS spectrum as the sipoglitazar-G detected in the bile of [¹⁴C]sipoglitazar-administered rats. Further analysis of sipoglitazar-G1 and sipoglitazar-G2 by LC-MS/MS and ¹H-NMR revealed that sipoglitazar-G1 was a β -1-*O*-acyl glucuronide and sipoglitazar-G2 was an α -2-*O*-acyl glucuronide (Table III-1, Figures III-3 and 4). These results showed that the sipoglitazar-G1 has been detected only in *in vitro* studies, whereas the sipoglitazar-G detected in the *in vivo* studies was sipoglitazar-G2.

To clarify the reason that only sipoglitazar-G2 was detected in *in vivo* studies, the stability and interconversion of the sipoglitazar glucuronides were examined. The different properties of these isomers between sipoglitazar-G1 and sipoglitazar-G2 were caused by irreversible internal migration of the glucuronides (Figure III-5). In the neutral condition, sipoglitazar-G1 was converted to sipoglitazar-G2, whereas sipoglitazar-G2 was not converted to sipoglitazar-G1. Moreover, sipoglitazar was formed by deconjugation from both sipoglitazar-G1 and sipoglitazar-G2. These conversions were significantly observed in rat bile and human plasma. From these results, it is believed that sipoglitazar-G1 is rapidly converted to sipoglitazar-G2 and sipoglitazar and is biotransformed to M-I simultaneously in *in vivo* conditions. Therefore, of the two isomers, only sipoglitazar-G2 was detected *in vivo*. Such conversion is generally known with acyl glucuronides for which β -1-*O*-acyl glucuronide is irreversibly converted to the 2-*O*-isomer [50]. The rates of acyl migration depend on the temperature and pH, with such compounds being more stable in low temperature and acidic conditions [47,48,51], and also depending on the solvent [48,52] and the nature of the aglycone [53,54]. These properties of the acyl glucuronides would support the clarification of the metabolic pathway of sipoglitazar.

To elucidate the metabolic pathways of sipoglitazar, [¹⁴C]sipoglitazar-G1 and [¹⁴C]sipoglitazar-G2 were metabolized by human liver microsomes with and without an NADPH-generating system (Figure III-6). In either condition, deglucuronidation of both sipoglitazar-G1 and sipoglitazar-G2 was observed. In contrast, M-I was formed only from sipoglitazar-G1, and the reaction was dependent on the presence of NADPH, whereas M-I was not formed from sipoglitazar-G2. These results indicate that CYP may be involved in the formation of M-I from sipoglitazar-G1. Further investigations to identify the CYP isoform revealed that CYP2C8 was involved in the oxidation of sipoglitazar-G1 (Table III-2 and Figure III-7). In total, it is considered that M-I formation occurs via the oxidation of sipoglitazar-G1 by CYP2C8, and it was clarified that the glucuronide is a substrate for oxidative metabolism by CYP.

This unusual metabolic pathway has already been reported in several studies showing that glucuronides of diclofenac, β -estradiol and MRL-C could be a substrate for oxidative

metabolism by CYP [55,56,57]. CYP2C8 is also involved in the oxidation of these compounds. These compounds are supposed to have easier access to the active site of CYP2C8 by the polarization of the compound by glucuronidation. This finding is a common feature with CYP2C8 substrates, revealed from the pharmacophore analysis of CYP2C8; CYP2C8 substrates have a long hydrophobic chain with an acidic or polar group and a hydrophobic or aromatic moiety, and another structural feature of CYP2C8 probably causing this is an active site, Arg [58,59,60]. Although sipoglitazar also has a similar structural property, there was a big difference between sipoglitazar and these compounds. Of interest, M-I was formed only when sipoglitazar was metabolized via glucuronidation, whereas the position subject to oxidation in the glucuronides of diclofenac and MRL-C could be also oxidized by other CYPs, and their glucuronidation was not always essential to form their oxidative metabolites. This difference suggests that the metabolism of sipoglitazar-G1 is more CYP2C8-selective than that of the other compounds and makes the metabolic pathway of sipoglitazar very unique. Furthermore, gemfibrozil-1-*O*- β -glucuronide is well known as CYP2C8 inhibitor and could cause drug-drug interactions at the level of transporters [61,62,63]. Sipoglitazar also has a similar property with gemfibrozil in terms of the structure and the involvement of CYP2C8 in its metabolic pathway. The effects of gemfibrozil on the *in vitro* oxidative metabolism and/or glucuronidation of sipoglitazar were investigated on the basis of the metabolite profile of sipoglitazar (Figure III-8). In this study, gemfibrozil could inhibit the glucuronidation of sipoglitazar concentration-dependently in the presence of UDPGA and M-I formation in the presence of an NADPH-generating system and UDPGA, resulting in sipoglitazar-G1 accumulation. These results indicate that the oxidation is affected more extensively than glucuronidation by gemfibrozil, which might be due to the gemfibrozil and gemfibrozil-1-*O*- β -glucuronide as an inhibitor of CYP2C8 and support the fact that the formation of M-I from sipoglitazar-G1 depended on CYP2C8. Therefore, sipoglitazar has a possibility of increasing the plasma level by inhibition of the oxidation metabolism when gemfibrozil is coadministered.

From the results of this study, the metabolic pathway of sipoglitazar is postulated as follows (Figure III-9). Sipoglitazar is metabolized via glucuronidation by UGT to give sipoglitazar-G1 as a first step, and sipoglitazar-G1 is deethylated by CYP2C8 to form M-I. Part of sipoglitazar-G1 is metabolized via deglucuronidation to sipoglitazar or is subsequently converted by acyl migration to sipoglitazar-G2. M-II was formed directly from sipoglitazar. In consideration of this metabolic pathway of sipoglitazar in detail, the deethylated sipoglitazar-G1, namely the acyl glucuronide of M-I, is expected to exist as the intermediate between sipoglitazar-G1 and M-I. Moreover, in the deglucuronidation of acyl glucuronide, an interesting metabolic pathway was reported for statins, namely hydroxymethylglutaryl-CoA reductase inhibitors [64,65]. Statin acyl glucuronide could be lactonized spontaneously and metabolized via deglucuronidation to the formed statin lactone when hydrolyzed to the open acid chemically or enzymatically. If structural similarity is

taken into consideration, the deethylated sipoglitazar-G1 has the possibility of being metabolized to M-I through the lactone or being induced chemically, because the structure of deethylated sipoglitazar-G1 could be superimposed on the structure of statin acyl glucuronide (Figure III-10). Unfortunately, a lactone-form intermediate could not be detected in the *in vitro* [^{14}C]sipoglitazar-G1 reactant. Too rapid hydrolysis of the lactone-form intermediate might be one of the reasons for this. Further investigation for M-I formation is also necessary.

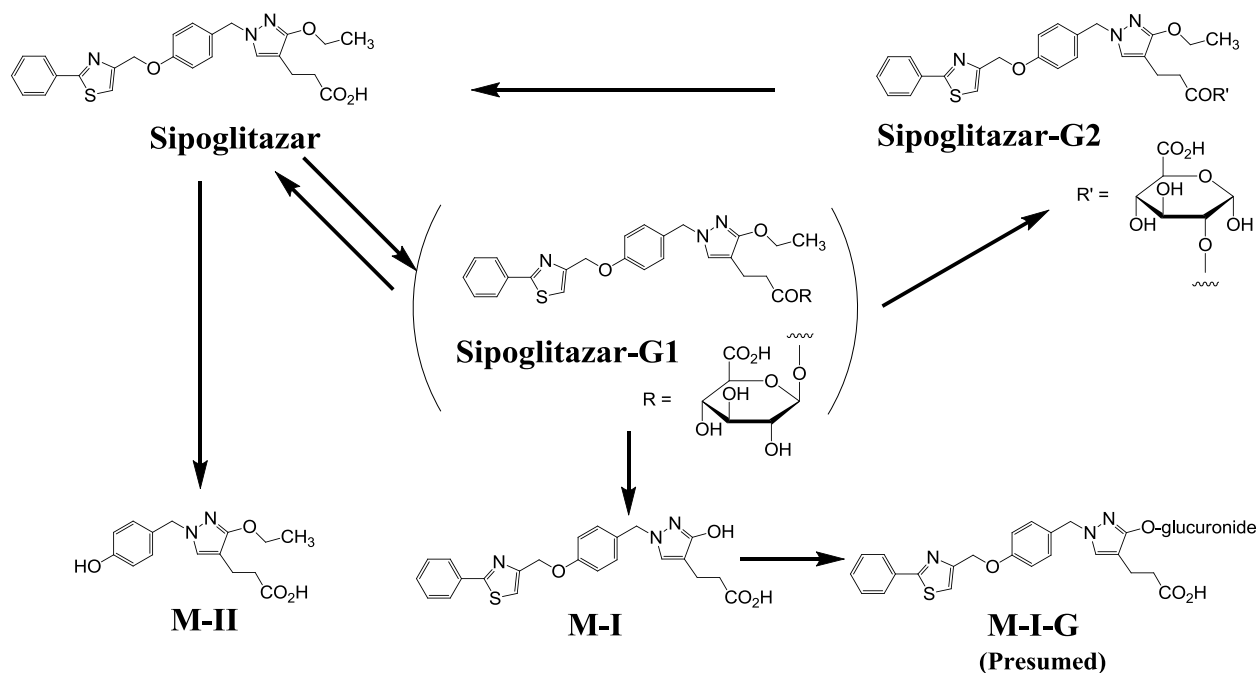


Figure III-9. Postulated metabolic pathways of sipoglitazar
M-I-G: glucuronide of M-I

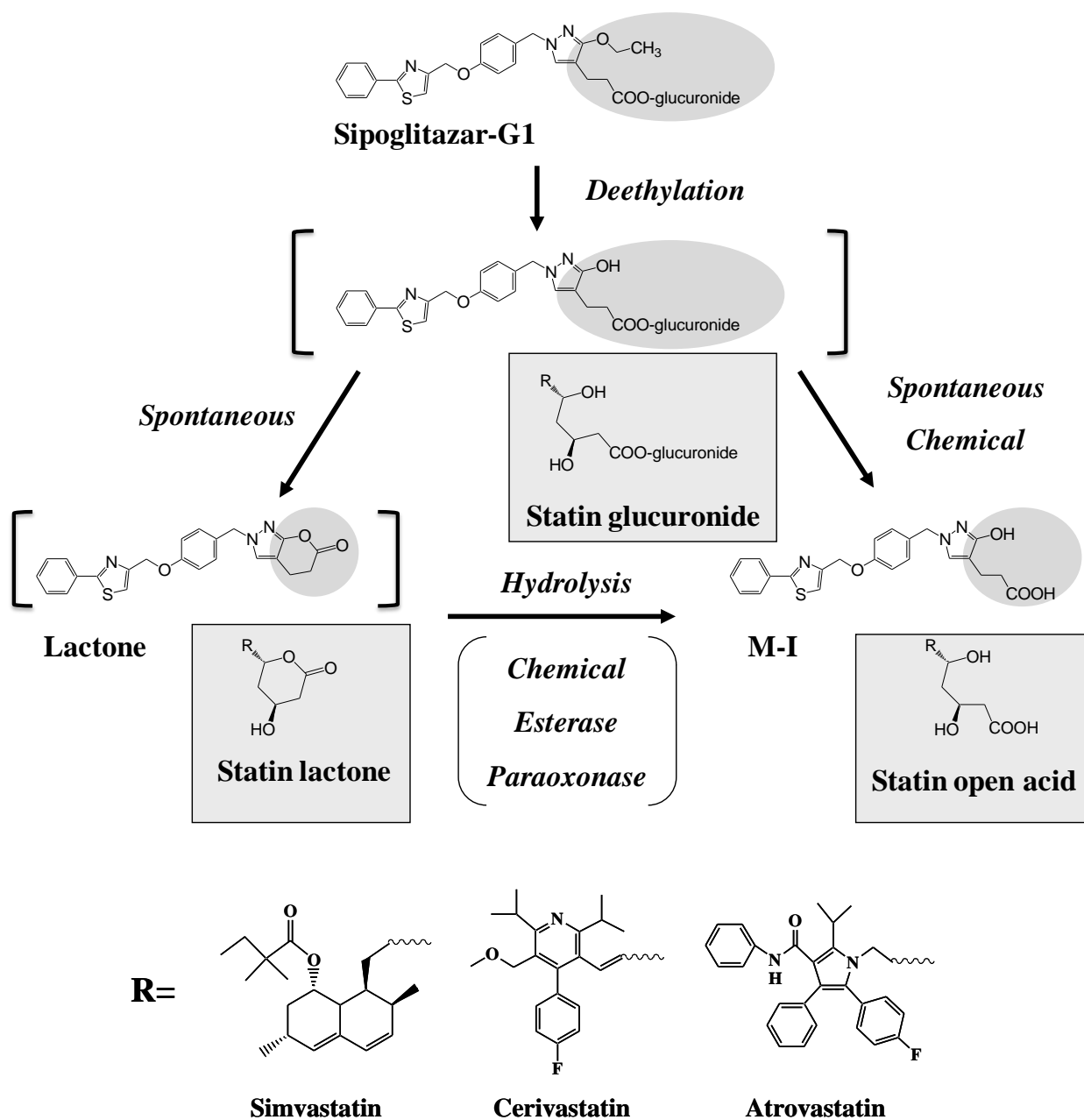


Figure III-10. Possible metabolic pathway of sipoglitazar-G1 via lactone-form and metabolic pathway of statin glucuronide

In conclusion, the present study demonstrates the unusual deethylation pathway of sipoglitazar, which is metabolized via glucuronidation by UGT, a phase II metabolic enzyme, as a first step to form an unstable β -1-*O*-acyl glucuronide, and this acyl glucuronide is deethylated by CYP2C8, a phase I metabolic enzyme. The deethylated sipoglitazar acyl glucuronides are immediately metabolized via deglucuronidation spontaneously or enzymatically to form M-I, deethylated sipoglitazar.

Summary

Animal pharmacokinetic studies of sipoglitazar, a novel anti-diabetic agent, showed that the deethylated metabolite (M-I) and the glucuronide conjugate of sipoglitazar (sipoglitazar-G) appeared to be the key metabolites in the elimination process. M-I was also measured as the main metabolite in the plasma of humans administered sipoglitazar. *In vitro* metabolic studies were performed to investigate the metabolic pathways from sipoglitazar to M-I in humans. The metabolic profile with human hepatocytes and liver microsomes indicated that M-I was not formed directly from sipoglitazar and that sipoglitazar-G was involved in the metabolism from sipoglitazar to M-I. Further studies of the metabolism of sipoglitazar-G revealed that the properties of the glucuronide conjugate and its metabolism are as follows: HPLC, LC-MS/MS and NMR analyses showed that sipoglitazar-G was composed of two glucuronides; sipoglitazar-G1, a β -1-*O*-acyl glucuronide and sipoglitazar-G2, an α -2-*O*-acyl glucuronide. The stability study of these glucuronides suggested that sipoglitazar-G1 could be converted to sipoglitazar-G2 and sipoglitazar, but sipoglitazar-G2 could not be converted to sipoglitazar-G1. The oxidative metabolic study of sipoglitazar-G1 and -G2 with human liver microsomes and CYP-expressing microsomes revealed that M-I was formed only from sipoglitazar-G1, not from sipoglitazar-G2, and that CYP2C8 was mainly involved in this process. From these results, it is shown that the metabolic pathway from sipoglitazar to M-I is an unusual one, in which sipoglitazar is initially metabolized to sipoglitazar-G1 by UGT and then sipoglitazar-G1 is metabolized to M-I by *O*-dealkylation by CYP2C8 and deconjugation. Sipoglitazar-G2 is sequentially formed by the migration of the β -site of sipoglitazar-G1.

CHAPTER IV

UDP-glucuronosyltransferase 2B15 (UGT2B15) Is the Major Enzyme Responsible for Sipoglitazar Glucuronidation in Humans: Retrospective Identification of the UGT Isoform by *In Vitro* Analysis and the Effect of UGT2B15*2 Mutation

Introduction

Sipoglitazar had been developed as a novel anti-diabetic with triple agonistic activities on the human peroxisome proliferator-activated receptors hPPAR- γ , hPPAR- α , and hPPAR- δ . Animal pharmacokinetic studies in rats and monkeys and *in vitro* studies using [^{14}C]sipoglitazar indicated that sipoglitazar is metabolized primarily by oxidation and glucuronidation [10]. Previous *in vitro* metabolic studies of sipoglitazar showed that it had a unique metabolic pathway in humans as follows: Sipoglitazar was metabolized to sipoglitazar-G1, β -1-*O*-acyl glucuronide by UGT and further metabolized to the deethylated metabolite (M-I) by CYP2C8 [11]. Part of sipoglitazar-G1 was sequentially converted to sipoglitazar-G2, α -2-*O*-acyl glucuronide. The sipoglitazar glucuronide was one of the main metabolites in human and monkey hepatocytes, but not in rat, indicating a species difference between humans and animals. Recently, clinical pharmacokinetic studies of sipoglitazar have revealed the existence of extensive and poor metabolizers (EM and PM) of sipoglitazar, which is largely related to the UGT2B15 genetic polymorphism [12,13]. In the present study, to identify the UGT isoform mainly responsible for the metabolism of sipoglitazar retrospectively, the *in vitro* metabolism of sipoglitazar was examined with human UGT-expressing supersomes and liver microsomes.

In humans, the UGT superfamily of genes is roughly divided into two families, UGT1 and UGT2, based on sequence similarity at the amino acid level [66]. To date, 19 human UGT isoforms have been identified [66,67]. Most UGT enzymes are expressed in the liver and UGT1A1, 1A3, 1A4, 1A6, 1A9, 2B4, 2B7, 2B15 and 2B17 are considered to be the isoforms of greatest importance in hepatic drug elimination, while the other UGTs appear to exhibit low or negligible activity towards drugs and xenobiotics [68]. Genetic polymorphisms have also been identified for many of the UGT isoforms and several studies have examined the relationship between their phenotypes and genotypes [69]. The genetic polymorphisms of the UGT1A family such as UGT1A1*28 and UGT1A6*2 are well-known and are associated with Gilbert's syndrome and the toxicity caused by irinotecan treatment [70,71,72]. Meanwhile, for the UGT2B family, genetic polymorphisms of UGT2B15 have been identified (UGT2B15*1[85D], *2[85Y]), and this functional significance is well-known for *S*-oxazepam, lorazepam and 5 α -androstene-3 α ,17 β -diol [73,74,75]. The UGT2B15*2 variant could have a significant impact because of its high population frequency (approximately 50% in Caucasians) [76]. Due to this frequency, 19-32% of the Caucasian

populations are homozygous for this allele with a potentially significant impact on their ability to metabolize drugs and other chemicals by this pathway [77,78]. Since understanding of the relationship between *in vitro* and *in vivo* glucuronidation by UGT2B15 may give some insight into the development of new drugs undergoing glucuronidation, the *in vitro* contribution of UGT2B15 to glucuronidation of sipoglitazar was evaluated. In this study, the effect of the mutation of UGT2B15 on the metabolism of sipoglitazar was also investigated by kinetic studies to support the results of UGT2B15*2 genotypes in clinical studies.

Materials and Methods

Chemicals

Sipoglitazar was prepared by Takeda Pharmaceutical Company Limited (Osaka, Japan). [¹⁴C]sipoglitazar with a specific radioactivity of 4.58 or 4.62 MBq/mg was synthesized by Amersham Pharmacia Biotech UK Ltd. (Buckinghamshire, UK). The radiopurity (>98%) and chemical identity of the labeled compound were verified by TLC and HPLC. Authentic samples of [¹⁴C]sipoglitazar-G, [¹⁴C]sipoglitazar-G1 and [¹⁴C]sipoglitazar-G2 were also prepared in house by the *in vitro* reaction of sipoglitazar with human liver microsomes [11]. The sources of the other chemicals used in this work were as follows: UDPGA was purchased from Sigma-Aldrich (St. Louis, MO). Alamethicin was from Sigma-Aldrich or MP Biomedicals, LLC (Solon, OH). (*R, S*)-Oxazepam glucuronide in methanol (0.1 mg/mL) was from Cerilliant Corporation (Round Rock, TX). (*R, S*)-Oxazepam, TFA, phenacetin, methanol, acetonitrile, and other reagents of analytical grade were purchased from Wako Pure Chemical Industries, Ltd. (Osaka, Japan).

UGT-expressing supersomes and liver microsomes

Baculovirus-infected-insect cell supersomes expressing 12 human UGT isoforms (UGT1A1, UGT1A3, UGT1A4, UGT1A6, UGT1A7, UGT1A8, UGT1A9, UGT1A10, UGT2B4, UGT2B7, UGT2B15 and UGT2B17) and control supersomes were purchased from BD Biosciences (Woburn, MA). For the enzyme kinetics studies, mixed pool human (8 males + 7 females) liver microsomes were obtained from Tissue Transformation Technologies, Inc. (Edison, NJ). For the correlation studies, human liver microsomes (16 individual and pooled samples) were obtained as the Reaction Phenotyping Kit (Ver. 7), which was commercially available from XenoTech, LLC (Lenexa, KS).

His-tagged UGT2B15*1 and UGT2B15*2 membrane fractions

Construction of the vector, recombinant virus and expression: The cDNAs of human UGT2B15*1[85D] with *Nru* I sites were synthesized based on GenBank Accession No. 001076 and the same synthesis was applied to those of human UGT2B15*2[85Y] with *Nru* I

sites (Hokkaido System Science Co, Ltd., Hokkaido, Japan). To confirm the expression of the UGT2B15 proteins and compare the expression amount between UGT2B15*1 and UGT2B15*2, a 6 His-tag was added at the C-terminus of the sequence. Those two types of cDNAs encoding His-tagged human UGT2B15s were inserted into the pPSC8 baculovirus transfer vector (Protein Sciences Corporation, Meriden, CT). The His-tagged UGT2B15*1 or *2 -pPSC8 was amplified by PCR according to the manufacture's instruction for KOD DNA polymerase (Toyobo Co. Ltd., Osaka, Japan). For typical PCR, two primers were designed (forward primer, ATG TCT CTG AAA TGG ACG TCA GTC; reverse primer, CTA GTG ATG GTG ATG GTG ATG ATC TCT TTT CTT CTT CTT TCC TG, underline means the His-tag site.) and the reaction condition was 30 cycles with the following cycle of 30 seconds at 94°C, 30 seconds at 50°C and 1 minute at 74°C. The obtained cDNA sequences were confirmed using an ABI PRISM BigDye Terminator Cycle Sequencing Kit Ver. 3 and an ABI PRISM[®] 310 genetic analyzer (Perkin-Elmer, Foster, CA). The His-tagged UGT2B15*1 or *2 plasmids were co-transfected into Sf9 insect cells (Invitrogen Corporation, Carlsbad, CA) with linearized Autographa California nuclear polyhedrosis virus (AcNPV) DNA (Protein Sciences Corporation) and the Cellfectin reagent (Invitrogen Corporation) in SF900 II SFM (Invitrogen Corporation). The obtained recombinant virus was propagated in Sf9 cells by static culture for 4 or 7 days at 28°C and purified from a single plaque by the plaque assay method. After amplification by the sequential culture for 3 days, the virus was cultured for 3 days at 28°C with expresSF+ cells (Protein Sciences Corporation) and obtained by centrifugation at 3,000×g for 30 minutes at 4°C. The N-terminal and C-terminal sequences of the obtained virus and the expression of His-tagged UGT2B15*1 or *2 proteins by Western-blotting as described later were confirmed.

Preparation of the membrane fractions: After selection based on the titer of the obtained virus, the expresSF+ cells were infected with the His-tagged UGT2B15*1 or *2 baculovirus at a multiplicity of infection (MOI) of 1 after the expresSF+ cell density was adjusted to around 1.5×10^6 cells/mL. Cells incubated at 28°C were collected at 60 or 72 hour post infection by centrifugation and resuspended in 0.1 M Tris-HCl buffer (pH 7.5). The cell suspension was sonicated in 5 seconds × 10 bursts and homogenized using a glass potter homogenizer for cooling on ice. The cell lysate was centrifuged at 500×g for 30 minutes and the supernatant was ultracentrifuged at 100,000×g for 60 minutes at 4°C to obtain the membrane fraction. The resulting pellet was resuspended in 0.1 M Tris-HCl buffer (pH 7.5) and stored at -80°C before use. The protein concentration was measured by the Coomassie Plus-the Bradford Assay Kit using albumin as a standard (Pierce, Rockford, IL). Proteins were separated by 12.5% SDS-PAGE and transferred to an Immobilon-P nitrocellulose transfer membrane (Millipore, Billerica, MA). The His-tagged recombinant UGTs were detected using Penta-His HRP antibodies (Qiagen, Valencia, CA). The Immobilon Western Chemiluminescent HRP Substrate (Millipore) was employed for visualization in the ECL Mini-Camera apparatus (GE-Healthcare, Buckinghamshire, UK). The relative amounts of

UGT2B15 expressed at the protein band peaks were measured with Scion Imaging software (Scion Corporation, Frederick, MD) and XL-Ladder Broad molecular marker (APRO Life Science Institute, Inc., Tokushima, Japan). The glucuronidation activity for 4-methylumbelliferone was also examined by HPLC analysis [79].

Assay of sipoglitazar glucuronidation with UGT-expressing supersomes

Sipoglitazar glucuronidation was measured in a reaction mixture containing recombinant human UGTs: UGT1A1, UGT1A3, UGT1A4, UGT1A6, UGT1A7, UGT1A8, UGT1A9, UGT1A10, UGT2B4, UGT2B7, UGT2B15, or UGT2B17. The UGT isoforms involved in the glucuronidation of sipoglitazar were examined by analysis of the glucuronide conjugates of [¹⁴C]sipoglitazar in the incubation mixture. An incubation mixture with a final volume of 0.25 mL consisted of 1 mg protein/mL UGT-expressing supersomes in 50 mM Tris-HCl buffer (pH7.5) containing 5 mM UDPGA, 5 mM MgCl₂ and 50 µg/mL alamethicin. A stock solution of 1 mM [¹⁴C]sipoglitazar in acetonitrile was prepared and added to the incubation mixture with a 1% volume of the reaction mixture. The reaction was initiated by the addition of UDPGA, conducted at 37°C for 1 hour and terminated by the addition of acetonitrile equivalent to the volume of the reaction mixture. After centrifugation at 1,500×g for 10 minutes, the supernatant was applied to the HPLC. All incubations were made in duplicate.

Kinetic assay of sipoglitazar glucuronidation

In advance of the kinetic study for human UGT-expressing supersomes and liver microsomes, the protein concentration and incubation time were examined up to 1 mg protein/mL and 90 minutes and the most suitable conditions were determined. [¹⁴C]sipoglitazar was incubated in the reaction mixtures described above with UGT1A1, UGT1A3, UGT1A6, UGT2B15 or human liver microsomes (each 0.25 mg protein/mL), and with UGT2B4 (0.5 mg protein/mL). The sipoglitazar concentration was set at 2.5-100 µM. The reaction was initiated by the addition of UDPGA and conducted at 37°C for 30 minutes for UGT1A1-, UGT1A3-, UGT2B15-expressing supersomes and human liver microsomes, 60 minutes for UGT1A6-expressing supersomes, and 90 minutes for UGT2B4-expressing supersomes, respectively. Other assay conditions were the same as in “Assay of sipoglitazar glucuronidation with UGT-expressing supersomes” as described above. In advance of the kinetic study for His-tagged UGT2B15*1, the protein concentration and incubation time were examined up to 3 mg protein/mL and 4 hours and the most suitable conditions were determined and applied to His-tagged UGT2B15*2. [¹⁴C]sipoglitazar was incubated in the reaction mixtures with 2 mg protein/mL of His-tagged UGT2B15*1 and UGT2B15*2 membrane fractions. The sipoglitazar concentration was set at 25-250 µM. The reaction was initiated by the addition of UDPGA and conducted at 37°C for 2 hours. Other assay conditions except the reaction volume of 0.3 mL were also the same as in “Assay of

sipoglitazar glucuronidation with UGT-expressing supersomes” as described above.

Determination of [¹⁴C]sipoglitazar and its glucuronides

[¹⁴C]sipoglitazar and its glucuronides in the incubation mixture were analyzed by HPLC. The supernatant was mainly analyzed by an HPLC (LC-10 gradient system; Shimadzu Corp., Kyoto, Japan) with an on-line RI detector (D505TR Flow Scintillation Analyzer, PerkinElmer, Inc., Waltham, MA). The HPLC analytical method was as follows: The column was an Inertsil ODS-3 (5- μ m particle size, 250 \times 4.6 mm I.D.; GL Sciences, Tokyo, Japan). The mobile phase (A) [MP(A)] was H₂O-acetonitrile-TFA (90:10:0.1, v/v) and the mobile phase (B) [MP(B)] was H₂O-acetonitrile-TFA (10:90:0.1, v/v). The column temperature and the flow-rate were 40°C and 1 mL/min. The scheduled program for the gradient elution was as follows: The concentration of MP(B) was linearly increased from 30% to 70% over a period of 40 minutes, held at 95% for 10 minutes and then cycled back to the initial condition (30%).

For the kinetic analysis by human UGT-expressing supersomes and liver microsomes, the amount of sipoglitazar-G was measured as sipoglitazar-G1 and sipoglitazar-G2 separately and the formation rate of sipoglitazar-G1, the first step product in the metabolism of sipoglitazar, was evaluated to investigate more precisely in this study. However, since the formation rate of sipoglitazar-G2 was too low to evaluate in this study, the formation rate of sipoglitazar-G was evaluated in other studies. Sipoglitazar-G1 was analyzed by modification of the HPLC conditions described above: The column temperature and the flow-rate were 4°C and 0.7 mL/min. The scheduled program for the gradient elution was as follows: The concentration of MP(B) was held at 44% for 25 minutes, jumped and held at 100% for next 10 minutes and then cycled back to the initial condition (44%). These systems were equilibrated with the initial mobile phase composition for 10 minutes prior to injection of the next sample. On-line RI detection was carried out using Ultima-Flo M (PerkinElmer, Inc.) as the flow scintillation cocktail.

Correlation study of sipoglitazar glucuronidation

Sipoglitazar glucuronidation activity was measured in microsomes from 16 individual human livers. The concentrations of sipoglitazar and the human liver microsomes were 30 μ M and 0.25 mg protein/mL, respectively. The reaction was initiated by the addition of the microsomes and conducted at 37°C for 30 minutes. The other assay conditions were the same as in “Assay of sipoglitazar glucuronidation with UGT-expressing supersomes” as described above. β -Estradiol was used as the substrate for UGT1A1, trifluoperazine was for UGT1A4, morphine was for UGT2B7 and *S*-oxazepam was for UGT2B15 [80,81]. The specific substrate for each UGT isoform was not fully found and the method could not be applied to UGT1A3 and UGT2B4 selected in the previous studies due to the lack of a substrate specific to each UGT isoform. As a UGT1A6 substrate, 1-naphthol was used in

this study, even though many recombinant UGTs are reported to metabolize this compound [83]. The correlation between sipoglitazar glucuronidation and the glucuronidation of *S*-oxazepam, β -estradiol at the 3-OH position, trifluoperazine, 1-naphthol and morphine at the 6-OH position was analyzed using the statistical software, pre-clinical statistical analysis package ver. 5.0 (SAS Institute). The glucuronidation activities of β -estradiol at the 3-OH position, trifluoperazine, 1-naphthol and morphine at the 6-OH position in the microsomes from 16 human livers were provided by the manufacturer as typical reference activity for UGT1A1, UGT1A4, UGT1A6 and UGT2B7. Determination of *S*-oxazepam glucuronidation activity for UGT2B15 is described below.

Assay of *S*-oxazepam glucuronidation

For the correlation study, the *S*-oxazepam glucuronidation activity in microsomes from 16 individual human livers was determined in an assay using HPLC [83]. The reaction mixture of 0.3 mL in 50 mM KPB (pH 7.4) containing 50 μ M oxazepam, human liver microsomes (0.5 mg protein/mL), 5 mM MgCl₂, 50 μ g/mL alamethicin, and 5 mM UDPGA was incubated at 37°C for 2 hours. The reaction was terminated by the addition of HClO₄ (30 μ L). The mixtures were centrifuged at 1,500 \times g for 5 minutes to obtain the supernatants. Aliquots (50 μ L) of the supernatants were injected into an HPLC system (Alliance 2695; Waters, Milford, MA). The HPLC analytical method was as follows: The column was a C₁₈ column (10- μ m particle size, 250 \times 4.6 mm I.D.; Phenomenax, Torrance, CA). The mobile phase (A) [MP(A)] was 20 mM KPB (pH 4.5) and the mobile phase (B) [MP(B)] was acetonitrile. The column temperature and the flow-rate were 30°C and 1 mL/min. The scheduled program for the gradient elution was as follows: The concentration of MP(B) was held at 25% for 15 minutes, linearly increased from 25% to 60% over a period of 10 minutes and then cycled back to the initial condition (25%). (*R*, *S*)-Oxazepam glucuronides were detected at a UV wavelength of 214 nm and *S*-oxazepam glucuronide was identified by the relative retention time of *R*-glucuronide and *S*-glucuronide as described in the COA provided by the manufacturer.

For the kinetic study of *S*-oxazepam glucuronidation, (*R*, *S*)-oxazepam was incubated in the reaction mixtures with 2 mg protein/mL of His-tagged UGT2B15*1 and UGT2B15*2 membrane fractions. The (*R*, *S*)-oxazepam concentration was set at 5 or 10-150 μ M. The reaction with a final volume of 0.3 mL was initiated by the addition of UDPGA, conducted at 37°C for 2 hours and terminated by the addition of methanol equivalent to the volume of the reaction mixture. The other assay conditions were the same as in “Assay of sipoglitazar glucuronidation with UGT-expressing supersomes” as described above. The mixtures were then centrifuged at 1,500 \times g for 5 minutes to obtain the supernatants. The supernatants (10 μ L) were analyzed by LC-MS/MS using a Sciex API3000 triple quadrupole mass spectrometer (Applied Biosystems, Foster City, CA). HPLC was conducted on a gradient HPLC system (Shiseido, Tokyo, Japan). Separation for *R*-oxazepam glucuronide and

S-oxazepam glucuronide was achieved on a Sunfire C₁₈ column (3.5 μm particle size, 2.1 × 100 mm I.D.; Waters) using the mobile phase described in “Determination of [¹⁴C]sipoglitazar and its glucuronides”. *S*-Oxazepam glucuronide was identified by the relative retention time of HPLC analysis. The scheduled program for the gradient elution was as follows: The concentration of MP(B) was held at 10% for 5 minutes, increased to 24% over 14 minutes, jumped and held at 100% for next 6 minutes and then cycled back to the initial condition (5%) at a constant flow rate of 0.2 mL/min. Selective reaction monitoring (SRM) and product ion scan were carried out using ESI in the positive ion mode. Product ion scans were conducted by using precursor ion at *m/z* 463 [M+H]⁺ for the *S*-oxazepam glucuronide or *m/z* 180.1 [M+H]⁺ for the I.S. (phenacetin). The SRM of *m/z* 463 → 287.1 or *m/z* 180.1 → 110.3 was used for quantitative measurement of the *S*-oxazepam glucuronide and the I.S., respectively. The concentrations of *S*-oxazepam glucuronide in the reaction mixtures were determined using a standard curve of the peak area ratios.

Data analysis of the kinetic studies

Glucuronidation kinetic models have been shown to vary with the UGT isoforms and/or with the substrate [82,84,85]. For analysis of the enzyme kinetic data, the substrate concentrations and formation rates of the glucuronides of each substrate were applied for fitting to three kinetic models, the Michaelis-Menten model (eq.1), the substrate inhibition model (eq. 2), and the Hill equation model (eq. 3), to derive the Michaelis constant and the maximum velocity. The equations for each model are as follows.

$$1) \quad V = V_{\max} \times [S] / (K_m + [S])$$

$$2) \quad V = V_{\max} \times [S] / (K_m + [S] + [S]^2 / K_{si})$$

$$3) \quad V = V_{\max} \times [S]^n / (S_{50}^n + [S]^n)$$

where *V* is the formation rate of glucuronide of each substrate, *V*_{max} is the maximum velocity, *K*_m is the Michaelis constant (substrate concentration at 0.5 *V*_{max}), [*S*] is the substrate concentration, *K*_{si} is the constant describing the substrate inhibition interaction, *S*₅₀ is the substrate concentration resulting in 50% of *V*_{max} (analogous to *K*_m), and *n* is the Hill coefficient. In this study, the fitting was performed using the Enzyme kinetics module (Sigma Plot. ver. 9.01) for selection of the best-fitting model. Goodness of fit to the models was assessed from the Akaike Information Criterion values and the model that showed the lowest value among the three models was selected as the best-fitting model.

Results

Glucuronidation of sipoglitazar in UGT-expressing supersomes

The UGT isoforms involved in the biotransformation of sipoglitazar were examined by the metabolism of sipoglitazar with supersomes expressing human UGT isoforms. The sipoglitazar-G formation activities of 12 UGT isoforms were integrated as the relative activities against UGT1A1, which showed the highest activity among them (Figure IV-1). The remaining ranking order was UGT2B15 (78.4% against UGT1A1 activity), UGT1A3 (60.6%), UGT1A6 (35.5%), and UGT2B4 (15.6%), while the 7 other UGT isoforms had activity below 10% of the UGT1A1 activity.

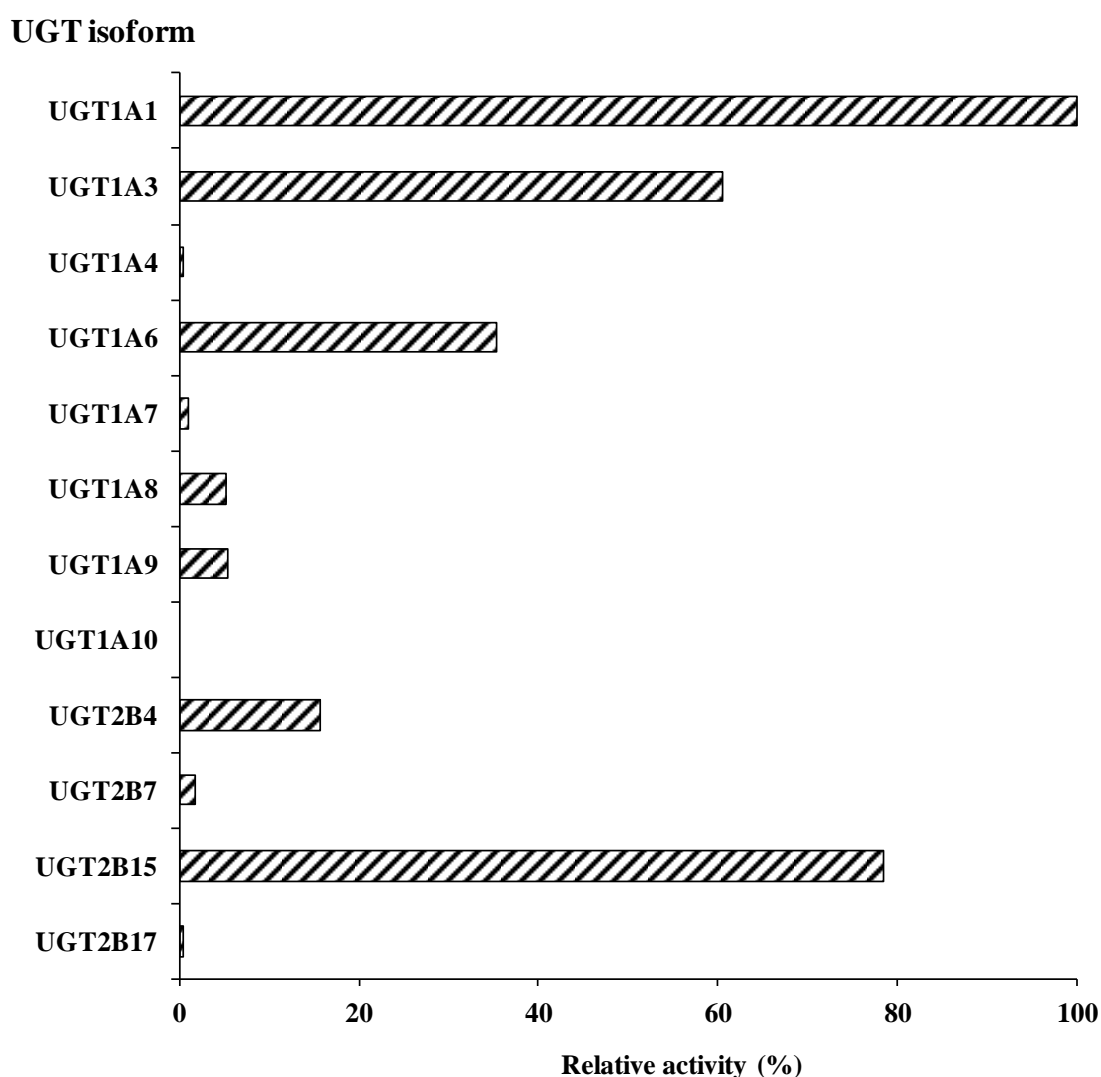


Figure IV-1. Relative glucuronosyltransferase activity of [^{14}C]sipoglitazar with human UGT-expressing supersomes

Relative activity shows the [^{14}C]sipoglitazar-G formation rates for each UGT isoform, when the activity of UGT1A1 is assumed to be 100%. Data represent the mean of duplicate determinations.

Kinetics of [¹⁴C]sipoglitazar glucuronidation by human UGT-expressing supersomes and liver microsomes

Kinetic analyses of glucuronidation by UGT isoforms and human liver microsomes were performed to determine the K_m and clearances of the UGT isoforms with sipoglitazar for further consideration of each isoform's contribution to sipoglitazar glucuronidation. UGT1A1, UGT1A3, UGT1A6, UGT2B4, and UGT2B15, for which activities were higher than 10% of the UGT1A1 activity, were selected for this study. The sipoglitazar-G1 formation rates in the other isoforms were not sufficient for kinetic analysis.

The results showed the substrate inhibition model was applicable for UGT1A6 and the Michaelis-Menten model was applicable for the other UGT-expressing supersomes and human liver microsomes (Table IV-1 and Figure IV-2). The K_m values were the lowest for UGT2B15 (17.0 μ M) followed by UGT1A6 (17.9 μ M), UGT1A3 (29.1 μ M), UGT1A1 (36.0 μ M) and UGT2B4 (over 100 μ M). The CL_{int} value was the highest for UGT1A1 (15 μ L/min/mg protein) followed by UGT2B15 (8.1 μ L/min/mg protein), UGT1A3 (6.2 μ L/min/mg protein), UGT1A6 (4.2 μ L/min/mg protein), while its value for UGT2B4 was not calculated. The K_m and CL_{int} values for human liver microsomes were 40.5 μ M and 54 μ L/min/mg protein, respectively.

Table IV-1. Kinetic parameters of [¹⁴C]sipoglitazar-G1 formation in human UGT1A1-, UGT1A3-, UGT1A6-, UGT2B4-, UGT2B15-expressing supersomes, and liver microsomes

UGT isoform	K_m or S_{50} (μ M)	V_{max} (pmol/min/mg protein)	CL_{int} (μ L/min/mg protein)
UGT1A1 ^{a)}	36.0	549	15
UGT1A3 ^{a)}	29.1	180	6.2
UGT1A6 ^{b)}	17.9	75.8	4.2
UGT2B4 ^{a)}	> 100	465	NC
UGT2B15 ^{a)}	17.0	138	8.1
Liver microsomes ^{a)}	40.5	2172	54

The kinetic parameters were calculated by the fitting models described below.

Fitting model: a) Michaelis-Menten, b) Substrate inhibition, K_{si} : 85.2 μ M

NC indicates not calculated.

Kinetic plots are presented in Figure IV-2.

Data represent the mean of duplicate determinations.

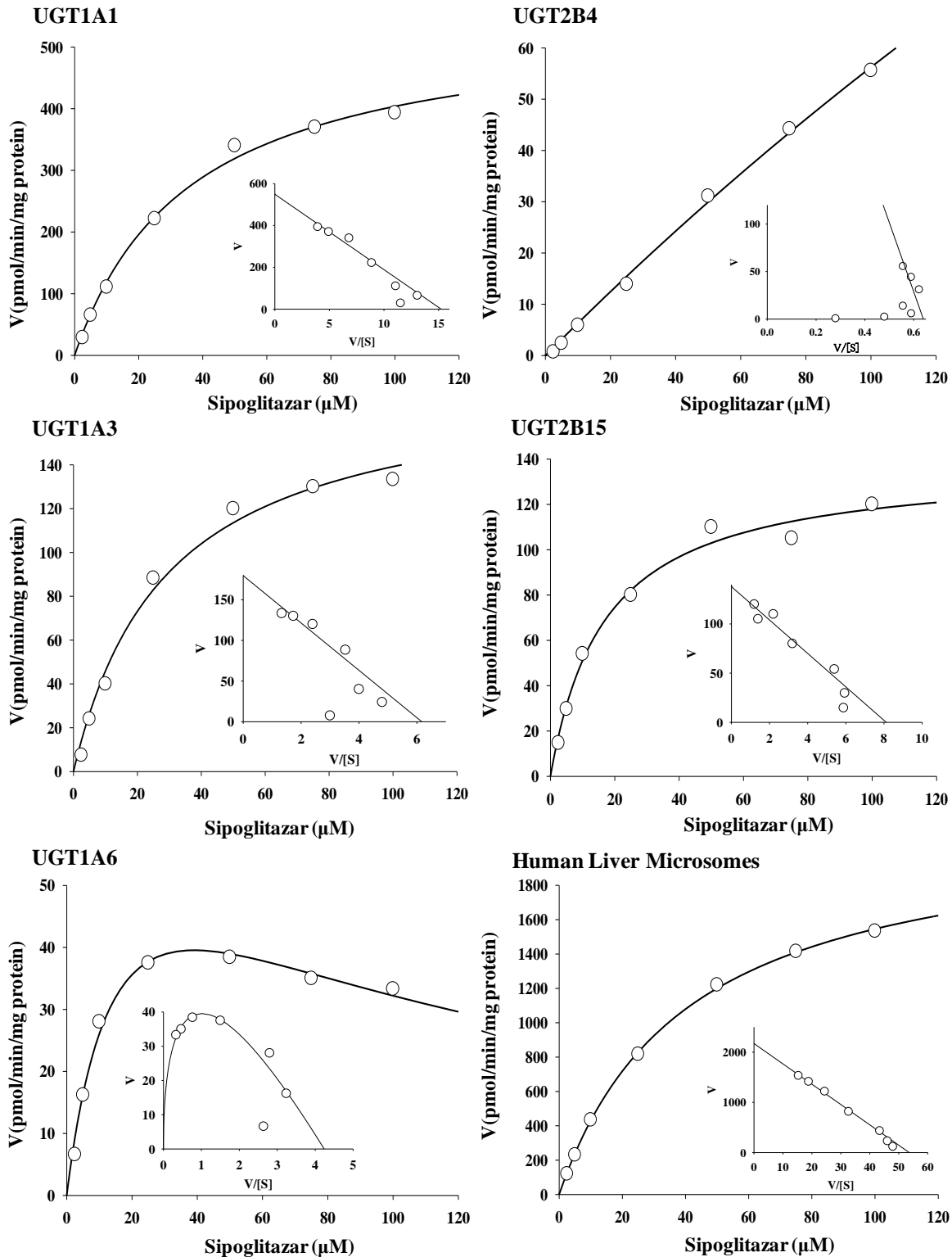


Figure IV-2. Kinetics of [^{14}C]sipoglitazar-G1 formation by UGT1A1-, UGT1A3-, UGT1A6-, UGT2B4-, UGT2B15-expressing supersomes and human liver microsomes

The concentrations of [^{14}C]sipoglitazar ([S]) ranged from 2.5 to 100 μM . V is the [^{14}C]sipoglitazar-G1 formation rate (pmol/min/mg protein). Each insert shows the Eadie-Hofstee plot of the experimental data. Data represent the mean of duplicate determinations.

Correlation analysis of [¹⁴C]sipoglitazar glucuronidation by human liver microsomes

Sipoglitazar-G formation strongly correlated with *S*-oxazepam glucuronidation activity ($r=0.90$) (Table IV-2 and Figure IV-3). Sipoglitazar-G formation also correlated with the glucuronidation activity of β -estradiol at the 3-OH position ($r=0.59$), trifluoperazine ($r=0.59$), and morphine at the 6-OH position ($r=0.50$), while these correlation coefficient values were much weaker than that for *S*-oxazepam glucuronidation and a similar correlation was observed between morphine and *S*-oxazepam ($r=0.63$) or morphine and trifluoperazine ($r=0.56$) (Table IV-2).

Table IV-2. The correlation coefficients among the glucuronidation of sipoglitazar, β -estradiol, trifluoperazine, 1-naphthol, morphine, and *S*-oxazepam

	β -Estradiol	Trifluoperazine	1-Naphthol	Morphine	<i>S</i> -oxazepam
Sipoglitazar	0.59 (0.016)	0.59 (0.015)	0.37 (0.15)	0.50 (0.049)	0.90 (< 0.001)
β -Estradiol	-	0.36 (0.17)	-0.04 (0.88)	-0.01 (0.96)	0.34 (0.20)
Trifluoperazine	-	-	0.16 (0.56)	0.56 (0.024)	0.44 (0.092)
1-Naphthol	-	-	-	0.23 (0.39)	0.41 (0.12)
Morphine	-	-	-	-	0.63 (0.0089)

The parenthetic figure represents the *p* value.

The correlation coefficients between the glucuronidation of sipoglitazar and β -estradiol, trifluoperazine, 1-naphthol, morphine, or *S*-oxazepam were derived from Figure IV-3.

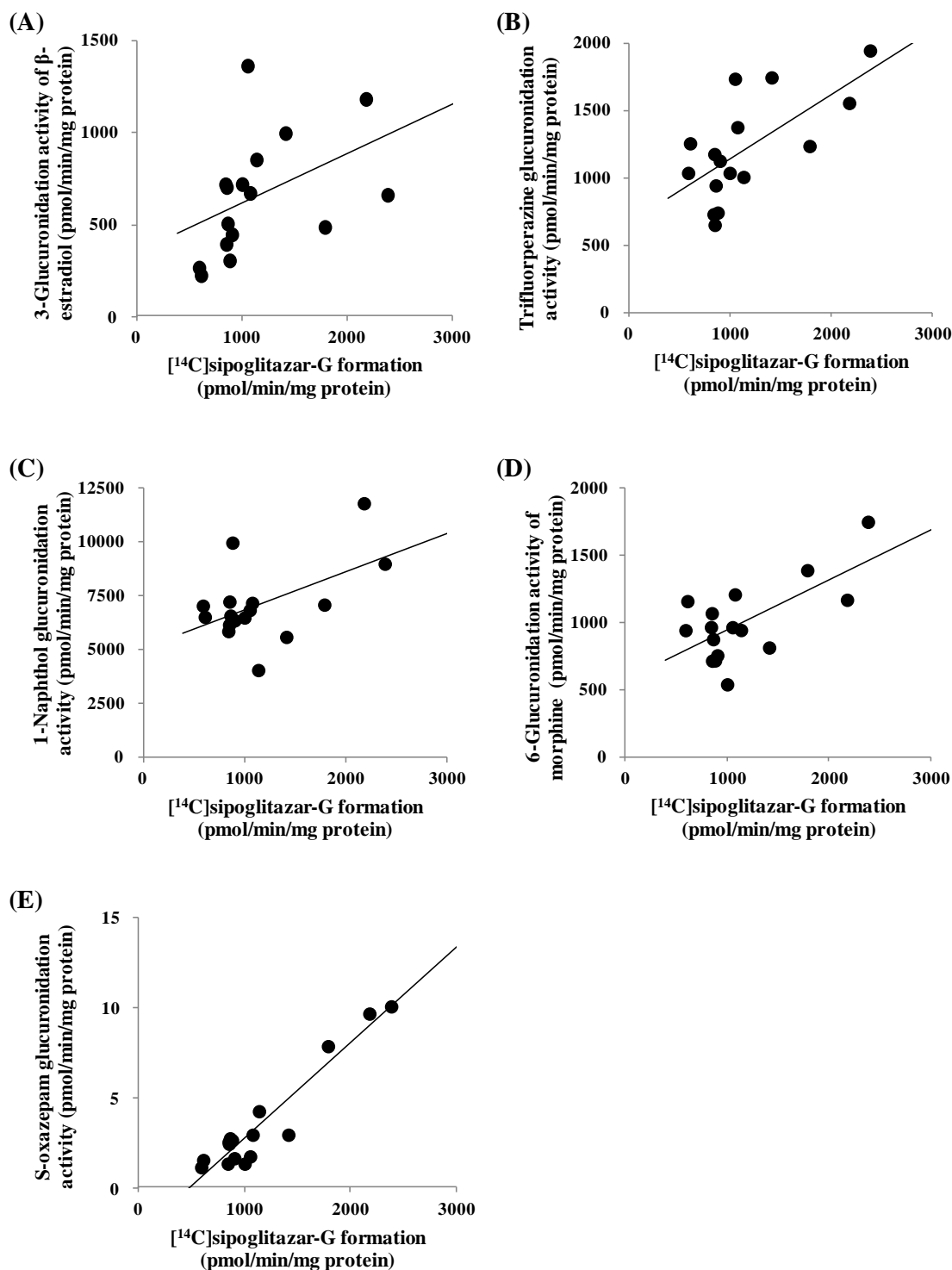


Figure IV-3. Correlation analysis between the glucuronidation of [¹⁴C]sipoglitazar and UGT isoform-specific activities in microsomes from 16 human livers

The x axis represents the [¹⁴C]sipoglitazar-G formation rate and the y axis represents the UGT1A1 activity for β-estradiol 3-glucuronidation (A), UGT1A4 activity for trifluoperazine glucuronidation (B), UGT1A6 activity for 1-naphthol glucuronidation (C), UGT2B7 activity for morphine 6-glucuronidation (D) and UGT2B15 activity for S-oxazepam glucuronidation (E). Data represent the mean of duplicate determinations.

Expression of His-tagged UGT2B15*1 and UGT2B15*2

The expression of the genes and proteins for His-tagged UGT2B15*1 and UGT2B15*2 in the membrane fractions was confirmed by Western blotting with Penta-His HRP antibodies. Protein concentrations of the membrane fractions measured by the Coomassie Plus-the Bradford Assay Kit were 13.6 mg protein/mL for His-tagged UGT2B15*1 and 19.6 mg protein/mL for His-tagged UGT2B15*2. The relative expression levels of each His-tagged UGT2B15 protein in the cell homogenates were determined by Western blotting using the protein band peak corresponding to the 50 kDa of the XL-Ladder Broad molecular marker as the His-tagged control protein (Figure IV-4). The protein band peak corresponds to 0.15 μ g protein/band when 5 μ L of the marker is applied following the description of the manufacturer. UGT2B15 protein concentrations of the membrane fractions measured by Western blotting were 1.9 mg for His-tagged UGT2B15*1 protein/mL and 1.1 mg for His-tagged UGT2B15*2 protein/mL.

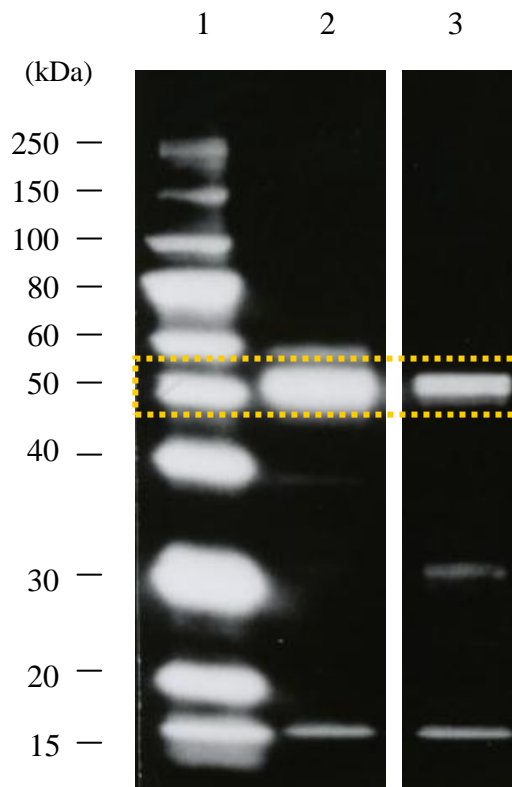


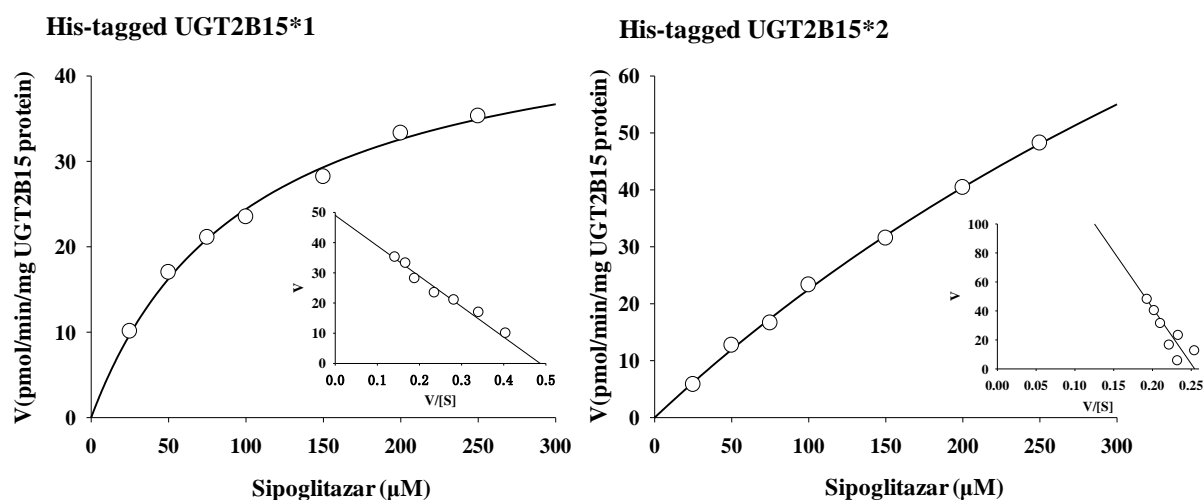
Figure IV-4. Identification of His-tagged UGT2B15*1 and UGT2B15*2 protein by Western blotting

- 1 : Molecular marker
- 2 : His-tagged UGT2B15*1 membrane fraction
- 3 : His-tagged UGT2B15*2 membrane fraction

Glucuronidation activity by His-tagged UGT2B15*1 and UGT2B15*2 membrane fractions

To investigate the effects of the mutation of UGT2B15 on the metabolism of sipoglitazar, kinetic analyses of glucuronidation by His-tagged UGT2B15*1 and UGT2B15*2 membrane fractions were performed (Figure IV-5). Affinities toward *S*-oxazepam were also evaluated as UGT2B15 specific substrates.

The K_m values of UGT2B15*1 and UGT2B15*2 for sipoglitazar glucuronidation were 100.7 and over 250 μM , their V_{max} values were 49.0 and 197.0 pmol/min/mg UGT2B15 protein, respectively and the CL_{int} value for UGT2B15*1 was 0.49 $\mu\text{L}/\text{min}/\text{mg}$ UGT2B15 protein while its value for UGT2B15*2 was not calculated. This correlation between the affinity and activity was also observed in the glucuronidation of *S*-oxazepam. The K_m values of UGT2B15*1 and UGT2B15*2 for *S*-oxazepam glucuronidation were 86.4 and 160.1 μM , their V_{max} values of UGT2B15*1 and UGT2B15*2 were 7.1 and 20.6 pmol/min/mg UGT2B15 protein, and their CL_{int} values were 0.08 and 0.13 $\mu\text{L}/\text{min}/\text{mg}$ UGT2B15 protein, respectively.



Kinetic parameter	His-tagged UGT2B15*1	His-tagged UGT2B15*2
K_m (μM)	100.7	> 250
V_{max} (pmol/min/mg UGT2B15 protein)	49.0	197.0
CL_{int} ($\mu\text{L}/\text{min}/\text{mg}$ UGT2B15 protein)	0.49	NC

NC indicates not calculated.

Figure IV-5. Kinetics of [^{14}C]sipoglitazar glucuronidation by His-tagged UGT2B15*1 and UGT2B15*2 membrane fractions

The concentrations of [^{14}C]sipoglitazar ($[S]$) ranged from 25 to 250 μM . V is the [^{14}C]sipoglitazar-G formation rate (pmol/min/mg UGT2B15 protein). Each insert shows the Eadie-Hofstee plot of the experimental data. The line indicates fitting of the data to the Michaelis-Menten equation by non-linear regression. Data represent the mean of duplicate determinations.

Discussion

The identification of the UGT isoform involved in the metabolism of sipoglitazar was retrospectively conducted by *in vitro* analysis. For a candidate primarily metabolized by CYP, the CYP isoforms responsible for the metabolism would be identified by some authorized studies, e.g. a metabolism study using recombinant CYP isoforms and the correlation analysis between the metabolic activities in the panel of individual human liver microsomes from multiple donors. In this study, the same methods were applied to the UGT identification using recombinant UGT isoforms and human liver microsomes.

The results of the metabolism study using 12 isoforms of recombinant UGT-expressing supersomes indicated that sipoglitazar is more extensively metabolized via glucuronidation by multiple UGT isoforms including UGT1A1, UGT1A3, UGT1A6, UGT2B4, and UGT2B15 than by other UGTs (Figure IV-1). Comparing the kinetic parameters of these five UGT isoforms, the CL_{int} value of sipoglitazar in each of the UGT-expressing supersomes was the highest for UGT1A1 followed by UGT2B15, UGT1A3, UGT1A6, while its value for UGT2B4 was not calculated, which was quite comparable to the result of the glucuronidation rate described before (Table IV-1 and Figure IV-1). However, the results cannot be directly extrapolated to humans *in vivo*, because the enzyme expression level in each of the UGT-expressing supersomes, which could have an effect on glucuronidation rate or V_{max} values, has not been decided. The K_m values might be less influenced by the enzyme expression level, which showed that sipoglitazar has the smallest K_m value toward UGT2B15, followed by UGT1A6, UGT1A3, and UGT1A1. The K_m value for UGT2B4 was obviously higher than those for the other 4 UGT isoforms, indicating that UGT2B4 has much lower affinity toward sipoglitazar and has little possibility to contribute in the glucuronidation. On the other hand, the CL_{int} value (54 $\mu\text{L}/\text{min}/\text{mg}$ protein) of sipoglitazar in pooled human liver microsomes was considerably higher than those of SN-38 (4.21 $\mu\text{L}/\text{min}/\text{mg}$ protein), serotonin (12.6 $\mu\text{L}/\text{min}/\text{mg}$ protein) and *S*-oxazepam (4.6-7.3 $\mu\text{L}/\text{min}/\text{mg}$ protein in 3 individual human donors), which are often used for UGT genetic polymorphism studies and have a wide range of CL_{int} [83,86,87]. These results revealed that UGT1A1, UGT1A3, UGT1A6 and UGT2B15 could be involved in the metabolism of sipoglitazar and the UGT isoform responsible for the glucuronidation of sipoglitazar in human liver would have a relatively high clearance ability. Following these results, the UGT isoform with the highest contribution to the sipoglitazar glucuronidation was investigated among UGT1A1, UGT1A3, UGT1A6 and UGT2B15. As mentioned above, the quantitative analysis method of the UGT enzyme expression level is not sufficiently established for the recombinant enzyme preparations and also for *in vivo* tissues. Some reports tried to elucidate the quantitative distribution of UGT isoforms in human tissues by mRNA expression analysis [88,89,90]. Even though the results in these reports are not fully consistent with each other, the expression amount of UGT1A3 in the liver is the lowest among the 4 UGT isoforms selected above and the amount of UGT1A6 is lower than the amount of UGT1A1 in all reports.

These facts suggest that the possibility of UGT1A3 and UGT1A6 involvement could be low in the metabolism of sipoglitazar. Between the others, UGT1A1 and UGT2B15, the correlation study showed the involvement of UGT2B15 is more significant than that of UGT1A1 in the glucuronidation of sipoglitazar (Table IV-2 and Figure IV-3). β -Estradiol used as a UGT1A1 probe could be metabolized partially by UGT1A3 [91], which could have some influence on the correlation analysis. However, the relative contribution is less than 20% and this correlation between sipoglitazar-G formation and β -estradiol glucuronidation activity had the same level as with trifluoperazine glucuronidation (UGT1A4; $r=0.59$) and morphine 6-glucuronidation (UGT2B7; $r=0.50$), which have been shown to be hardly involved in sipoglitazar glucuronidation in the metabolic study using recombinant UGT isoforms. This finding was partially due to the internal correlation between UGT2B7 and UGT2B15 ($r=0.63$) or UGT2B7 and UGT1A4 ($r=0.56$) (Table IV-2). Moreover, the involvement of either UGT1A1 or UGT2B15 should be examined from the view of species difference for the formation of sipoglitazar glucuronide, which was one of the main metabolites in human and monkey hepatocytes, but not in rat [10]. According to a phylogenetic analysis of the mammalian UGT2B subfamily, the human UGT2B family is classified into the same group with monkey UGT2Bs and human UGT2B15 in particular is very close to monkey UGT2B20, while most rat UGT2B isoforms are classified into a group separated from human UGT2B15 and the sequence identity to human UGT2B15 is lower in rats than in monkeys [92]. On the other hand, human UGT1A1 shares close identity with rat and monkey UGT1A1 orthologous in their amino acid sequences and has a similar substrate specificity and protein function [93,94]. These findings could account for the species differences for the formation of sipoglitazar glucuronide among humans, rats and monkeys and strengthen the possibility of UGT2B15 rather than UGT1A1 in the involvement of sipoglitazar glucuronidation in humans. Thus, these results and findings indicated that UGT2B15 is mainly responsible for the glucuronidation of sipoglitazar and the contribution of UGT1A1 and the other UGT isoforms to the sipoglitazar glucuronidation could be minor. Finally, this result has been confirmed by recent clinical pharmacokinetic studies of sipoglitazar, which showed inter-subject variability in the plasma concentration profiles of sipoglitazar and that approximately two-thirds of the inter-subject variability in sipoglitazar plasma exposure is explained by UGT2B15 genetic variation [12,13]. In addition, no relationship between sipoglitazar plasma exposure and variants of the other UGT isoforms was found.

In determining the genetic polymorphisms of UGT2B15, the kinetic analysis for *S*-oxazepam using the individual human liver microsomes divided into UGT2B15*1 and *2 is well-known [83]. Furthermore, to support this mutation effect of UGT2B15 from other *in vitro* analysis, UGT2B15*1- and UGT2B15*2-expressing membrane fractions were prepared and the examination of their properties for glucuronidation of sipoglitazar and *S*-oxazepam was attempted. In this study, a 6 His-tag was introduced at the C-terminal end of the UGT2B15

protein because of the lack of an available antibody specific to UGT2B15 [95]. The His-tag was utilized to compare the expression amount of UGT2B15*1 and UGT2B15*2 and to correct the protein concentration based on the UGT2B15 expression (Figure IV-4). Consequently, the K_m values of His-tagged UGT2B15*2 for sipoglitazar and *S*-oxazepam indicated that the mutation from D to Y at position 85 reduced the affinity of UGT2B15 enzyme toward sipoglitazar and *S*-oxazepam and the result showed a similar tendency to the reported results for other compounds metabolized by UGT2B15 (Figure IV-5) [83,96]. However, the K_m value for sipoglitazar in His-tagged UGT2B15*1 is approximately six-fold higher than that in UGT2B15 supersomes (Table IV-1 and Figure IV-5). Furthermore, the CL_{int} value of His-tagged UGT2B15*1 for *S*-oxazepam is lower than that of His-tagged UGT2B15*2, which is due to their inverted V_{max} values and contrary to the results which have been reported so far that UGT2B15 activity is reduced by the mutation [73]. These data indicate that His-tagged UGT proteins might have a different enzymatic property from actual UGTs. One of the possibilities to explain this difference is that the addition of a short peptide to the *C*-terminal end of the UGT2B15 might be expected to affect enzymatic activity [97]. Of interest, a previous report for dihydrotestosterone and androstane-3 α -diol also showed that the UGT2B15*2 variant has a two-fold higher V_{max} compared with the UGT2B15*1 even in the absence of a short peptide to the *C*-terminal end [77]. If these results are true, another possible explanation would be that the protein expression condition or the stability of UGT2B15*1 and UGT2B15*2 might be different under the conditions used to prepare their membrane fractions. However, the true reason for these differences is unclear. These results indicate the limitation and fluctuation of kinetic studies using His-tagged UGT proteins, although the reduction of the affinity to UGT2B15 enzyme by the mutation was at least confirmed in the same recombinant His-tagged UGT2B15*1- or *2-membrane fractions.

In conclusion, UGT2B15 was predictable as the main metabolic enzyme for glucuronidation of sipoglitazar from *in vitro* studies using human UGT-expressing supersomes and liver microsomes. For the glucuronidation of sipoglitazar, these *in vitro* study results supported the clinical finding that the genetic polymorphism causes the pharmacokinetic phenotypes, and the clinical study results confirmed the reliability of these *in vitro* study results. Thus, sipoglitazar is a good example to elucidate the relationship between phenotype and genotype for UGT2B15 from *in vitro* analysis. However, all the *in vitro* results might not be definitive enough to determine that UGT2B15 is responsible for the glucuronidation of sipoglitazar in humans without clinical data, suggesting the present limitations for *in vitro* UGT identification. Hereafter, further investigation for each UGT isoform will be essential such as the findings of each specific substrate or inhibitor and their contribution in human liver.

Summary

Recently, genotyping in clinical studies has revealed that UGT2B15 genetic polymorphism has an influence on the clinical pharmacokinetics of sipoglitazar. In this study, the UGT responsible for sipoglitazar was retrospectively identified by *in vitro* analysis. A study using UGT-expressing supersomes revealed that sipoglitazar glucuronidation was more extensively catalyzed by UGT1A1, 1A3, 1A6, 2B4, and 2B15 than by other UGTs. Enzyme kinetic studies for sipoglitazar glucuronidation and recent findings related to mRNA expression analysis of UGTs narrowed the involved isoforms down to UGT1A1 and UGT2B15 among these five human UGTs. In a correlation study between sipoglitazar glucuronidation and UGT isoform-specific activities, the glucuronidation of *S*-oxazepam, a specific substrate for UGT2B15, strongly correlated with that of sipoglitazar, as compared with that of β -estradiol, a representative UGT1A1 substrate. The analysis of the species difference strengthens the possibility of UGT2B15 rather than that of UGT1A1. These *in vitro* findings indicate that UGT2B15 is principally responsible for sipoglitazar glucuronidation. Moreover, the UGT2B15*2 mutation significantly increased the K_m value of sipoglitazar in the kinetic analysis using recombinant His-tag UGT2B15*1- or *2- membrane fractions. These results show that sipoglitazar is a good example to elucidate the relationship between phenotype and genotype for UGT2B15 from *in vitro* analysis.

CONCLUSION

The present studies have been originally initiated to elucidate the metabolic profiles of TAK-802 and sipoglitazar as a requisite non-clinical study to assess DDI liability of these compounds and to predict the metabolite's structure detected in human plasma. As a result, non-CYP enzymes were revealed to be involved in the metabolism of these compounds. However, in contrast to CYP enzymes which have been well characterized, the basic information of non-CYP enzymes is insufficient and only few reports evaluated the clinical relevancies of non-CYP metabolism from the *in vivo* and *in vitro* correlations. In these studies, the evaluation method of these non-CYP enzymes was developed, the species differences and polymorphic variation were examined and the clinical impacts of these non-CYP enzymes were exemplified through the evaluation of these two compounds.

In Chapter I, by comparing the metabolite profiles of TAK-802 *in vivo* and *in vitro*, M-IV, a reductive metabolite, was found as the major metabolite specific to humans. The *in vitro* metabolism studies revealed that M-IV was formed by human 11 β -HSD1, but not rat 11 β -HSD1, which may account for high plasma exposure of M-IV in humans. Fluorobenzyl group of TAK-802 seems to be a key chemical structure for affinity to 11 β -HSD1 and contributes to the species differences in the metabolic profiles between humans and animals. In addition, the present study proposed a methodology to elucidate the metabolic profiles with multiple pathways including both oxidative and reductive metabolism.

In Chapter II, the pharmacokinetic profiles of sipoglitazar were evaluated in rats and monkeys. The formation of deethylated metabolite (M-I) and glucuronides (sipoglitazar-G and M-I-G) was detected in plasma and excreta in rats and monkeys, which suggested that both oxidation and glucuronidation are the main elimination route of sipoglitazar from the body. On the other hand, the use of hepatocytes from humans and animals was the promising approach to postulate the metabolic pathway of compounds which simultaneously undergo oxidation and glucuronidation and to predict the metabolic property in humans.

In Chapter III, sipoglitazar was found to primarily undergo glucuronidation by UGT and sequentially metabolized to a deethylated metabolite by CYP2C8. This metabolic pathway is very unique, since conjugation reaction generally follows oxidative metabolism. In this study, hepatocytes and microsomes were utilized in combination for the elucidation of the metabolic pathway in humans. These findings indicate that more attention should be paid to glucuronides as well in investigating the metabolite profile for NCEs.

In Chapter IV, the *in vitro* analysis using human liver microsomes and UGT-expressing supersomes revealed that the responsible UGT isoform for sipoglitazar glucuronidation was UGT2B15 and the identification was shown to be possible. Moreover, *in vitro* study using His-tagged UGT2B15 membrane fractions demonstrated clinical relevance of polymorphic variation of UGT2B15 to the inter-individual variability in sipoglitazar levels in human

plasma. To date, the universal method of UGT identification has not been established due to the lack of specific substrate or inhibitor to each UGT isoform, and thus the clinical impacts of polymorphism still remain unclear. To address this issue, it might be essential to accumulate further knowledge and clinical cases related to UGTs.

In conclusion, through *in vitro* studies to clarify the metabolic profiles of TAK-802 and sipoglitazar, I exemplified that 11 β -HSD1 and UGT2B15 could play key roles in species differences and inter-individual variability in their pharmacokinetics. The obtained results would intensify the importance of *in vitro* studies in bridging non-clinical and clinical studies. Moreover, the approaches taken in this study would contribute to predict human pharmacokinetics and mitigate risks which may surface in the early clinical study.

ACKNOWLEDGEMENTS

I wish to express my sincere gratitude to Dr. Tatsuo Kurihara, Professor of the Laboratory of Molecular Microbial Science, Institute for Chemical Research, Kyoto University, for his kind advice and valuable discussion.

I would like to express my gratitude to Dr. Satoru Asahi, Senior Director, Drug Metabolism and Pharmacokinetics Research Laboratories, Pharmaceutical Research Division, Takeda Pharmaceutical Company Limited, for his kind encouragement and many helpful discussions.

I would like to express my gratitude to Mr. Junzo Takahashi, Associate Director, Drug Metabolism and Pharmacokinetics Research Laboratories, Pharmaceutical Research Division, Takeda Pharmaceutical Company Limited, for many helpful discussions in carrying out these studies.

I am deeply grateful to Dr. Takahiro Kondo, Director, Drug Metabolism and Pharmacokinetics Research Laboratories, Pharmaceutical Research Division, Takeda Pharmaceutical Company Limited, for his pointed advice and kind encouragement.

I am deeply grateful to Dr. Hideki Hirabayashi, Associate Director, Drug Metabolism and Pharmacokinetics Research Laboratories, Pharmaceutical Research Division, Takeda Pharmaceutical Company Limited, for his helpful discussions.

I am deeply grateful to Dr. Toshiya Moriwaki, Director, Drug Metabolism and Pharmacokinetics Research Laboratories, Pharmaceutical Research Division, Takeda Pharmaceutical Company Limited, for his kind encouragement and support.

I would like to express my gratitude to Dr. Nobuyoshi Esaki, Executive Vice-President of Kyoto University and former Professor of the Laboratory of Molecular Microbial Science, Institute for Chemical Research, Kyoto University, for his kind encouragement after my graduation.

I am greatly indebted to Mr. Naohiro Kawaguchi, Ms. Miyako Sudo, Mr. Yuto Hiura, Mr. Hidenori Kamiguchi, Mr. Yoshihiro Maeshiba, Mr. Yutaka Kiyota and Dr. Yoshihiko Tagawa of Pharmaceutical Research Division, Takeda Pharmaceutical Company Limited who have contributed to the studies discussed in this thesis.

I am greatly indebted to Dr. Kiyoshi Miwa, Mr. Kouji Mouri, and Ms. Frances Stringer of Pharmaceutical Development Division, Takeda Pharmaceutical Company Limited who have contributed to the studies discussed in this thesis.

I would like to thank all of their colleagues of Drug Metabolism and Pharmacokinetics Research Laboratories and Mr. Mitsuharu Matsumoto, Dr. Nozomi Katayama, Mr. Tomohiro Kawamoto, and Dr. Tetsuo Miwa at Takeda Pharmaceutical Company Limited for their kind support.

I would like to thank Ms. Ai Bernards, Ms. Chie Shiojima, the late Mr. Masahiro Kawase, Dr. Masaki Yamamoto, Dr. Kenji Yamashita, Dr. Katsumi Iga, and Dr. Kenji Okonogi for their

kind support.

Finally, I would like to express my hearty gratitude to my wife, Miho and my children, Yuga and Yurina for their immense understanding, support and the countless other things they have done for me.

REFERENCES

- 1) Thompson T. N. (2000) Early ADME in support of drug discovery: the role of metabolic stability studies. *Curr. Drug Metab.*, **1**:215-241.
- 2) Zhao S. X., Forman D., Wallace N., Smith B. J., Meyer D., Kazolias D., Gao F., Soglia J., Cole M., Nettleton D. (2005) Simple strategies for reducing sample loads in *in vitro* metabolic stability high-throughput screening experiments: a comparison between traditional, two-time-point and pooled sample analyses. *J. Pharm. Sci.*, **94**:38-45.
- 3) Strolin B. M., Whomsley R., Baltes E. (2006) Involvement of enzymes other than CYPs in the oxidative metabolism of xenobiotics. *Expert Opin. Drug Metab. Toxicol.*, **2**:895-921.
- 4) Williams J. A., Hyland R., Jones B. C., Smith D. A., Hurst S., Goosen T. C., Peterkin V., Koup J. R., Ball S. E. (2004) Drug-drug interactions for UDP-glucuronosyltransferase substrates: a pharmacokinetic explanation for typically observed low exposure (AUC_i/AUC) ratios. *Drug Metab. Dispos.*, **32**:1201-1208.
- 5) Hutzler J. M., Obach R. S., Dalvie D., Zientek M. A. (2013) Strategies for a comprehensive understanding of metabolism by aldehyde oxidase. *Expert Opin. Drug Metab. Toxicol.*, **9**:153-168.
- 6) Akabane T., Gerst N., Masters J. N., Tamura K. (2012) A quantitative approach to hepatic clearance prediction of metabolism by aldehyde oxidase using custom pooled hepatocytes. *Xenobiotica*, **42**:863-871.
- 7) Jones J. P., Korzekwa K. R. (2013) Predicting intrinsic clearance for drugs and drug candidates metabolized by aldehyde oxidase. *Mol. Pharm.*, **10**:1262-1268.
- 8) Nishihara M., Takahashi J., Kondo T., Mouri K., Asahi S. (2014) Main metabolic pathways of TAK-802, a novel drug candidate for voiding dysfunction, in humans: The involvement of carbonyl reduction by 11 β -hydroxysteroid dehydrogenase 1. *Drug Res.*, *in press*.
- 9) FDA (2012) Drug Interaction Studies—Study Design, Data Analysis, Implications for Dosing, and Labeling Recommendations. Draft Guidance. US Food and Drug Administration, Silver Spring, MD
(<http://www.fda.gov/Drugs/GuidanceComplianceRegulatoryInformation/Guidances>)
- 10) Nishihara, M., Sudo, M., Kamiguchi, H., Kawaguchi, N., Maeshiba, Y., Kiyota, Y., Takahashi, J., Tagawa, Y., Kondo, T., Asahi, S. (2012) Metabolic fate of sipoglitazar, a novel oral PPAR agonist with activities for PPAR- γ , - α and - δ , in rats and monkeys and comparison with humans *in vitro*. *Drug Metab. Pharmacokinet.*, **27**:1-9.
- 11) Nishihara, M., Sudo, M., Kawaguchi, N., Takahashi, J., Kiyota, Y., Kondo, T., Asahi, S. (2012) An unusual metabolic pathway of sipoglitazar, a novel anti-diabetic agent: Cytochrome P450-catalyzed oxidation of sipoglitazar acyl glucuronide. *Drug Metab.*

- Dispos.*, **40**:249-258.
- 12) Stringer, F., Ploeger, B., Jongh, J. de., Scott, G., Urquart, R., Karim, A., Danhof, M. (2013) Evaluation of the impact of UGT polymorphism on the pharmacokinetics and pharmacodynamics of the novel PPAR agonist, sipoglitazar. *J. Clin. Pharmacol.*, **53**:256-263.
 - 13) Stringer, F., Scott, G., Valbuena, M., Kinley, J., Nishihara, M., Urquhart, R. (2013) The effect of genetic polymorphisms in UGT2B15 on the pharmacokinetic profile of sipoglitazar, a novel anti-diabetic agent. *Eur. J. Clin. Pharmacol.*, **69**:423-430.
 - 14) Nishihara M., Hiura Y., Kawaguchi N., Takahashi J., Asahi S. (2013) UDP-glucuronosyltransferase 2B15 (UGT2B15) is the major enzyme responsible for sipoglitazar glucuronidation in humans: Retrospective identification of the UGT isoform by *in vitro* analysis and the effect of UGT2B15*2 mutation. *Drug Metab. Pharmacokinet.*, **28**:475-484.
 - 15) Ishichi Y., Sasaki M., Setoh M., Tsukamoto T., Miwatashi S., Nagabukuro H., Okanishi S., Imai S., Saikawa R., Doi T., Ishihara Y. (2005) Novel acetylcholinesterase inhibitor as increasing agent on rhythmic bladder contractions: SAR of 8-{3-[1-(3-fluorobenzyl)piperidin-4-yl]propanoyl}-1,2,5,6-tetrahydro-4*H*-pyrrolo[3,2,1-*ij*]quinolin-4-one (TAK-802) and related compounds. *Bioorg. Med. Chem.*, **13**:1901-1911.
 - 16) Nagabukuro H., Okanishi S., Doi T. (2004) Effects of TAK-802, a novel acetylcholinesterase inhibitor, and various cholinomimetics on the urodynamic characteristics in anesthetized guinea pigs. *Eur. J. Pharmacol.*, **494**:225-232.
 - 17) Hashimoto T., Nagabukuro H., Doi T. (2005) Effects of the selective acetylcholinesterase inhibitor TAK-802 on the voiding behavior and bladder mass increase in rats with partial bladder outlet obstruction. *J. Urol.*, **174**:1137-1141.
 - 18) Nagabukuro H., Okanishi S., Imai S., Ishichi Y., Ishihara Y., Doi T. (2004) Effects of TAK-802, a novel acetylcholinesterase inhibitor, on distension-induced rhythmic bladder contractions in rats and guinea pigs. *Eur. J. Pharmacol.*, **485**:299-305.
 - 19) Kakehi M., Tagawa Y., Kondo T., Asahi S. (2013) Disposition of the new potent acetylcholinesterase inhibitor 8-[3-[1-[(3-fluorophenyl)methyl]-4-piperidiny]-1-oxopropyl]-1,2,5,6-tetrahydro-4*H*-pyrrolo[3,2,1-*ij*]quinolin-4-one (TAK-802) in rats, dogs and monkeys. *Drug Res.*, **63**:293-299.
 - 20) Rosemond M. J., Walsh J. S. (2004) Human carbonyl reduction pathways and a strategy for their study *in vitro*. *Drug Metab. Rev.*, **36**:335-361.
 - 21) Skarydová L., Wsól V. (2012) Human microsomal carbonyl reducing enzymes in the metabolism of xenobiotics: well-known and promising members of the SDR superfamily. *Drug Metab. Rev.*, **44**:173-191.
 - 22) Oppermann U. C., Maser E. (2000) Molecular and structural aspects of xenobiotic carbonyl metabolizing enzymes. Role of reductases and dehydrogenases in xenobiotic phase I reactions. *Toxicology*, **144**:71-81.

- 23) Forrest G. L., Gonzalez B. (2000) Carbonyl reductase. *Chem. Biol. Interact.*, **129**: 21-40.
- 24) Rosemond M. J., St John-Williams L., Yamaguchi T., Fujishita T., Walsh J. S. (2004) Enzymology of a carbonyl reduction clearance pathway for the HIV integrase inhibitor, S-1360: role of human liver cytosolic aldo-keto reductases. *Chem. Biol. Interact.*, **147**:129-139.
- 25) Oppermann U. C., Filling C., Jörnvall H. (2001) Forms and functions of human SDR enzymes. *Chem. Biol. Interact.*, **130-132**:699-705.
- 26) Odermatt A., Nashev L. G. (2010) The glucocorticoid-activating enzyme 11 β -hydroxysteroid dehydrogenase type 1 has broad substrate specificity: Physiological and toxicological considerations. *J. Steroid Biochem. Mol. Biol.*, **119**:1-13.
- 27) Maser E. (1995) Xenobiotic carbonyl reduction and physiological steroid oxidoreduction. The pluripotency of several hydroxysteroid dehydrogenases. *Biochem. Pharmacol.*, **49**:421-440.
- 28) Maser E., Friebertshäuser J., Völker B. (2003) Purification, characterization and NNK carbonyl reductase activities of 11 β -hydroxysteroid dehydrogenase type 1 from human liver: enzyme cooperativity and significance in the detoxification of a tobacco-derived carcinogen. *Chem. Biol. Interact.*, **143-144**:435-448.
- 29) Sawada H., Hara A., Nakayama T., Usui S., Hayashibara M. (1982) Comparative studies on distribution and properties of carbonyl reductase in mammalian tissues. *Prog. Clin. Biol. Res.*, **114**:275-289.
- 30) Matsuura K., Bunai Y., Ohya I., Hara A., Nakanishi M., Sawada H. (1994) Ultrastructural localization of carbonyl reductase in mouse lung. *Histochem. J.*, **26**:311-316.
- 31) Nakanishi M., Deyashiki Y., Ohshima K., Hara A. (1995) Cloning, expression and tissue distribution of mouse tetrameric carbonyl reductase. Identity with an adipocyte 27-kDa protein. *Eur. J. Biochem.*, **228**:381-387.
- 32) Arampatzis S., Kadereit B., Schuster D., Balazs Z., Schweizer R. A., Frey F. J., Langer T., Odermatt A. (2005) Comparative enzymology of 11 β -hydroxysteroid dehydrogenase type 1 from six species. *J. Mol. Endocrinol.*, **35**:89-101.
- 33) Meyer A., Vuorinen A., Zielinska A. E., Strajhar P., Lavery G. G., Schuster D., Odermatt A. (2013) Formation of threohydrobupropion from bupropion is dependent on 11 β -hydroxysteroid dehydrogenase 1. *Drug Metab. Dispos.*, **41**:1671-1678.
- 34) Meyer A., Vuorinen A., Zielinska A. E., Da Cunha T., Strajhar P., Lavery G. G., Schuster D., Odermatt A. (2013) Carbonyl reduction of triadimefon by human and rodent 11 β -hydroxysteroid dehydrogenase 1. *Biochem. Pharmacol.*, **85**:1370-1378.
- 35) Desvergne B., Wahli W. (1999) Peroxisome proliferator-activated receptors: nuclear control of metabolism. *Endocr. Rev.*, **20**:649-688.
- 36) Balfour J. A., McTavish D., Heel R. C. (1990) Fenofibrate.: A review of its pharmacodynamic and pharmacokinetic properties and therapeutic use in dyslipidaemia. *Drugs*, **40**:260–290.

- 37) Despres J. P. (2001) Increasing high-density lipoprotein cholesterol: an update on fenofibrate. *Am. J. Cardiol.*, **88**:30N–36N.
- 38) Packard K. A., Backes J. M., Lenz T. L., Wurdeman R. L., Destache C., Hilleman D. E. (2002) Comparison of gemfibrozil and fenofibrate in patients with dyslipidemic coronary heart disease. *Pharmacotherapy*, **22**:1527-1532.
- 39) Haffner S. M., D'Agostino R. Jr., Mykkanen L., Tracy R., Howard B., Rewers M., Selby J., Savage P. J., Saad M. F. (1999) Insulin sensitivity in subjects with T2DM. Relationship to cardiovascular risk factors: the Insulin Resistance Atherosclerosis Study. *Diabetes Care*, **22**:562-568.
- 40) Balfour J. A., Plosker G. L. (1999) Rosiglitazone. *Drugs*, **57**:921-930.
- 41) Gillies P. S., Dunn C. J. (2000) Pioglitazone. *Drugs*, **60**:333-343.
- 42) Sprecher D. L. (2007) Lipids, lipoproteins, and peroxisome proliferator activated receptor-delta. *Am. J. Cardiol.*, **100**:20N-24N.
- 43) Kim S. N. (1988) Preclinical toxicology and pharmacology of dimethylacetamide with clinical notes. *Drug Metab. Rev.*, **19**:345-368.
- 44) Li A. P., Lu C., Brent J. A., Pham C., Fackett A., Ruegg C. E., Silber P. M. (1999) Cryopreserved human hepatocytes: characterization of drug-metabolizing enzyme activities and applications in higher throughput screening assays for hepatotoxicity, metabolic stability, and drug-drug interaction potential. *Chem. Biol. Interact.*, **121**:17-35.
- 45) Loretz L. J., Li A. P., Flye M. W., Wilson, A. G. (1989) Optimization of cryopreservation procedures for rat and human hepatocytes. *Xenobiotica*, **19**:489-498.
- 46) Kintscher U., Law R. E. (2005) PPAR γ -mediated insulin sensitization: the importance of fat versus muscle. *Am. J. Physiol. Endocrinol. Metab.*, **288**:E287-291.
- 47) Hyneck M. L., Munafo A., Benet L. Z. (1988) Effect of pH on acyl migration and hydrolysis of tolmetin glucuronide. *Drug Metab. Dispos.*, **16**:322-324.
- 48) Smith P. C., Hasegawa J., Langendijk P. N., Benet L. Z. (1985) Stability of acyl glucuronides in blood, plasma, and urine: Studies with zomepirac. *Drug Metab. Dispos.*, **13**:110-112.
- 49) Yan Z., Caldwell G. W. (2003) Metabolic assessment in liver microsomes by co-activating cytochrome P450s and UDP-glycosyltransferases. *Eur. J. Drug Metab. Pharmacokinet.*, **28**:223-232.
- 50) Skordi E., Wilson I. D., Lidon J. C., Nicholson J. K. (2005) Kinetic studies on the intramolecular acyl migration of β -1-*O*-acyl glucuronides: Application to the glucuronides of (*R*)- and (*S*)-ketoprofen, (*R*)- and (*S*)-hydroxy-ketoprofen metabolites, and tolmetin by ¹H-NMR spectroscopy. *Xenobiotica*, **35**:715-725.
- 51) Dickinson R. G., Hooper W. D., Eadie M. J. (1984) pH-Dependent rearrangement of the biosynthetic ester glucuronide of valproic acid to β -glucuronidase-resistant forms. *Drug Metab. Dispos.*, **12**:247-252.
- 52) Mortensen R. W., Sidemann U. G., Tjornelund J., Hansen S. H. (2002) Stereospecific

- pH-dependent degradation kinetics of R- and S-naproxen- β -1-*O*-acyl-glucuronide. *Chirality*, **14**:305-312.
- 53) Nicholls A. W., Akira K., Lindon J. C., Farrant R. D., Wilson I. D., Harding J., Killick D. A., Nicholson J. K. (1996) NMR spectroscopic and theoretical chemistry studies on the internal acyl migration reactions of the 1-*O*-acyl- β -D-glucopyranuronate conjugates of 2-, 3-, and 4-(trifluoromethyl)benzoic acids. *Chem. Res. Toxicol.*, **9**:1414-1424.
 - 54) Vanderhoeven S. J., Troke J., Tranter G. E., Wilson I. D., Nicholson J. K., Lindon J. C. (2004) Nuclear magnetic resonance (NMR) and quantitative structure–activity relationship (QSAR) studies on the transacylation reactivity of model 1- β -*O*-acyl glucuronides. II: QSAR modeling of the reaction using both computational and experimental NMR parameters. *Xenobiotica*, **34**:889-900.
 - 55) Kumar S., Samuel K., Subramanian R., Braun M. P., Stearns R. A., Chiu S-H., Evans D. C., Baillie T. A. (2002) Extrapolation of diclofenac clearance from *in vitro* microsomal metabolism data: role of acyl glucuronidation and sequential oxidative metabolism of the acyl glucuronide. *J. Pharmacol. Exp. Ther.*, **303**:969-978.
 - 56) Delaforge M., Pruvost A., Perrin L., André F. (2005) Cytochrome P450-mediated oxidation of glucuronide derivatives: example of estradiol-17 β -glucuronide oxidation to 2-hydroxy-estradiol-17 β -glucuronide by CYP2C8. *Drug Metab. Dispos.*, **33**:466-473.
 - 57) Kochansky C. J., Xia Y. Q., Wang S., Cato B., Creighton M., Vincent S. H., Franklin R. B., Reed J. R. (2005) Species differences in the elimination of a peroxisome proliferator-activated receptor agonist highlighted by oxidative metabolism of its acyl glucuronide. *Drug Metab. Dispos.*, **33**:1894-1904.
 - 58) Melet A., Marques-Soares C., Schoch G. A., Macherey A. C., Jaouen M., Dansette P. M., Sari M. A., Johnson E. F., Mansuy D. (2004) Analysis of human cytochrome P450 2C8 substrate specificity using a substrate pharmacophore and site-directed mutants. *Biochemistry*, **43**:15379-15392.
 - 59) Schoch G. A., Yano J. K., Wester M. R., Griffin K. J., Stout C. D., Johnson E. F. (2004) Structure of human microsomal cytochrome P450 2C8. Evidence for a peripheral fatty acid binding site. *J. Biol. Chem.*, **279**:9497-9503.
 - 60) Johnson E. F., Stout C. D. (2005) Structure diversity of human xenobiotic-metabolizing cytochrome P450 monooxygenases. *Biochem. Biophys. Res. Commun.*, **338**:331-336.
 - 61) Ogilvie B. W., Zhang D., Li W., Rodrigues A. D., Gipson A. E., Holsapple J., Toren P., Parkinson A. (2006) Glucuronidation converts gemfibrozil to a potent, metabolism-dependent inhibitor of CYP2C8: Implications for drug-drug interactions. *Drug Metab. Dispos.*, **34**:191-197.
 - 62) Baer B. R., DeLisle R. K., Allen A. (2009) Benzylic oxidation of gemfibrozil-1-*O*- β -glucuronide by P450 2C8 leads to heme alkylation and irreversible inhibition. *Chem. Res. Toxicol.*, **22**:1298-1309.
 - 63) Shitara Y., Hirano M., Sato H., Sugiyama Y. (2004) Gemfibrozil and its glucuronide

- inhibit the organic anion transporting polypeptide 2 (OATP2/OATP1B1:SLC21A6)-mediated hepatic uptake and CYP2C8-mediated metabolism of cerivastatin: analysis of the mechanism of the clinically relevant drug-drug interaction between cerivastatin and gemfibrozil. *J. Pharmacol. Exp. Ther.*, **311**:228-236.
- 64) Prueksaritanont T., Ma B., Fang X., Subramanian R., Yu J., Lin J. H. (2001) β -Oxidation of simvastatin in mouse liver preparations. *Drug Metab. Dispos.*, **29**:1251-1255.
- 65) Prueksaritanont T., Subramanian R., Fang X., Ma B., Qiu Y., Lin J. H., Pearson P. G., Baillie T. A. (2002) Glucuronidation of statins in animals and humans: a novel mechanism of statin lactonization. *Drug Metab. Dispos.*, **30**:505-512.
- 66) Mackenzie, P. I., Bock, K. W., Burchell, B., Guillemette, C., Ikushiro, S., Iyanagi, T., Miners, J. O., Owens, I. S., Nebert, D. W. (2005) Nomenclature update for the mammalian UDP glycosyltransferase (UGT) gene superfamily. *Pharmacogenet. Genomics*, **15**:677-685.
- 67) Guillemette, C., Lévesque, E., Harvey, M., Bellemare, J., Menard, V. (2010) UGT genomic diversity: beyond gene duplication. *Drug Metab. Rev.*, **42**:24-44.
- 68) Miners, J. O., Mackenzie, P. I., Knights, K. M. (2010) The prediction of drug-glucuronidation parameters in humans: UDP-glucuronosyltransferase enzyme-selective substrate and inhibitor probes for reaction phenotyping and *in vitro-in vivo* extrapolation of drug clearance and drug-drug interaction potential. *Drug Metab. Rev.*, **42**:196-208.
- 69) Argikar, U. A., Iwuchukwu, O. F., Nagar, S. (2008) Update on tools for evaluation of uridine diphosphoglucuronosyltransferase polymorphisms. *Expert Opin. Drug Metab. Toxicol.*, **4**:879-894.
- 70) Peters, W. H., te Morsche, R. H., Roelofs, H. M. (2003) Combined polymorphisms in UDP-glucuronosyltransferases 1A1 and 1A6: implications for patients with Gilbert's syndrome. *J. Hepatol.*, **38**:3-8.
- 71) Massacesi, C., Terrazzino, S., Marcucci, F., Rocchi, M. B., Lippe, P., Bissoni, R., Lombardo, M., Pilone, A., Mattioli, R., Leon A. (2006) Uridine diphosphate glucuronosyl transferase 1A1 promoter polymorphism predicts the risk of gastrointestinal toxicity and fatigue induced by irinotecan-based chemotherapy. *Cancer*, **106**:1007-1016.
- 72) Nagar, S., Blanchard, R. L. (2006) Pharmacogenetics of uridine diphosphoglucuronosyltransferase (UGT) 1A family members and its role in patient response to irinotecan. *Drug Metab. Rev.*, **38**:393-409.
- 73) Court, M. H., Hao, Q., Krishnaswamy, S., Bekaii-Saab, T., Al-Rohaimi, A., von Moltke, L. L., Greenblatt, D. J. (2004) UDP-glucuronosyltransferase (UGT) 2B15 pharmacogenetics: UGT2B15 D85Y genotype and gender are major determinants of oxazepam glucuronidation by human liver. *J. Pharmacol. Exp. Ther.*, **310**:656-665.
- 74) Chung, J. Y., Cho, J. Y., Yu, K. S., Kim, J. R., Jung, H. R., Lim, K. S., Jang, I. J., Shin, S. G. (2005) Effect of the UGT2B15 genotype on the pharmacokinetics, pharmacodynamics,

- and drug interactions of intravenous lorazepam in healthy volunteers. *Clin. Pharmacol. Ther.*, **77**:486-494.
- 75) Swanson, C., Mellström, D., Lorentzon, M., Vandenput, L., Jakobsson, J., Rane, A., Karlsson, M., Ljunggren, O., Smith, U., Eriksson A. L., Bélanger A., Labrie F., Ohlsson C. (2007) The uridine diphosphate glucuronosyltransferase 2B15 D85Y and 2B17 deletion polymorphisms predict the glucuronidation pattern of androgens and fat mass in men. *J. Clin. Endocrinol. Metab.*, **92**:4878-4882.
- 76) Gsur, A., Preyer, M., Haidinger, G., Schatzl, G., Madersbacher, S., Marberger, M., Vutuc, C., Micksche, M. (2002) A polymorphism in the UDP-Glucuronosyltransferase 2B15 gene (D85Y) is not associated with prostate cancer risk. *Cancer Epidemiol. Biomarkers Prev.*, **11**:497-498.
- 77) Lévesque, E., Beaulieu, M., Green, M. D., Tephly, T. R., Bélanger, A., Hum, D. W. (1997) Isolation and characterization of UGT2B15(Y85): a UDP-glucuronosyltransferase encoded by a polymorphic gene. *Pharmacogenetics*, **7**:317-325.
- 78) Guillemette, C. (2003) Pharmacogenomics of human UDP-glucuronosyltransferase enzymes. *Pharmacogenomics J.*, **3**:136-158.
- 79) Lovdahl, M. J., Reher, K. E., Mann, H. J., Rimmel, R. P. (1994) Determination of 4-methylumbelliferone and metabolites in Williams E medium and dog plasma by high performance liquid chromatography. *J. Liq. Chromatogr.*, **17**:1795-1809.
- 80) Court, M. H. (2005) Isoform-selective probe substrates for *in vitro* studies of human UDP-glucuronosyltransferases. *Methods Enzymol.*, **400**:104-116.
- 81) Court, M. H., Krishnaswamy, S., Hao, Q., Duan, S. X., Patten, C. J., Von Moltke, L. L., Greenblatt, D. J. (2003) Evaluation of 3'-azido-3'-deoxythymidine, morphine, and codeine as probe substrates for UDP-glucuronosyltransferase 2B7 (UGT2B7) in human liver microsomes: specificity and influence of the UGT2B7*2 polymorphism. *Drug Metab. Dispos.*, **31**:1125-1133.
- 82) Uchaipichat, V., Mackenzie, P. I., Guo, X. H., Gardner-Stephen, D., Galetin, A., Houston, J. B., Miner, J. O. (2004) Human UDP-glucuronosyltransferases: Isoform selectivity and kinetics of 4-methylumbelliferone and 1-naphthol glucuronidation, effects of organic solvents, and inhibition by diclofenac and probenecid. *Drug Metab. Dispos.*, **32**:413-423.
- 83) Court, M. H., Duan, S. X., Guillemette, C., Journault, K., Krishnaswamy, S., Von Moltke, L. L., Greenblatt, D. J. (2002) Stereoselective conjugation of oxazepam by human UDP-glucuronosyltransferases (UGTs): *S*-oxazepam is glucuronidated by UGT2B15, while *R*-oxazepam is glucuronidated by UGT2B7 and UGT1A9. *Drug Metab. Dispos.*, **30**:1257-1265.
- 84) Bauman, J. N., Goosen, T. C., Tugnait, M., Peterkin, V., Hurst, S. I., Menning, L. C., Milad, M., Court, M. H., Williams, J. A. (2005) UDP-glucuronosyltransferase 2B7 is the major enzyme responsible for Gemcabene glucuronidation in human liver microsomes. *Drug Metab. Dispos.*, **33**:1349-1354.

- 85) Kaji, H., Kume, T. (2005) Identification of human UDP-glucuronosyltransferase isoform(s) responsible for the glucuronidation of 2-(4-chlorophenyl)-5-(2-furyl)-4-oxazoleacetic acid (TA-1801A). *Drug Metab. Pharmacokinet.*, **20**:212-218.
- 86) Hanioka, N., Tanabe, N., Jinno, H., Tanaka-Kagawa, T., Nagaoka, K., Naito, S., Koeda, A., Narimatsu, S. (2010) Functional characterization of human and cynomolgus monkey UDP-glucuronosyltransferase 1A1 enzymes. *Life Sci.*, **87**:261-268.
- 87) Krishnaswamy, S., Hao, Q., Al-Rohaimi, A., Hesse, L. M., von Moltke, L. L., Greenblatt, D. J., Court, M. H. (2005) UDP glucuronosyltransferase (UGT) 1A6 pharmacogenetics: II. Functional impact of the three most common nonsynonymous UGT1A6 polymorphisms (S7A, T181A, and R184S). *J. Pharmacol. Exp. Ther.*, **313**:1340-1346.
- 88) Izukawa T., Nakajima M., Fujiwara R., Yamanaka H., Fukami T., Takamiya M., Aoki Y., Ikushiro S., Sakaki T., Yokoi T. (2009) Quantitative analysis of UDP-glucuronosyltransferase (UGT) 1A and UGT2B expression levels in human livers. *Drug Metab. Dispos.*, **37**:1759-1768.
- 89) Ohno S., Nakajin S. (2009) Determination of mRNA expression of human UDP-glucuronosyltransferases and application for localization in various human tissues by real-time reverse transcriptase-polymerase chain reaction. *Drug Metab. Dispos.*, **37**:32-40.
- 90) Court, M. H., Zhang, X., Ding, X., Yee, K. K., Hesse, L. M., Finel, M. (2012) Quantitative distribution of mRNAs encoding the 19 human UDP-glucuronosyltransferase enzymes in 26 adult and 3 fetal tissues. *Xenobiotica*, **42**:266-277.
- 91) Lépine, J., Bernard, O., Plante, M., Têtu, B., Pelletier, G., Labrie, F., Bélanger, A., Guillemette, C. (2004) Specificity and regioselectivity of the conjugation of estradiol, estrone, and their catecholestrogen and methoxyestrogen metabolites by human uridine diphospho-glucuronosyltransferases expressed in endometrium. *J. Clin. Endocrinol. Metab.*, **89**:5222-5232.
- 92) Soars M. G., Fettes M., O'Sullivan A. C., Riley R. J., Ethell B. T., Burchell B. (2003) Cloning and characterisation of the first drug-metabolising canine UDP-glucuronosyltransferase of the 2B subfamily. *Biochem. Pharmacol.*, **65**:1251-1259.
- 93) King C. D., Green M. D., Rios G. R., Coffman B. L., Owens I. S., Bishop W. P., Tephly T. R. (1996) The glucuronidation of exogenous and endogenous compounds by stably expressed rat and human UDP-glucuronosyltransferase 1.1. *Arch. Biochem. Biophys.*, **332**:92-100.
- 94) Dean B., Chang S., Stevens J., Thomas P. E., King C. (2002) Isolation and characterization of a UDP-glucuronosyltransferase (UGT1A01) cloned from female rhesus monkey. *Arch. Biochem. Biophys.*, **402**:289-295.
- 95) Kurkela, M., García-Horsman, J. A., Luukkanen, L., Mörsky, S., Taskinen, J., Baumann,

- M., Kostiainen, R., Hirvonen, J., Finel, M. (2003) Expression and characterization of recombinant human UDP-glucuronosyltransferases (UGTs). *J. Biol. Chem.*, **278**:3536-3544.
- 96) Patel, M., Tang, B. K., Grant, D. M., Kalow, W. (1995) Interindividual variability in the glucuronidation of (*S*)-oxazepam contrasted with that of (*R*)-oxazepam. *Pharmacogenetics*, **5**:287-297.
- 97) Meech, R., Mackenzie, P. I. (1998) Determinants of UDP glucuronosyltransferase membrane association and residency in the endoplasmic reticulum. *Arch. Biochem. Biophys.*, **356**:77-85.